Radiocarbon: detection, contamination, and determination

Paul, Dipayan

Radiocarbon: Detection, Contamination, and Determination

Dipayan Paul

Radiocarbon: Detection, Contamination, and Determination

Dipayan Paul

PhD thesis, 2016
University of Groningen
the Netherlands
ISBN: 978-90-367-8730-7 (printed version)
ISBN: 978-90-367-8729-1 (digital version)
Printing: Ridderprint BV, the Netherlands

Cover designed by: Swati B Vartak and Dipayan Paul

The research described in this thesis was performed at the Centre for Isotope Research (CIO), which is part of the Energy and Sustainability Research Institute Groningen (ESRIG), University of Groningen, the Netherlands.

The research described in this thesis was funded by the electricity company RWE/Essent.

university of groningen

Radiocarbon: Detection, Contamination, and Determination

PhD thesis

to obtain the degree of PhD at the
University of Groningen
on the authority of the
Rector Magnificus Prof. E. Sterken
and in accordance with
the decision by the College of Deans.

This thesis will be defended in public on

Monday 11 April 2016 at 12:45 hours

by

Dipayan Paul

born on 14 November 1982
in Jamshedpur, India

Supervisor
Prof. H. A. J. Meijer

Assessment committee
Prof. J. van der Plicht
Prof. E. Kerstel
Prof. W. Peters

Table of Contents

Chapter 1:

General Introduction

1

Introduction

Carbon, the building block of all living organisms on our planet, naturally exists in the form of three isotopes. Carbon-12 (^{12}C, 98.9%) being the most abundant and followed by carbon-13 (^{13}C, 1.1%) are the two stable isotopes of carbon. Carbon-14 (^{14}C, ≈ 1 ppt), which is radioactive and therefore is usually called radiocarbon, is the third naturally occurring isotope ($t_{½}$ = 5730 ± 40 years) of carbon. Formation of ^{14}C occurs in the higher atmosphere (Lingenfelter 1963) by the reaction of ^{14}N with thermalized neutrons, produced through cosmic radiation. ^{14}C is then oxidized in the atmosphere to $^{14}CO_2$. Thus, $^{14}CO_2$ forms a trace component of carbon dioxide (CO_2). ^{14}C in the form of $^{14}CO_2$ is then taken up by plants through photosynthesis, and is subsequently transferred to animals that feed on plants. In this way radiocarbon is taken up by all living organisms, and, since the decay of ^{14}C is very slow compared to the C turnover time in living organisms, all living matter is in ^{14}C equilibrium with atmospheric $^{14}CO_2$ (although there are some complications with marine and aquatic life). When an organism dies, the uptake of radiocarbon stops and the leftover radiocarbon slowly decays to ^{14}N. Thus, the older the sample gets, the lower the radiocarbon content gets. This process forms the very basis of the well-known radiocarbon dating. ^{14}C is present in the atmosphere predominantly in the form of $^{14}CO_2$ and CO_2 is by far the largest carbon containing fraction in the atmosphere. CO_2 is a naturally occurring greenhouse gas produced mainly through respiration by aerobic organisms, decay of organic materials and volcanic activities. It is also produced anthropogenically through the combustion of fossil fuels and biomass burning. The concentration of CO_2 in the atmosphere has been continuously rising since the beginning of industrialization. $^{14}CO_2$ is an important atmospheric tracer, which helps in the understanding and quantification of the levels of anthropogenic emissions from fossil fuels (examples of such work in our group Zondervan and Meijer 1996; Palstra et al. 2008; Van der Laan et al. 2010). This is due to the fact that fossil fuel is virtually radiocarbon-free, which upon combustion produces radiocarbon-free CO_2 which dilutes the atmospheric $^{14}CO_2$ concentration upon release. Figure 1a shows the increase in the concentration of atmospheric CO_2 (top panel, green curve), the annual mean growth rate (top panel,

magenta curve) and the activity of ^{14}C in CO_2 from different zones in the northern and southern hemisphere (bottom panel). The activity of ^{14}C is given in $\Delta^{14}C$ (‰), which indicates the enrichment/depletion in $^{14}C/C$ of CO_2 with respect to the preindustrial level of 0‰ (Stuiver and Polach 1977; Mook and van der Plicht 1999). Due to the dilution of atmospheric $^{14}CO_2$ by CO_2 produced from fossil fuel alone, one would have expected a continuous decrease in the $^{14}CO_2$ concentration. However, as seen in Figure 1, the above-ground nuclear bomb tests conducted during the 1950's and 1960's introduced a huge amount of $^{14}CO_2$ in the atmosphere, such that the atmospheric concentration of $^{14}CO_2$ almost doubled. Following the ratification of Nuclear Test Ban Treaty, signed in 1963, the surplus $^{14}CO_2$ in the atmosphere has gradually equilibrated with the terrestrial biosphere and the oceans.

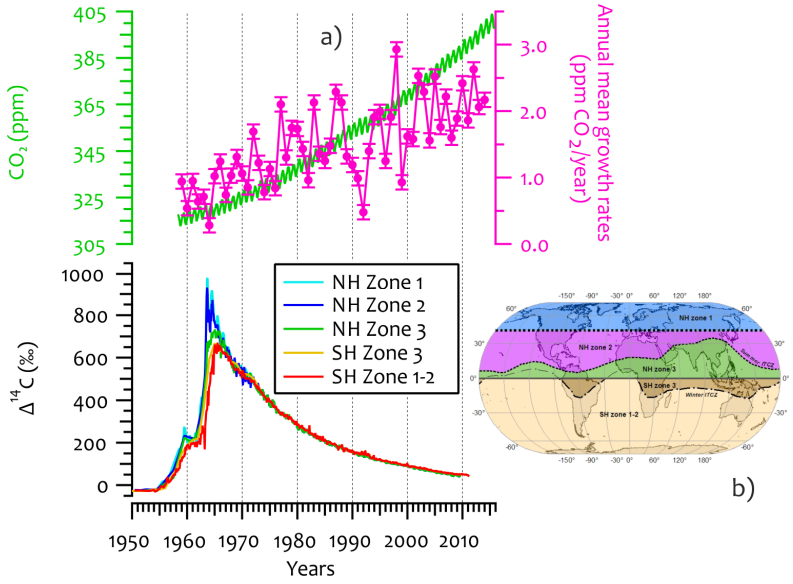

Figure 1: (a) Top panel, Left: Monthly mean atmospheric carbon dioxide at Mauna Loa Observatory, Hawaii; Right: Annual mean growth rate of carbon dioxide at Mauna Loa Observatory, Hawaii (*www.esrl.noaa.gov/gmd/ccgg/trends/*); Bottom panel: Compiled monthly atmospheric $\Delta^{14}C$ (‰) curves for 5 different zones shown on the world map in (b): adapted from (Hua et al. 2013).

Only since the 21st century, the dilution effect by CO_2 produced from fossil fuel has become visible. As the concentration of CO_2 in our atmosphere is rising

continuously at a current growth rate of ≈ 2 ppm/year, monitoring of this greenhouse gas, and understanding of its sources, sinks and transport mechanisms has become extremely important. Radiocarbon is a prominent tracer to better understand the global carbon cycle. Apart from dating of archaeological discoveries and atmospheric applications, radiocarbon is also used in determining the age of ground water reservoirs, oceanic water masses, food authenticity, and various forensic and pharmaceutical applications.

High sensitivity detection of radiocarbon was traditionally performed using proportional gas counting, invented in our laboratory (de Vries and Barendsen 1953). Although accurate, this method had a very low throughput (one measurement took typically 48 hours) and required very large samples (1 gram C or more). With the advent of Accelerator Mass Spectrometry (AMS), an atom counting method, high precision ^{14}C measurements of relatively small samples were made possible (Bennett et al. 1977; Purser et al. 1979). To perform AMS measurements of ^{14}C, a sample is combusted to CO_2, which is then reduced to graphite. The reduction of CO_2 to graphite is either performed using the Zn-reduction method or the Bosch reaction. In the method using the Bosch reaction, which is the method used at the Groningen AMS facility, CO_2 is heated in the presence of H_2 and Fe (Aerts-Bijma et al. 1997). Byproduct of this reaction, H_2O, is either removed with Peltier cooled traps or chemically through the use of anhydrous $Mg(ClO_4)_2$ (Santos et al. 2007). This produced graphite is then pressed on aluminum cathodes (also known as “target”) and measured.

In this thesis, three different research topics have been dealt with, each described in a separate chapter. Although broadly diverse, the projects are linked by their common factor: radiocarbon. In the following sections, a brief introduction of each chapter has been provided.

Chapter 2: Intracavity OptoGalvanic Spectroscopy not suitable for ambient level radiocarbon detection.

This chapter describes the development and evaluation of Intracavity OptoGalvanic Spectroscopy (ICOGS) as a tool to detect radiocarbon (^{14}C) for applications such

as radiocarbon dating, atmospheric monitoring and industrial flue gas analysis. ICOGS was developed by the Murnick group at Rutgers University, Newark for radiocarbon detection with subattomole sensitivity (Murnick et al. 2008). Due to the underlined features the technique was presented with, many research groups around the world, including us at the University of Groningen, were motivated to explore the technique at various frontiers of research. Since the sensitivity of ICOGS was described to be very similar to that of the Accelerator Mass Spectrometer (AMS), which back then was the only technique for radiocarbon detection at contemporary levels and below, it brought in hopes for an affordable, and perhaps even on-line, analytical technique for various radiocarbon-related studies.

At Groningen, the ICOGS facility was developed in close collaboration with the Murnick Group at Rutgers. ICOGS in principle is inspired by a combination of two spectroscopic detection techniques i.e., IntraCavity Absorption Spectroscopy (ICAS) and OptoGalvanic Spectroscopy (OGS). The sample cell (containing pure CO_2 or CO_2 in a buffer gas) is placed inside the optical cavity of a CO_2 laser. The sample cell is maintained at a low pressure (1-10 mbar) to produce a RF-induced glow discharge. The optogalvanic signal is a measure of the change in impedance of a discharge due to resonant laser interaction with atomic or molecular transitions of an analyte present in the discharge. The ICOGS setup constructed in Groningen is similar to the setup built by the Murnick group and features several modifications made to improve the detection. Thus, the ICOGS setup comprised of a modified $^{14}CO_2$ laser with an extended cavity, where the sample and the reference cells were placed. The setup also comprised of a $^{12}CO_2$ laser used for signal normalization, several beam steering optics, RF excitation and detection electronics, laser power meters, a spectrum analyzer, and the sample handling system. The construction of the ICOGS setup was completed in mid-2012. Since then, numerous experiments have been performed to unambiguously detect radiocarbon in CO_2 samples, containing different levels of ^{14}C concentrations. Initially, all experiments were performed with CO_2 containing contemporary levels of ^{14}C ("modern", 1.2×10^{-10} % $^{14}C/^{12}C$) and CO_2 highly depleted in ^{14}C ("dead", ≤

1×10^{-13} % $^{14}C/^{12}C$). Later, due to repeated failures in that range of ^{14}C concentrations, we prepared several enriched CO_2 samples (up to 1 billion times the natural abundance) for determining the achievable limits of detection with our setup. We have recently reported our findings, and concluded that ICOGS is not at all a viable analytical technique for radiocarbon detection (Paul and Meijer 2015).

Chapter 3: Contamination on Accelerator Mass Spectrometric sample targets by modern carbon is inevitable.

Accelerator Mass Spectrometric (AMS) determination of radiocarbon for applications such as radiocarbon dating and atmospheric monitoring requires very careful sample handling to avoid contaminations. Since radiocarbon is a trace component in natural CO_2, any "foreign" carbon contamination would lead to erroneous results. Thus, extreme care is required during the preparation steps. After preparation, the samples often have to be stored before the actual AMS measurements are performed. This makes the storage conditions very important as well to minimize the post-preparation contamination.

In this chapter, the process of post-preparation contamination of background (highly depleted in radiocarbon, older than 30000 years) AMS samples is investigated. For such old samples, dead carbon contamination (DCC, $\leq 1 \times 10^{-13}$ % $^{14}C/^{12}C$) hardly affects the age determination, if anything, making the sample appear only slightly older depending on the ^{14}C activity of the sample and the contaminant. However, contaminations arising from modern carbon contaminants (MCC, 1.2×10^{-10} % $^{14}C/^{12}C$) make the background samples appear much younger, the severity of the effect depending also on the mass of the sample and the contaminant. Contamination of AMS samples possibly happens in every stage of sample handling. During an AMS measurement, a sample is measured at eight different spots on the sample graphite surface, and every spot is measured ten times with each measurement lasting 30 sec. This results in a total of eighty measurements and each measurement is called a "block". It has been known for long that, when a pressed background target is left in open air, and is then measured, the initial blocks always produce higher number of counts than the later

ones. This indicates the presence of an enriched surface relative to the inner bulk, which is exposed during the sputtering process. The only possible explanation to this phenomenon is the presence of an additional carbonaceous material, with higher ^{14}C activity, on the target surface. Although the source of this carbonaceous material was not known, one may speculate the source to be atmospheric CO_2. Since the concentration of CO_2 in atmosphere surpasses any other carbon containing fraction by at least 2 orders of magnitude, it being the culprit is plausible. Thus, several storage tests were performed with targets stored in humidified laboratory air spiked with CO_2 containing various levels of radiocarbon. Results of these storage tests are discussed in this chapter. Additional experiments were performed to understand the chemical nature of the graphitization product, the nature of attachment of this contamination and whether or not the catalyst mediates the contamination. Probably one of the most important findings during this study was the fact that a phenomenon similar to what is discussed in this chapter is known in the field of material science. In this field of science, it is known that a thin carbonaceous layer "automatically" and unavoidably appears on a clean surface when exposed to air, which is known as Adventitious Carbon (AC). The formation of an adventitious carbon layer on clean surfaces likely explains the type of contamination we observe with the graphite targets. From the available literature on AC, it appears that the complete avoidance of such a contaminating layer is probably impossible. One may have strict strategies and protocols which could help minimize the extent of contamination, but possibly none to stop it completely.

Chapter 4: Determination of radiocarbon in stratospheric CO_2 retrieved from AirCore sampling.

Radiocarbon is one of the important atmospheric tracers that helps differentiating natural from anthropogenic sources of emitted CO_2. Since CO_2 is a major component of the global carbon budget, proper understanding of its sources, sinks and transport is essential. In this chapter we describe a proof-of-principle project in which the radiocarbon concentration in stratospheric CO_2 samples, collected using AirCore sampling method, is determined. AirCore is an innovative atmospheric sampling method developed at National Oceanic and Atmospheric Administration

(NOAA) for measuring the vertical distribution of several greenhouse gases in the atmosphere (Karion et al. 2010). In Europe, regular AirCore samplings are being organized from our group (Dr. Huilin Chen), and performed at Sodankylä, Northern Finland. Two such AirCore samples from Sodankylä were collected in July 2014 and stored for the purpose of determination of radiocarbon in stratospheric CO_2. The samples were later brought to Groningen, where they were processed and measured at the Groningen AMS facility. The stratospheric part of each AirCore profile was divided into six sections that were preserved in a stratospheric air sampler. Each section of the stratospheric air sampler contained ≈ 50 ml air (≈ 35 µg CO_2). Due to the small sample size, a small-volume extraction system (≈ 20 ml) was constructed for quantitative extraction of CO_2. Additionally, a small-volume graphitization system (≈ 1.5 ml) was also constructed and an optimized protocol was adopted for efficient graphitization of these small samples. This chapter provides a detailed description of the sampling technique, extraction steps, graphitization step, and the data normalization procedure. Finally, through the results it is shown that the AirCore sampling technique is a viable sample collection technique for the detection of radiocarbon in stratospheric air samples.

References

Aerts-Bijma AT, Meijer HAJ, van der Plicht J. 1997. AMS sample handling in Groningen. Nuclear Instruments & Methods in Physics Research Section B-Beam Interactions with Materials and Atoms 123(1-4):221-5.

Bennett CL, Beukens RP, Clover MR, Gove HE, Liebert RB, Litherland AE, Purser KH, Sondheim WE. 1977. Radiocarbon Dating Using Electrostatic Accelerators: Negative Ions Provide the Key. Science 198(4316):508-10.

de Vries H, Barendsen GW. 1953. Radio-carbon dating by a proportional counter filled with carbondioxide. Physica 19(1-12):987-1003.

Hua Q, Barbetti M, Rakowski AZ. 2013. Atmospheric Radiocarbon for the Period 1950–2010. Radiocarbon 55(4):2059-72.

Karion A, Sweeney C, Tans P, Newberger T. 2010. AirCore: An Innovative Atmospheric Sampling System. Journal of Atmospheric and Oceanic Technology 27(11):1839-53.

Lingenfelter RE. 1963. Production of Carbon 14 by Cosmic-Ray Neutrons. Reviews of Geophysics 1(1):35-55.

Mook WG, van der Plicht J. 1999. Reporting ^{14}C activities and concentrations. Radiocarbon 41(3):227-39.

Murnick DE, Dogru O, Ilkmen E. 2008. Intracavity optogalvanic spectroscopy. An analytical technique for C-14 analysis with subattomole sensitivity. Analytical Chemistry 80(13):4820-4.

Palstra SWL, Karstens U, Streurman HJ, Meijer HAJ. 2008. Wine ethanol C-14 as a tracer for fossil fuel CO_2 emissions in Europe: Measurements and model comparison. Journal of Geophysical Research-Atmospheres 113(D21).

Paul D, Meijer HAJ. 2015. Intracavity OptoGalvanic Spectroscopy Not Suitable for Ambient Level Radiocarbon Detection. Analytical Chemistry 87(17):9025-32.

Purser KH, Litherland AE, Gove HE. 1979. Ultra-sensitive particle identification systems based upon electrostatic accelerators. Nuclear Instruments and Methods 162(1-3):637-56.

Santos GM, Southon JR, Druffel-Rodriguez KC, Griffin S, Mazon M. 2007. Magnesium perchlorate as an alternative water trap in AMS graphite sample preparation; a report on sample preparation at KCCAMS at the University of California, Irvine. Radiocarbon 46(1):165-73.

Stuiver M, Polach HA. 1977. Discussion: reporting of ^{14}C data. Radiocarbon 19(3):355-63.

Van der Laan S, Karstens U, Neubert REM, Van der Laan-Luijkx IT, Meijer HAJ. 2010. Observation-based estimates of fossil fuel-derived CO_2 emissions in the Netherlands using $\Delta^{14}C$, CO and ^{222}Radon. Tellus Series B-Chemical and Physical Meteorology 62(5):389-402.

Zondervan A, Meijer HAJ. 1996. Isotopic characterisation of CO_2 sources during regional pollution events using isotopic and radiocarbon analysis. Tellus Series B-Chemical and Physical Meteorology 48(4):601-12.

Chapter 2:

Intracavity OptoGalvanic Spectroscopy not suitable for ambient level radiocarbon detection

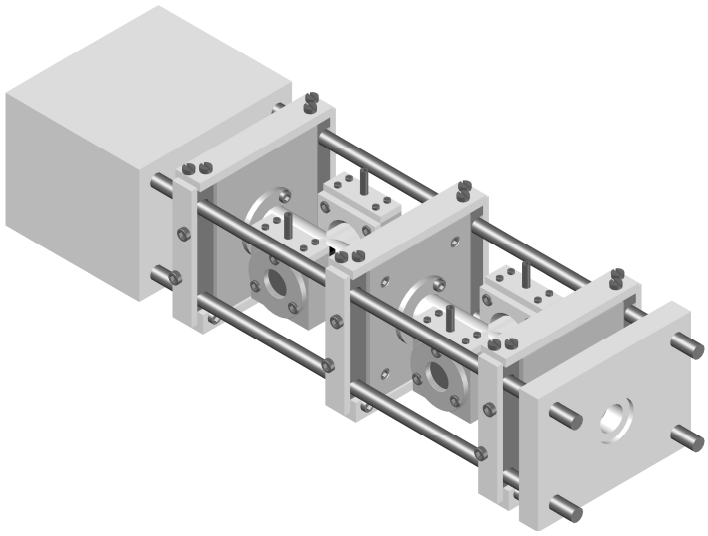

This chapter has been published as:

Paul, D.; Meijer, H. A. J., Analytical Chemistry 2015, 87, 9025-9032.

Cover image shows the intracavity cells placed inside the $^{14}CO_2$ laser gain medium for optogalvanic detection of radiocarbon described in this chapter.

Abstract

IntraCavity OptoGalvanic Spectroscopy (ICOGS) as a radiocarbon detection technique was first reported by the Murnick group at Rutgers University, Newark, USA in 2008. This technique for radiocarbon detection was presented with tremendous potentials for applications in various fields of research. Significantly cheaper, this technique was portrayed as a possible complementary technique to the more expensive and complex Accelerator Mass Spectrometry. Several groups around the world started developing this technique for various radiocarbon related applications. The ICOGS setup at the University of Groningen was constructed in 2012 in close collaboration with the Murnick group for exploring possible applications in the fields of radiocarbon dating and atmospheric monitoring. In this chapter we describe a systematic evaluation of the ICOGS setup at Groningen for radiocarbon detection. Since the ICOGS setup was strictly planned for dating and atmospheric monitoring purposes, all the initial experiments were performed with CO_2 samples containing contemporary levels and highly depleted levels of radiocarbon. Because of recurring failures in differentiating the two CO_2 samples, with radiocarbon concentration 3 orders of magnitude apart, CO_2 samples containing elevated levels of radiocarbon were prepared in-house and experimented with. All results obtained thus far at Groningen are in sharp contrast to the results published by the Murnick group and rather support the results put forward by the Salehpour group at Uppsala University. From our extensive test work, we must conclude that the method is unsuited for ambient level radiocarbon measurements, and even highly enriched CO_2 samples yield insignificant signal.

2.1 Introduction

In 2008, Murnick et al. (will be referred as “Mu2008” throughout this chapter), introduced ICOGS as a highly sensitive technique for radiocarbon (^{14}C) detection (Murnick et al. 2008). ICOGS evolved from its predecessor Laser Assisted Ratio Analyzer (LARA) which was developed and successfully used for $\delta^{13}C$ measurements for breath analysis (Murnick and Peer 1994; Murnick et al. 1995; Cave et al. 1999; Van der Hulst et al. 1999; Savarino et al. 2000) and in atmospheric CO_2 (Okil 2004). ICOGS was presented with tremendous potentials due to the underlined capabilities and did bring in hopes for an accelerator-free, thus affordable, laser-based radiocarbon detection method(Murnick and Okil 2005; Murnick et al. 2007; Murnick et al. 2008; Ilkmen 2009; Ilkmen and Murnick 2010; Murnick et al. 2010). The key features that made ICOGS attractive were: 1) minimal sample handling since samples were measured in the form of pure CO_2 or CO_2 mixed with a buffer gas such as N_2; 2) depending on the sample size measurements were possible in continuous flow-through and batch mode; 3) relatively simple and inexpensive construction when compared to an Accelerator Mass Spectrometer; and 4) projected detection limits close to or better than possible with AMS ($^{14}C/^{12}C \approx 10^{-15}$). With all these salient features, ICOGS could have potentially been useful in several fields of research, such as radiocarbon dating, industrial flue gas analysis, atmospheric monitoring, drug-metabolism studies, to name but a few.

ICOGS claimed its “allegedly” extraordinary sensitivity due to the combination of optogalvanic effect (OGE) and the intracavity enhancements achieved by the placement of sample cell inside the laser cavity. To reduce the interferences from the much more abundant molecular species e.g., $^{12}C^{16}O_2$, $^{13}C^{16}O_2$, $^{12}C^{18}O_2$, $^{13}C^{18}O_2$, $^{12}C^{17}O_2$, $^{13}C^{17}O_2$ etc., wavelengths around 11–12 µm were used. A commercially available CO_2 laser was modified to accommodate the sample cell inside the laser cavity. The CO_2 in the gas mixture, inside the laser gain medium, was replaced with $^{14}CO_2$ to generate the $^{14}CO_2$ specific wavelengths (11–12 µm) for higher specificity and sensitivity.

Following the 2008 publication, at least four groups around the world, including us at the University of Groningen got involved in the development of ICOGS for various applications. The ICOGS setup at Groningen was started in 2012, prior to which both authors spent a considerable time (DP ≈ 11 months, HAJM ≈ 3 months) in the Murnick group at Rutgers University, Newark. During the stay, we were involved in the day-to-day experiments conducted in the Murnick group, apart from understanding the technical details concerning the instrumentation. Experiments described in Mu2008 (Murnick et al. 2008) and elsewhere (Ilkmen 2009; Murnick et al. 2010) were repeated numerous times, using pure CO_2 and CO_2 mixed in different buffer gases (N_2 and Air), but none produced any reproducible results and conclusive evidence. Because of these severe reproducibility problems we encountered during the stay, it was extremely difficult to ascertain and conclude the feasibility of ICOGS. This led us to doubt the truthfulness of the previously published data and hence we decided to continue with the project in Groningen, with several modifications and careful evaluation criteria in mind.

Recently, the Salehpour group at Uppsala University have published their findings and reported their failure to reproduce the claim published in Mu2008 (Eilers et al. 2013; Persson et al. 2013; Persson and Salehpour 2015). The authors have extensively tested their ICOGS system in the ^{14}C concentration range of 29-970 percent of Modern Carbon (pMC) (Persson and Salehpour), so up to about tenfold the ^{14}C concentration in modern organic material. Several improvements in the excitation and detection methods were made but nevertheless, none of the experiments supported the claimed sensitivities of Mu2008 (Persson et al. 2014a; Persson et al. 2014b; Persson and Salehpour 2015).

Here we show results obtained using CO_2 samples for a very wide range of the $^{14}CO_2/^{12}CO_2$ ratio, from 10^{-15} to 10^{-3}. Initially all experiments were performed with CO_2 containing depleted levels of radiocarbon ($^{14}CO_2/^{12}CO_2 \leq 10^{-15}$) and CO_2 containing natural levels of radiocarbon ($^{14}CO_2/^{12}CO_2 \approx 10^{-12}$). Experiments were repeated numerous times, and under different conditions, but no obvious difference in OptoGalvanic Signal (OGS) from the two CO_2 samples was observed. Hence, CO_2 samples containing levels of radiocarbon elevated by many orders of

magnitude ($^{14}CO_2/^{12}CO_2 \approx 10^{-11}$ - 10^{-3}) were later prepared in-house to investigate the concentration range where a clear signal arising from radiocarbon could be detected.

2.2 Experimental setup

The ICOGS setup at Groningen (pictures shown in Figures 1 and 2 of Appendix II) is similar to the setup at Rutgers with some distinct modifications. As described in Mu2008 and elsewhere(Murnick et al. 2008; Ilkmen 2009), the setup at Rutgers consisted of a sealed reference cell positioned outside the laser cavity with highly elevated $^{14}CO_2$ concentration (1-10% $^{14}CO_2/^{12}CO_2$), and a sample cell that was placed inside the laser cavity. In contrast to the Rutgers setup, we placed both the sample and the reference cell inside the laser cavity. The reference cell was also a flow-through cell, identical to the sample cell, and was filled with contemporary reference CO_2 instead of enriched CO_2. The positioning of the reference cell inside the laser cavity was motivated by the principle of identical treatment of sample and reference materials, as is a common procedure for stable isotope measurements. This principle leads in general to higher measurement precision and reproducibility for relative measurement methods. In addition, it prevented the presence and use of extremely enriched $^{14}CO_2$ samples in the vicinity of our AMS ^{14}C dating facility.

The schematic of our ICOGS setup is shown in **Figure 1**. The setup consists of two isotopic CO_2 lasers; a $^{12}CO_2$ laser (Merit-SZ, Access Laser Co., USA) and a customized $^{14}CO_2$ laser (Lasy-20GZ, Access Laser Co., USA) with emission lines between 10.532-10.741 μm and 11.258-11.891 μm, respectively. A list of all the laser lines emitted by the $^{14}CO_2$ laser is shown in **Table 1** (Freed 1995). With help from the manufacturer, the output coupler (1%) mounting block (OCMB in Figure 1) of the $^{14}CO_2$ laser was moved away from the gain medium, such that both the cells could be accommodated inside the extended cavity. The cells have a cross-shaped geometry (64 mm × 38 mm, OD = 15 mm, wall thickness = 2 mm) and are constructed from fused silica. For a clearer picture, one representative cell is shown in the inset of Figure 1 with a blue background. Two copper tapes (5 mm wide) are placed 25 mm apart along the long axis and are connected to the RF

excitation and detection electronics through coaxial cables. The RF excitation and detection electronics were based on the design of May et al. (May and May 1986). They were obtained from the Murnick Group, and are similar to the ones used at Rutgers. Using a custom built cell-mount, the two cells are precisely positioned inside the laser cavity. The ZnSe (II-VI Incorporated) windows along the $^{14}CO_2$ laser axis are connected to the cell through the cell mount. Additional mounts with the sample inlet/exit ports were used to connect the ZnSe windows to the transverse arms of the cells through which the $^{12}CO_2$ laser beam was directed into the two cells. The ZnSe windows were mounted parallel to each other, and no significant power loss was observed, so a Brewster angled window as in the Rutgers setup was deemed unnecessary. Two power meters (30A-BB-18 for the $^{12}CO_2$ laser and 3A for the $^{14}CO_2$ laser, Ophir Photonics) were installed to continuously monitor the laser power. A spectrum analyzer (16E-C14, Macken Instruments Inc., USA) was used to verify the laser wavelength whenever the $^{14}CO_2$ laser was tuned to a desired wavelength. Since it was extremely difficult to spot the laser beam on the spectrum analyzer's infrared sensitive phosphor screen when the laser power was below 70 mW, an infrared camera (FLIR, i7) was often used to detect the diffracted beam on the screen. Gold-coated mirrors (Part number 43-733, Edmund Optics) were used to steer the beam through the cells to the power meters. Two mass flow controllers (πMFC-LP P2A, MKS) were used to introduce CO_2 into each cell and two pressure controllers (Model-640B, MKS) were used upstream to regulate the cell pressure. The flow rates and pressures explored were in the range of 0.2-0.5 sccm (standard cubic centimeters per minute) and 100-1200 Pa, respectively.

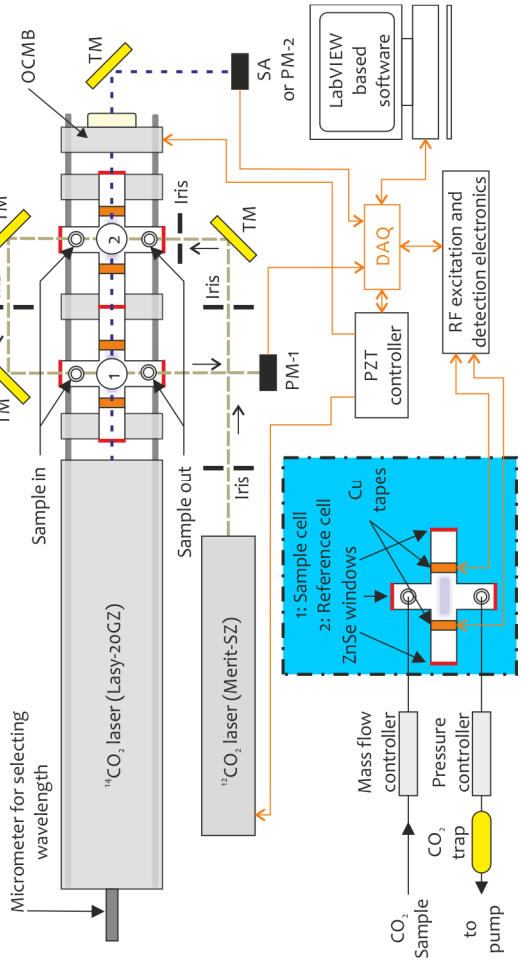

Figure 1: Schematic diagram showing the ICOGS setup at the University of Groningen. The setup consists of two isotopic CO_2 lasers, two sample cells, beam steering optics, a spectrum analyzer and two power meters. The sample and reference cell are both located inside the $^{14}CO_2$ laser cavity. The two copper electrodes are placed 2.5 cm apart (shown in the inset with blue background) and are connected to the RF excitation and detection electronics. The other components indicated with abbreviations are as follows: TM Turning Mirror; OCMB Output Coupler Mounting Block; PM Power Meter; SA Spectrum Analyzer; PZT Piezoelectric Transducer; DAQ Data Acquisition and Control; RF Radio Frequency. The laser beams are shown with dashed lines and the data handling with solid lines.

Line	Wavenumber (cm^{-1})	Wavelength (μm)	Frequency (MHz)
P(30)	841.00066805	11.8906	25212565.7454
P(28)	842.78929784	11.8654	25266187.5176
P(26)	844.56171722	11.8405	25319323.3138
P(24)	846.31793897	11.8159	25371973.5173
P(22)	848.05797276	11.7916	25424138.4180
P(20)	849.78182521	11.7677	25475818.2143
P(18)	851.48949996	11.7441	25527013.0154
P(16)	853.18099777	11.7208	25577722.8440
P(14)	854.85631653	11.6979	25627947.6369
P(12)	856.51545136	11.6752	25677687.2478
P(10)	858.15839460	11.6529	25726941.4470
P(8)	859.78513592	11.6308	25775709.9249
R(8)	872.95574563	11.4553	26170554.8708
R(10)	874.42754754	11.4361	26214678.3820
R(12)	875.88287985	11.4171	26258308.1470
R(14)	877.32170194	11.3983	26301442.9481
R(16)	878.74397043	11.3799	26344081.4848
R(18)	880.14963923	11.3617	26386222.3753
R(20)	881.53865943	11.3438	26427864.1533
R(22)	882.91097929	11.3262	26469005.2677
R(24)	884.26654418	11.3088	26509644.0807
R(26)	885.60529650	11.2917	26549778.8656
R(28)	886.92717564	11.2749	26589407.8052
R(30)	888.23211790	11.2583	26628528.9900

Table 1: List of all the laser lines emitted by the $^{14}CO_2$ laser (LASY-20GZ)[18]. Optogalvanic response of CO_2 containing depleted levels of ^{14}C and CO_2 containing natural levels of ^{14}C were evaluated at all lines the laser emitted. More extensive experiments were performed between P(20) and P(28).

2.3 Samples used

Based on our experience with the ICOGS setup at Rutgers, we were more inclined towards testing our ICOGS setup with pure CO_2. This was mostly because of the severe reproducibility issues we faced at Rutgers with the CO_2-in-N_2 based system in almost all experimental conditions we worked with, and also that the pure CO_2

based system was relatively less explored. Taking advantage of the in-house AMS facility at Groningen, we could use several well-characterized AMS local reference gases, in the whole natural range. To establish the optimal experimental conditions required for the best signal discrimination, we worked with a CO_2 gas highly depleted in ^{14}C ($^{14}C/^{12}C$ < 0.1 pMC), called "dead" from now on, and a CO_2 gas with a contemporary ^{14}C concentration ($^{14}C/^{12}C$ ≈ 108.8 pMC), called "modern" from now on. According to the claims from Mu2008 it should have been easy to see clear differences in the optogalvanic response at the P(20) transition (11.7677 μm) from the two gases with ^{14}C concentrations ≈3 orders of magnitude apart. Over a period of more than a year, many attempts were made to reproduce the claims, but none yielded evidence of unambiguous radiocarbon detection. During the same period, Persson et al. (Persson et al. 2013), also published their findings and questioned the validity of ICOGS, which also supported our findings. We then suspected that the actual detection limit achievable was much above the claimed detection limits. Hence, we decided to prepare a series of CO_2 local reference gases containing elevated levels of $^{14}CO_2$. A 0.5% $^{14}CO_2/CO_2$ sample was ordered from ViTrax Radiochemicals, USA to prepare these local reference gases (listed in **Table 2**). The 0.5% $^{14}CO_2/CO_2$ was diluted in steps with dead CO_2 to prepare a series of nine local reference gases ($^{14}CO_2/CO_2 \approx 10^{-3}$ to 10^{-11}) with very similar $\delta^{13}C$ values. To avoid any additional contribution to the OGS arising from the variations in the ^{13}C concentration, we diluted the nine samples with a single gas, the dead CO_2. To ensure the correctness of this dilution procedure, the last sample in the series containing the lowest amount of radiocarbon, namely one order of magnitude higher than contemporary based on the dilution scheme, was analyzed at the Groningen AMS facility. For obvious reasons of contamination in the AMS facility, other samples in the series containing 100 - 1 billion times contemporary radiocarbon concentrations were not measured. The activities of these enriched samples were then calculated, based on knowledge of the dilution ratio and the activity of the last sample, as determined by the AMS measurement. The AMS measurement of the last sample yielded $^{14}C/^{12}C \approx 9.5\times10^{-12}$ (or a normalized activity of 951.1 ± 2.3 % to be exact), which matched the targeted value within the concentration uncertainty of the original 0.5% sample, thereby demonstrating the

correctness of our dilution process (the results imply that the 0.5% $^{14}CO_2/CO_2$ sample in fact had a $^{14}CO_2/CO_2$ ratio of 0.47%). The $\delta^{13}C$ value of the original $^{14}CO_2$ gas is unknown, but according to the supplier it is in the natural range. This means that due to the high level of dilution of the samples, the $\delta^{13}C$ value for all except perhaps the first are virtual identical to that of the dilution gas.

Sample	Intended ($^{14}CO_2/^{12}CO_2$)	Calculated ($^{14}CO_2/^{12}CO_2$)
1	1.01×10^{-3}	9.57×10^{-4}
2	1.01×10^{-4}	9.56×10^{-5}
3	1.01×10^{-5}	9.57×10^{-6}
4	1.01×10^{-6}	9.55×10^{-7}
5	1.01×10^{-7}	9.52×10^{-8}
6	1.01×10^{-8}	9.54×10^{-9}
7	1.01×10^{-9}	9.55×10^{-10}
8	1.01×10^{-10}	9.53×10^{-11}
9	1.01×10^{-11}	**9.50×10^{-12} ***

Table 2: Summary of the samples enriched in radiocarbon prepared by diluting commercially available 0.5% $^{14}CO_2/CO_2$ with CO_2 highly depleted in radiocarbon. The $^{14}C/^{12}C$ value for the last sample in the series was determined by AMS measurement at Groningen (indicated by *). The $\delta^{13}C$ value for all except perhaps the first (see text) are virtually identical to that of the dilution gas, which has a $\delta^{13}C$ value of -3.4 ‰.

2.4 Results and discussions

As mentioned earlier, ICOGS for radiocarbon detection was presented with several attractive features, one of the most appealing being the ability to perform measurements on pure CO_2 in both flow and batch mode, depending on the sample size. To optimize the experimental parameters of ICOGS, all the initial experiments were performed with both dead and modern CO_2 in a continuous flow mode. Since unambiguous detection of radiocarbon in the range of dead to modern, with a pure CO_2 based system, was not achieved even after many attempts, we decided to reexamine the claimed detection limits. This was only possible if several CO_2 samples containing different and elevated concentrations of $^{14}CO_2$ would be introduced and the change in optogalvanic signal as a function of

concentration derived. Hence, as described in the earlier section, nine enriched CO_2 samples were prepared in-house to investigate the achievable detection limits. These experiments with elevated radiocarbon concentration were performed only in batch mode because of reasons described later.

2.4.1 Continuous-flow mode measurement

Several different reactions take place inside a CO_2 glow discharge(Williams and Smith 2000; Okil 2004; Spencer and Gallimore 2010), the most important being the dissociation of CO_2 to CO. Since different gases influence the optogalvanic response of the analyte gas in different ways, by affecting the rate of ionization, it is very important to have a consistent gas mixture. Continuous-flow mode measurements ensure that the gas inside the discharge is always refreshed and thus one would avoid the accumulation of dissociated product that may influence the optogalvanic response in undesirable ways. Hence flow mode experiments became the very obvious choice to probe the ^{14}C detection capabilities of ICOGS. A multitude of different pressure and flow ranges were examined to document the optogalvanic response and the corresponding signal-to-noise ratio. The OptoGalvanic Signal (OGS) for both the dead and modern CO_2 was investigated at almost all $^{14}CO_2$ laser emission lines mentioned in **Table 1** which includes R(8)-R(30) and P(10)-P(30). The largest OGS was always achieved at the resonant P(20) transition and this transition was also used extensively by the Murnick group(Murnick et al. 2008; Ilkmen 2009), hence this transition was used with the continuous flow through experiments. A typical example of those many experiments performed to see the optogalvanic response of CO_2 with different radiocarbon concentration is shown in **Figure 2**. During this experiment, pure CO_2 was continuously flushed through the system at a flow rate of 0.2 sccm with a pressure of 800 Pa. The $^{14}CO_2$ and the $^{12}CO_2$ lasers were electronically chopped at a frequency of 131 Hz and 97 Hz respectively. By applying a Fast Fourier Transformation (FFT) to the resultant optogalvanic waveform obtained from each cell, the signal amplitudes at the two fundamental chopping frequencies are calculated. These amplitude signals from the sample and reference cells

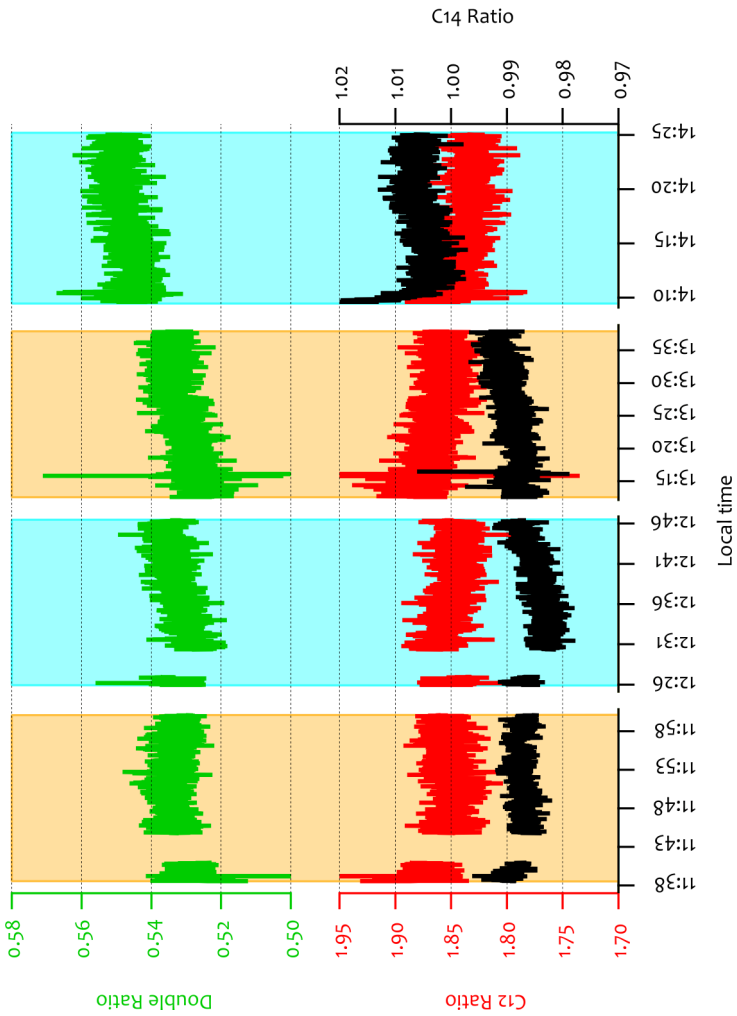

Figure 2: A data set showing continuous measurement of CO_2 through the reference and the sample cell. The C12 and the C14 ratios, shown in the lower part of the figure, are represented by the red line and black line, respectively. The green line shows the corresponding double ratio in the upper half of the figure. The orange background indicates the ratios when identical gas, dead CO_2, was introduced in both cells. Indicated with blue backgrounds are the ratios when different gases, dead CO_2 in the reference cell and modern CO_2 in the sample cell, were introduced. No significant difference in the double ratio is observed.

corresponding to the $^{14}CO_2$ and $^{12}CO_2$ laser chopping are called $^{14}C_{Sam}$,$^{14}C_{ref}$ and $^{12}C_{Sam}$,$^{12}C_{ref}$ respectively. At 800 Pa, the OGS produced by the $^{14}CO_2$ laser chopping at the P(20) transition was more than 3 times higher than at 130 Pa, while the OGS produced by the $^{12}CO_2$ laser chopping was reduced by a factor of 2. As described in Mu2008 and elsewhere(Ilkmen 2009), the fluctuations arising from the laser can be eliminated by dividing the sample signal with the corresponding reference signal, producing the single ratios (C14 ratio = $^{14}C_{Sam}$ /$^{14}C_{ref}$; C12 ratio = $^{12}C_{Sam}$ /$^{12}C_{ref}$). To eliminate the discharge fluctuations, the two single ratios were then used to calculate the double ratio (i.e. ratio of ratios) [$^{14}C_{Sam}$ /$^{14}C_{ref}$]/[$^{12}C_{Sam}$ /$^{12}C_{ref}$], which is equivalent to [$^{14}C_{Sam}$ /$^{12}C_{Sam}$]/[$^{14}C_{ref}$ /$^{12}C_{ref}$]. This latter expression is identical to the double ratios that are commonly used in stable isotope analysis, and from which delta values are derived. In **Figure 2**, the C12 ratio (red line) and the C14 ratio (black line) are shown in the lower half of the plot. The corresponding double ratio (green line) is shown in the upper half of the plot. First, the reference and the sample cells were both filled with dead CO_2, shown with yellow background. The dead CO_2 from the sample cell was then evacuated and replaced with the modern CO_2, shown with blue background. This switching of the gas in the sample cell, while keeping the same gas in the reference cell, was performed multiple times. Differences in the optogalvanic response of gases containing varying concentrations of radiocarbon should have been clearly visible in this example, had the corresponding OGS been noticeably different. Through a series of similar experiments, with varying parameters e.g., pressure, flow, $^{14}CO_2$ laser chopping frequency etc., we noted again and again that our instrument was not capable of unambiguously differentiating modern from dead CO_2. On the other hand, we learned that small changes in pressure and flow had notable influence in the resultant signal, which could be misinterpreted as $^{14}CO_2$ signal if a careful evaluation and continuous monitoring of all parameters was not performed.

2.4.2 Batch mode measurement

From flow mode experiments described in the previous section it was clear that our instrument could not differentiate modern from dead CO_2. This made us believe

that the $^{14}CO_2$ sensitivity, based on the assumption of a degree of enhancement because of intracavity operation of ≈ 10^7, as in the case of Mu2008, was possibly not true with our system (or in fact not at all). It must be emphasized that, based on our experience with the ICOGS system described in Mu2008, an enhancement factor of ≈ 10^7, leading to high sensitivity, may be an exaggeration. Therefore we decided to carefully determine the true sensitivity of our ICOGS setup through experiments with CO_2 samples enriched in ^{14}C. Since CO_2 gases containing elevated levels (10^1 – 10^9 × natural abundance) of ^{14}C concentrations are unavailable commercially, we prepared these desired local reference gases with elevated levels of radiocarbon in-house. As a precautionary measure because of the possibility of ^{14}C contamination in the AMS facility, samples were prepared in an isotope laboratory located in a different building, a few hundred meters away from the AMS facility. For the same reason, the ICOGS laboratory, where the samples were used and stored after preparation, is also located far away from the AMS laboratory (albeit in the same building complex). Because of both the strict European regulation on release of radioactive material and limited sample size, the experiments with these samples were performed in batch mode. In contrast to the continuous flow measurements, the batch mode experiments were performed with only one cell. A one-cell measurement was preferred since it was practically impossible to identically tune the two discharges in batch mode. This would lead to a difference in the rate of dissociation of CO_2, indicated by difference in the rate of change of pressure in the cell. Since the OGS from the C-12 and the C-14 channels are non-linearly dependent on pressure, it would make the correction to the single and hence the double ratio complicated and error-prone. Therefore, to keep the analysis simple, we chose to use only one cell as it would allow us to investigate the initial levels of detection.

To prevent the enriched CO_2 from escaping into the laboratory, a trap containing Carbo-Sorb® was placed between the pressure controller and the vacuum pump. The Carbo-Sorb® adsorbent was later disposed according to the University of Groningen's radiochemical disposal procedure. Experimental conditions, between experiments, were kept as similar as possible in order to have a realistic

comparison. An example experiment showing the optogalvanic response of a CO_2 discharge, performed with Sample No. 1 ($^{14}C/^{12}C$ 9.57×10^{-4}, refer Table 1), at five different laser transitions is presented in **Figure 3**. CO_2 is introduced into the cell to a pressure of about 400 Pa. Once the pressure in the cell stabilized, the discharge was turned ON, which is characterized by a sharp, but small, rise in pressure. The laser was then tuned to a desired wavelength and allowed to stabilize, shown in white background. The length of the laser cavity was detuned by scanning a PZT placed on the output coupler. The selected voltage range (0-500 V) reveals one longitudinal mode, shown by a peak observed in the laser power, marked with gray background. The laser power was then stabilized on the maximum of the OGS, marked with yellow background. The DC offset associated with the discharge was determined by blocking the $^{14}CO_2$ laser, shown with orange background and is ≈ 0.4 mV in our case. To reduce the risk of contamination arising because of memory effects, the cell was evacuated for at least an hour before it was discharge cleaned with helium, shown with the pink background. This extra step of discharge cleaning was included in the cleaning procedure to remove the residual CO_2 from the glass surface (suggested by Prof. Daniel Murnick through personal communication), although the effectiveness was not verified. Following the helium discharge-cleaning step, the cell was evacuated again. This cleaning procedure was repeated every time before a new sample was introduced into the cell.

The objective with these one-cell experiments was to look for differences in the power normalized OGS as a function of the changing ^{14}C concentration in samples, and to do so at different laser transitions. OGS for the dead, modern and enriched CO_2 samples were measured in batch mode at the P(18)-P(30) range of $^{14}CO_2$ laser transitions listed in **Table 1**. The most extensive studies were performed between P(20)-P(28), such as illustrated in **Figure 3**. The most striking feature seen in **Figure 3** is the large OGS produced at the P(20) transition, which is not evident on any other laser transition we experimented with (mind the logarithmic vertical OGS axis in Figure 3). Unlike the other laser transitions, the peak optogalvanic signal at the P(20) transition is not located on the peak laser power, but on its shoulder. This feature indicated a possible coincidental resonance with

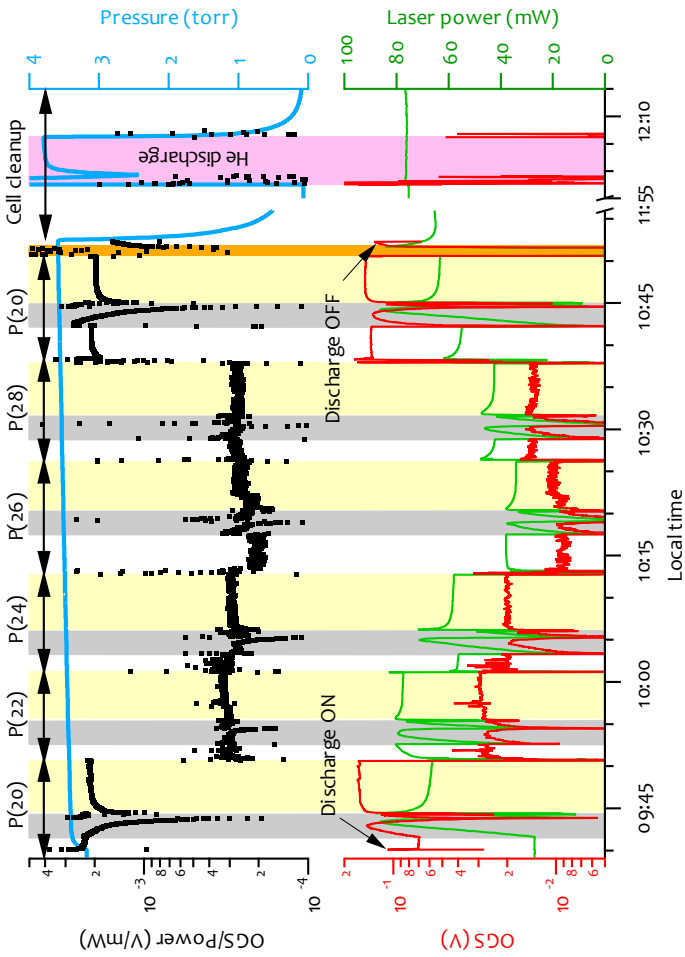

Figure 3: Experiment, performed in batch mode, showing the OGS of a pure CO_2 ($^{14}C/^{12}C \approx 0.1\%$) discharge at various $^{14}CO_2$ laser lines. A PZT scan to stabilize the OGS at the maximum, shown with gray background, is performed selecting the desired laser line. The laser is allowed to stabilize on the peak of the OGS for some time, shown with yellow background, before switching to, and stabilizing on, the next $^{14}CO_2$ laser line (white background). The OGS and the laser power are shown in the lower half of the graph. The power normalized OGS and the cell pressure are shown in the upper half of the graph. To reduce the memory effect, the cell is first evacuated, then discharge cleaned with helium, shown in pink background, and evacuated again before performing the next measurement. The DC offset on the OGS is determined by blocking the laser, shown with the orange background.

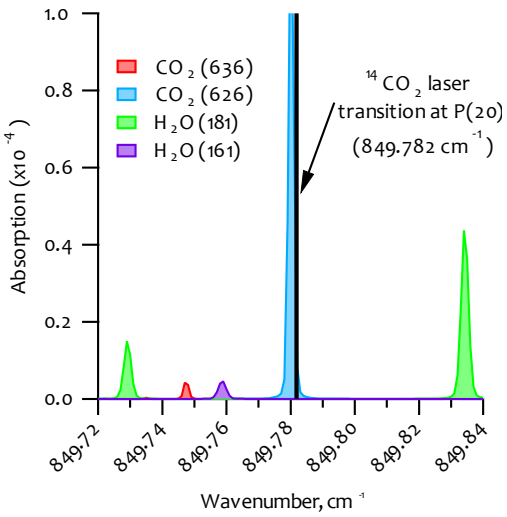

Figure 4: Simulation performed using HITRAN on the web (http://hitran.iao.ru/) to show the possible source of the enhanced OGS at the P(20) laser transition. An energetically high $^{12}C^{16}O_2$ transition is probably responsible for the large signal enhancements as seen in Figure 3. For the purpose of verification other molecules like $^{13}C^{16}O_2$, $H_2{}^{16}O$, and $H_2{}^{18}O$ have also been shown. For the different isotopologues, Air Force Geophysics Laboratory (AFGL) shorthand notations have been used (e.g., $^{16}O^{12}C^{16}O$ is represented as 626).

another, more abundant, interfering species in the discharge. From previous studies in the Murnick Group (Okil 2004), influence of water vapor leading to OGS enhancement was already known. It was thus predicted that water vapor contamination in the CO_2 samples might be the cause of the P(20) signal enhancement. We did a few tests to check the extent of signal enhancement by humidifying the samples. Results indicated that water vapor contamination in our system quenched the OGS instead of enhancing it. HITRAN simulations (performed at http://hitran.iao.ru/) then revealed the presence of an energetically high lying $^{12}C^{16}O_2$ transition ≈51 MHz from the P(20) laser transition, shown in **Figure 4**. It seems quite likely that this $^{12}C^{16}O_2$ transition accounts for the large intracavity OGS enhancement on the P(20) laser transition. This corruption of the OGS makes the P(20) transition unsuited for $^{14}CO_2$ detection in pure CO_2.

A summary of all the measurements made with six enriched working standards and the dead CO_2 are shown in **Figure 5a**. Every sample, shown in Figure 5a, was measured three consecutive times in the order of their increasing activity. The OGS corresponding to each sample is an average of the three measurements, and the error bars indicate 1σ standard deviation. The results indicate that there is no clear dependence of the OGS amplitude on the radiocarbon concentration. A few initial measurements with the highly ^{14}C enriched samples did, however, produce a noticeably higher OGS amplitude in the 10^{-4}-10^{-3} $^{14}C/^{12}C$ range. Similar to the detection sensitivities achieved by LARA, OGS at these ranges would be more realistic if there is no intracavity enhancement as claimed in Mu2008. Unfortunately, these results were not reproduced in the later set of measurements that contributed to Figure 5a. For all transitions (leaving the P(20) aside) the average OGS for dead CO_2 is higher than for all higher ^{14}C level gases. However, for three out of four transitions this is no significant effect: the large error bars for P(22) and P(24) are the result of considerable scatter of the individual measurements. Furthermore, from extensive tests described above, we know that there is no significant OGS difference between the dead and modern (10^{-12}) levels. Figure 5b shows an example of six independent batch mode measurements performed with the dead (D) and modern (M) CO_2 (3 each) at different laser lines. This example demonstrates the large variability in the OGS that frequently leads to substantial spread. It also shows that the difference in the OGS of dead and 10 × modern sample (10^{-11}), shown in Figure 5a, is not real and that the signals are all within the variability of the OGS. This large variability in the OGS leading to unsuccessful discrimination of OGS produced by CO_2 containing different levels of ^{14}C was also demonstrated by Persson et al., at Uppsala University (Persson et al. 2013). With this extra information, it is clear that these higher points at the lowest ^{14}C level are coincidental.

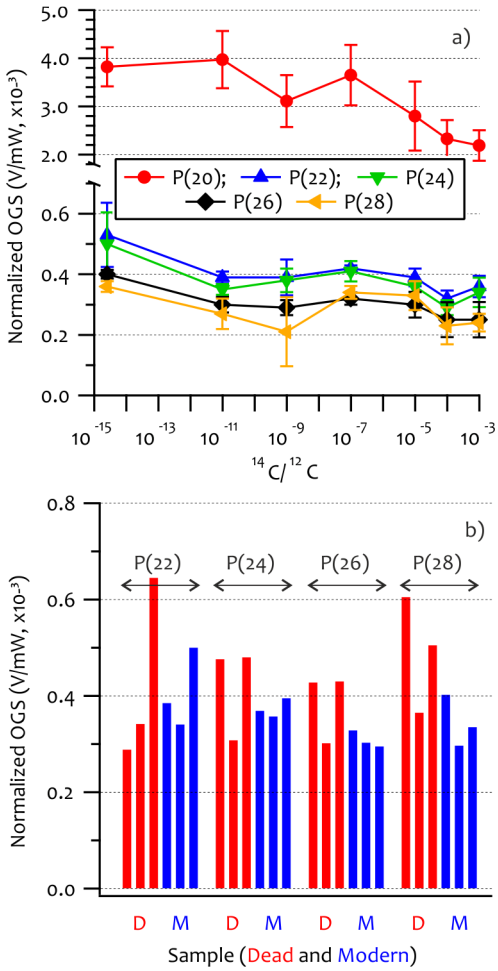

Figure 5: a) Summary of a series of twenty-one experiments performed with dead CO_2 and six enriched CO_2 samples in the sequence of their increasing activity. Each sample was measured three consecutive times; one such experiment is shown in Figure 4. The vertical error bars indicate 1σ standard deviation. No evidence showing dependence of the amplitude of OGS to the radiocarbon concentration was observed. **b)** Results showing OGS of a set of six independent batch-mode measurements of dead and modern CO_2 demonstrating the large variability in the OGS. These results demonstrate that the apparent difference in the dead and 10 × modern CO_2 OGS at P(22)–P(28), shown in a), are insignificant as they are within the detection variability.

2.5 Conclusions

Motivated by the claimed potentials of ICOGS described in Mu2008, at least four other research groups, including the University of Groningen, participated in developing ICOGS for various applications in collaboration with Rutgers. The construction of the ICOGS setup at Groningen was completed by mid-2012. Since then, extensive work has been done and a range of experimental strategies was employed with the goal to unambiguously detect radiocarbon signal in pure CO_2 samples. Because of repeated failures in the dead to modern range, we decided to also explore the range beyond the natural one, with CO_2 containing several-to-many orders of magnitude higher concentrations of radiocarbon, even though this concentration range was well beyond our area of interest. Even with these enriched CO_2 samples, we could not detect a clear OGS dependency on the radiocarbon concentration. Moreover, reproducing discharge conditions, which is another key parameter, was difficult and introduces the large variability observed in the signal. This problem of reproducibility, probably leading to false positive signal in the data presented in Mu2008 was suggested by the Uppsala group(Persson et al. 2013). From our extensive and detailed studies, we conclude that the level of detection is at the 10^{-3} level, to 10^{-4} at best. Further optimization would of course probably be feasible, but as the technique with even 10^{-5} level of detection would still be useless for our, and probably all, intended applications, we decided not to invest further time and resources.

From the results presented in the previous sections, we could not demonstrate ICOGS as a viable radiocarbon detection technique. Instead, through all our efforts as well as those of the group at Uppsala we have come as close as possible to proving that ICOGS is unsuited as a viable radiocarbon technique. Similar, unsuccessful results were also obtained at the Columbia University (through personal communications with Dr. Cantwell G. Carson). Even though there are some distinct differences in the setup, the RF excitation/detection electronics and our measurement/analysis scheme are very similar to the ones used by the Murnick group. Through our extensive experiments, we are very sure that the

results presented in Mu2008 are highly suspicious and for the purpose of scientific integrity must be withdrawn.

Of course, Optogalvanic Spectroscopy is a viable and proven trace gas detection technique. The LARA (Murnick and Peer 1994; Minoli et al. 1998; Cave et al. 1999; Van der Hulst et al. 1999; Savarino et al. 2000; Braden et al. 2001; Okil 2004; Murnick and Okil 2005) instrument is capable of measuring $^{13}CO_2/^{12}CO_2$ ratios in exhaled breath at a precision and accuracy level that makes it useful in clinical breath analysis applications. Based on that, we can estimate the level of detection of this, optimized flow-through system as $\geq 10^{-5}$, loosely based on a 10^{-3} (equivalent to 1 ‰ in $\delta^{13}C$ (Murnick and Okil 2005)) precision in detecting the 1.1% level of $^{13}CO_2$. The precision in the detection of a substantial signal is usually higher than the level of detection of a rare species, as in the former case signal averaging is used. For a fully optimized IntraCavity Optogalvanic System, the detection limit may even be better still, thanks to the higher intracavity laser power ($\approx \times 100$). This, however, would only be feasible by using a flow-through system of CO_2 in Nitrogen, as this dilution in Nitrogen gas is known to enhance the OGS considerably (Okil 2004). Measurement of such a mixture, however, introduces additional uncertainty effects. Because of the complex nature of optogalvanic spectroscopy and poor understanding of the magnitude of OGS generation at different wavelength, it becomes very difficult to ascertain the limit of detection as is possible in the case of absorption spectroscopy. The batch-mode measurements using a single cell, and pure CO_2 do definitely have a worse level of detection, such that the 10^{-3} or 10^{-4} level we cautiously report above are quite realistic. The alleged intracavity enhancement term introduced in Mu2008 has not been proven so far, and has not been underpinned theoretically either. In this work, we have come as closely as possible to proving that the results claimed in Mu2008 are incorrect. Thus, AMS is still the best possible method for high-precision ^{14}C measurements at subcontemporary levels, especially for age determination (“dating”). However, several laser based spectroscopic methods for radiocarbon detection have recently been demonstrated (McCartt et al. ; Galli et al. 2011; Galli et al. 2013; Genoud et al. 2015). Although some of these methods realize ^{14}C detection limits below 10^{-13},

currently none of them can compete with AMS in that respect. Most of the methods are more suitable and, in fact, designed for pharmaceutical and other applications that make use of ^{14}C labeling.

2.6 References

Braden B, Gelbmann C, Dietrich CF, Caspary WF, Scholmerich J, Lock G. 2001. Qualitative and quantitative clinical evaluation of the laser-assisted ratio analyser for detection of Helicobacter pylori infection by C-13-urea breath tests. European Journal of Gastroenterology & Hepatology 13(7):807-10.

Cave DR, Veldhuyzen van Zanten S, Carter E, Halpern EF, Klein S, Prather C, Stolte M, Laine L. 1999. A multicentre evaluation of the laser assisted ratio analyser (LARA): a novel device for measurement of $^{13}CO_2$ in the ^{13}C-urea breath test for the detection of Helicobacter pylori infection. Alimentary Pharmacology & Therapeutics 13(6):747-52.

Eilers G, Persson A, Gustavsson C, Ryderfors L, Mukhtar E, Possnert G, Salehpour M. 2013. The Radiocarbon Intracavity Optogalvanic Spectroscopy Setup at Uppsala. Radiocarbon 55(3–4):237-50.

Freed C. 1995. 4 - CO_2 Isotope Lasers and Their Applications in Tunable Laser Spectroscopy. In: Duarte FJ, editor. Tunable Lasers Handbook. San Diego: Academic Press. p 63-165.

Galli I, Bartalini S, Borri S, Cancio P, Mazzotti D, De Natale P, Giusfredi G. 2011. Molecular Gas Sensing Below Parts Per Trillion: Radiocarbon-Dioxide Optical Detection. Physical Review Letters 107(27):270802.

Galli I, Bartalini S, Cancio P, De Natale P, Mazzotti D, Giusfredi G, Fedi ME, Mando PA. 2013. Optical detection of radiocarbon dioxide: First results and AMS intercomparison. Radiocarbon 55(2-3):213-23.

Genoud G, Vainio M, Phillips H, Dean J, Merimaa M. 2015. Radiocarbon dioxide detection based on cavity ring-down spectroscopy and a quantum cascade laser. Optics Letters 40(7):1342-5.

Ilkmen E. 2009. Intracavity Optogalvanic Spectroscopy for Radiocarbon Analysis with Attomole Sensitivity [Doctoral Thesis]. Newark: Rutgers, The State University of New Jersey.

Ilkmen E, Murnick DE. 2010. High sensitivity laboratory based C-14 analysis for drug discovery. Journal of Labelled Compounds & Radiopharmaceuticals 53(5-6):304-7.

May RD, May PH. 1986. Solid-state radio frequency oscillator for optogalvanic spectroscopy: Detection of nitric oxide using the 2-0 overtone transition. Review of Scientific Instruments 57(9):2242.

McCartt AD, Ognibene T, Bench G, Turteltaub K. 2015. Measurements of carbon-14 with cavity ring-down spectroscopy. Nuclear Instruments and Methods in Physics Research Section B: Beam Interactions with Materials and Atoms 361:277-80.

Minoli G, Prada A, Schuman R, Murnick D, Rigas B. 1998. A simplified urea breath test for the diagnosis of Helicobacter pylori infection using the LARA system. Journal of Clinical Gastroenterology 26(4):264-6.

Murnick D, Dogru O, Ilkmen E. 2010. C-14 analysis via intracavity optogalvanic spectroscopy. Nuclear Instruments & Methods in Physics Research Section B-Beam Interactions with Materials and Atoms 268(7-8):708-11.

Murnick DE, Peer BJ. 1994. Laser-based analysis of carbon-isotope ratios. Science 263(5149):945-7.

Murnick DE, Schuman R, Rigas B. 1995. C-13 Urea breath test with the LARA$^{(TM)}$ system. Gastroenterology 108(4):A172-A.

Murnick DE, Okil JO. 2005. Use of the optogalvanic effect (OGE) for isotope ratio spectrometry of $^{13}CO_2$ and $^{14}CO_2$. Isotopes in Environmental and Health Studies 41(4):363-71.

Murnick DE, Dogru O, Ilkmen E. 2007. Laser based ^{14}C counting, an alternative to AMS in biological studies. Nuclear Instruments and Methods in Physics Research Section B: Beam Interactions with Materials and Atoms 259(1):786-9.

Murnick DE, Dogru O, Ilkmen E. 2008. Intracavity optogalvanic spectroscopy. An analytical technique for C-14 analysis with subattomole sensitivity. Analytical Chemistry 80(13):4820-4.

Okil JO. 2004. Optogalvanic Spectroscopy for Atmospheric Carbon-dioxide Concentration and Isotopic Ratio Measurement [Doctoral Thesis]. Newark: Rutgers, The State University of New Jersey.

Persson A, Eilers G, Ryderfors L, Mukhtar E, Possnert G, Salehpour M. 2013. Evaluation of Intracavity Optogalvanic Spectroscopy for Radiocarbon Measurements. Analytical Chemistry 85(14):6790-8.

Persson A, Berglund M, Salehpour M. 2014a. Improved optogalvanic detection with voltage biased Langmuir probes. Journal of Applied Physics 116(24):243301.

Persson A, Berglund M, Thornell G, Possnert G, Salehpour M. 2014b. Stripline split-ring resonator with integrated optogalvanic sample cell. Laser Physics Letters 11(4):045701.

Persson A, Salehpour M. 2015. Intracavity optogalvanic spectroscopy: Is there any evidence of a radiocarbon signal? Nuclear Instruments and Methods in Physics Research Section B: Beam Interactions with Materials and Atoms Article in Press.

Savarino V, Landi F, Dulbecco P, Ricci C, Tessieri L, Biagini R, Gatta L, Miglioli M, Celle G, Vaira D. 2000. Isotope ratio mass spectrometry (IRMS) versus laser-assisted ratio analyzer (LARA): a comparative study using two doses of. Digestive diseases and sciences 45(11):2168-74.

Spencer LF, Gallimore AD. 2010. Efficiency of CO_2 Dissociation in a Radio-Frequency Discharge. Plasma Chemistry and Plasma Processing 31(1):79-89.

Van der Hulst RWM, Lamouliatte H, Megraud F, Pounder RE, Stoltes M, Vaira D, Williams M, Tytgat GNJ. 1999. Laser assisted ratio analyser C-13-urea breath testing, for the detection of H-pylori: a prospective diagnostic European multicentre study. Alimentary Pharmacology & Therapeutics 13(9):1171-7.

Williams GCR, Smith ALS. 2000. Plasma chemistry of RF discharges in CO_2 laser gas mixtures. Journal of Physics D: Applied Physics 18(3):335-46.

Chapter 3:

Contamination on AMS sample targets by modern carbon is inevitable

This chapter has been published as:

***Paul, D.**, Been, H. A., Aerts-Bijma, A. T., and Meijer, H. A. J., Radiocarbon, 2016, DOI: 10.1017/RDC.2016.9.*

Cover image shows the storage test containers used during this study.

Abstract

AMS measurements of the radiocarbon content in very old samples are often challenging and carry large relative uncertainties due to possible contaminations acquired during the preparation and storage steps. In case of such old samples, the natural surrounding levels of radiocarbon from gases in the atmosphere, which may well be the source of contamination among others, are 2-3 orders of magnitude higher than the samples themselves. Hence, serious efforts are taken during the preparation steps to have the samples pristine till measurements are performed. As samples often have to be temporarily stored until AMS measurements can be performed, storage conditions also become extremely crucial. Here we describe an assessment of this process of contamination in background AMS samples. Samples, both as pressed graphite (on AMS targets) and graphite powder, were stored in various storage conditions (CO_2 spiked air) to investigate the extent of contamination. The experiments clearly show that the pressed targets are more vulnerable to contamination than the unpressed graphite. Experiments conducted with enriched CO_2 spiked laboratory air also reveal that the contaminating carbon is not only limited to the target surface but also penetrates into the matrix. A combination of measurements on understanding the chemical nature of the graphitization product, combined with long-available knowledge on "adventitious carbon" from the surface science community, brought us to the conclusion that contamination is to a certain extent inevitable. However, it can be minimized, and for the rest should be dealt with by sputter-cleaning the samples individually before the actual measurement.

3.1 Introduction

Contamination is generally a serious concern for any high sensitivity measurement technique, and this is certainly the case for radiocarbon (^{14}C) detection by Accelerator Mass Spectrometry (AMS). For ^{14}C measurements by AMS, the samples are, mostly after pretreatment, combusted to CO_2, which is then reduced to graphite. The produced solid graphite samples are then pressed in sample holders ("targets" or "cathodes") and are subsequently measured in the AMS by sputtering the surface with Cs ions. The released C^- ions are then used for the actual measurement. Due to the number of steps involved, from sample preparation to measurement, utmost care and attention is required to reduce the contamination accumulated over the whole process. For larger samples (1-2 mgC), with near-contemporary radiocarbon concentrations, contaminations accumulated after careful preparation may be barely discernible. On the contrary, for background materials and small(er) samples (1-200 µgC), measurements can be seriously affected by the inevitable contaminants accumulated during the preparation steps (Kirner, Taylor et al. 1995; Brown and Southon 1997; Santos, Southon et al. 2007; de Rooij, van der Plicht et al. 2010). This is one of the reasons why radiocarbon dating beyond 50000 years is so challenging. The "age", that is the ^{14}C content of the contaminating material matters: by the very nature of the radiocarbon dating technique, contamination of (sub)-modern samples by old carbon (for example from synthetic chemicals used in the preparation steps) only dilutes the sample, and the effects stay marginal. Contamination of old samples by modern carbon (for example atmospheric CO_2 from the laboratory), on the other hand can have massive impact. These effects are summarized in Figure 1, which shows the influence of modern carbon contamination (MCC, ^{14}C activity = 100 pMC: percent Modern Carbon) and dead carbon contamination (DCC, 0 pMC) on age determination. As shown in Figure 1a, MCC affects the age determination of older samples close to background, whereas DCC affects near-contemporary samples, as shown in Figure 1b. Contamination of a background (42500 years old) and a near-contemporary (105 years old) sample with a fixed mass of modern or

dead contaminants (1, 4, 7, and 10 µg C) with respect to a change in sample size is shown in Figures 1c & d.

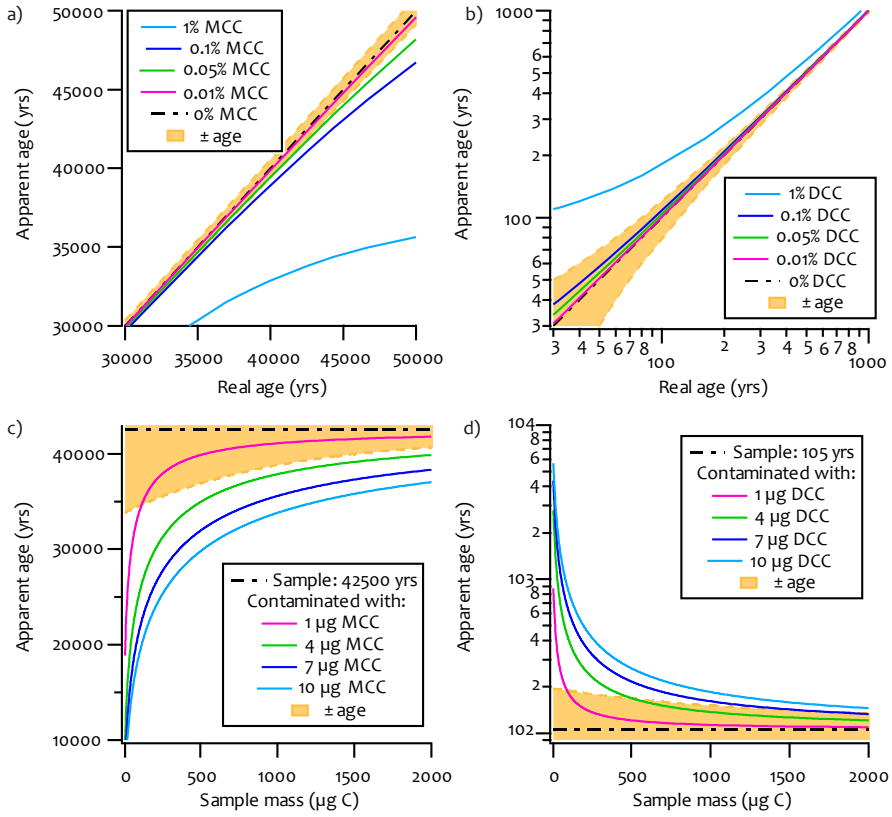

Figure 1: Plots illustrating the impact of modern carbon contamination (MCC) and dead carbon contamination (DCC) on age determination. a) Impact of MCC on age determination. b) Impact of DCC on age determination (for clarity shown with log-log axes). c) Impact of MCC on age determination of a background sample (42500 years) with respect to sample size. d) Impact of DCC on age determination of a near-contemporary sample (105 years) with respect to sample size. Typical uncertainties in age determination as performed in Groningen are shown with orange background. Modern carbon contaminations have the largest effects on samples containing close-to background levels of radiocarbon and on very small samples.

The uncertainties in age determination, shown with orange background, are the typical uncertainties at the Groningen AMS facility, based on many years of

operation. Thus, Figure 1 aims to illustrate that the contamination arising solely from DCC affects a very narrow range of sample age, i.e., near contemporary, whereas contamination arising solely from MCC affects a far-wider range of sample age especially near background. In reality, of course, the contamination is a combination of both MCC and DCC, where the extent of contamination from each component may vary depending on the precautionary measures adopted with the sample preparation. Although understanding the source and mechanism of contamination through DCC is important, it is of less concern for near-background measurements. In this chapter we concentrate on near-background samples, and thus performed experiments to understand the possible sources of MCC.

When performing an AMS measurement, a sample is measured for a substantial time period to reduce the measurement uncertainties. Depending on the type of ion source in use, it is either sputtered at a single position or at multiple positions on the target. At the Centre for Isotope Research (CIO), Groningen, we perform measurements at eight different positions on the target. A measurement at each position is performed for 30 s, before moving to the next position. Such a 30s measurement is referred to as a "block". Each position on the target is measured ten times, thus producing a total of eighty blocks with a total measurement time of 40 minutes.

During the measurements of very old samples and background material, the initial measurements always yield higher radiocarbon counts that eventually decline, after a few blocks of measurements, to lower and stable values. The higher values during the initial measurements, if not removed, invariably influence the age determination. To reduce the undesirable influence from the initial blocks, we perform a so-called "cleaning run" of eight blocks of only 10 s each, before performing the actual eighty-block measurement. This cleaning run is performed for a whole "batch" of up to 58 samples, before starting the actual measurements. This means that the time between cleaning run and actual measurement varies from ≈ 2 hours to more than 40 hours from the first to the last sample in the batch. This approach with the cleaning run step preceding the actual measurements has additional advantages apart from cleaning the surface: it provides adequate time

for source stabilization and also provides a quick overview of the sample quality in the whole batch. Still, in the light of the findings of this work, we are seriously considering to change our cleaning approach.

The initial higher counts during the course of measurement indicate the presence of a carbonaceous layer with higher radiocarbon content on top of the background sample material. We have been investigating this phenomenon for some years now and here we describe the understandings we gained over these years.

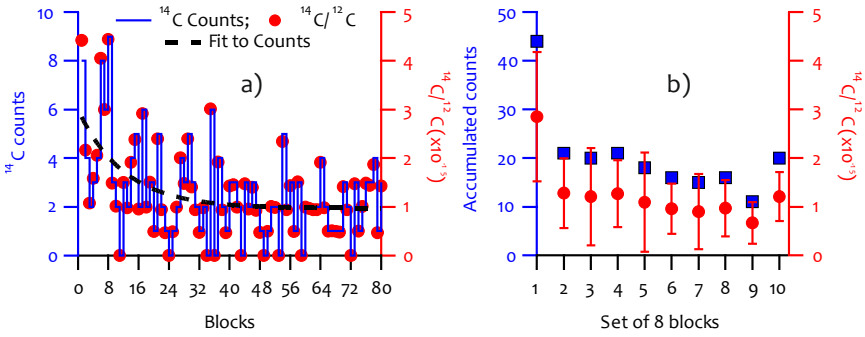

Figure 2: Data showing a typical background target measurement. a) The ^{14}C counts are shown with solid blue line, the corresponding $^{14}C/^{12}C$ with solid red circles and an exponential fit to the counts with dashed line. b) Counts accumulated in ten consecutive sets of 8 blocks, shown with blue squares, and the corresponding $^{14}C/^{12}C$ averages, shown with red circles (error bars representing 1σ standard deviation). Higher counts are observed during the initial part of the measurement due to carbonaceous contaminants on the surface of the target. As the measurement proceeds, cleaner surface is exposed, indicated by the reduced number of counts representative of the background material.

The phenomenon of surface contamination we observe is illustrated in Figure 2, which shows a typical background sample measurement. The target was pressed and left in open air for one day before it was measured. In Figure 2a, the ^{14}C counts are shown with a solid blue line, the corresponding $^{14}C/^{12}C$ ratio with solid red circles and an exponential fit to the counts with a dashed line. In Figure 2b the accumulated counts in the ten consecutive sets of eight blocks (blue squares) and their corresponding average $^{14}C/^{12}C$ ratios (red circles) are shown. Due to

contaminants on the surface of the target, the count rates observed during the initial parts of the measurement are higher than later in the measurement, where the average count rate gradually decays to lower values. It appears that the contamination causing this elevated count rate generally disappears in the second–third set of 8 blocks, so when each position in the target has experienced ≈ two times 30 s of sputtering by the Cs ions.

In a quest to understand the source of the surface contamination that leads to these initial higher counts, several storage tests were performed. During these tests, samples were exposed to various ^{14}C contamination sources in a controlled environment. The possible carbon containing molecules for such a contamination from air are CO_2, CH_4, CO and several other volatile organic compounds (VOC), partly already present in the atmosphere and partly from solvents used in the laboratory. CO_2 is by far the largest C-containing fraction (with modern levels of ^{14}C) in laboratory air with concentrations typically between 400-1000 ppm, depending on the number of occupants at a given time. CH_4 is the second largest C-containing fraction in laboratory air (typically 2 ppm, so roughly two orders of magnitude lower than CO_2) followed by CO (typically 0.2 ppm). Other hydrocarbons present in typical laboratory air have even smaller concentrations. Therefore we decided to test the extent of sample contamination with samples stored in air spiked with CO_2. Following these storage tests we learned, to our surprise, that the pressed targets carried more contamination than the unpressed graphite powders. It was also revealed during these experiments that, while some storage conditions were worse than others, almost all storage conditions affected the pressed targets. The unpressed graphite powder was mostly unaffected, only storage in a ^{14}C enriched CO_2 environment lead to noticeable increase of the ^{14}C activity. A detailed description of these experiments is the main subject of this chapter, and they will be discussed below. Basically, we will describe the production of sample material, and its storage under varying CO_2-spiked laboratory air conditions, and the effects on the count rate, both for the initial and steady state phase of the measurement.

We learned recently that this process of surface contamination with a carbonaceous layer is not only a concern during AMS measurements, but also in the field of material sciences. In that field of research, it has been known for a long time that any clean surface (not necessarily Carbon), when exposed to air, is immediately coated with a thin layer of carbonaceous material. This process even occurs under high vacuum, although at a much lower rate, where the carbonaceous contaminants are believed to have originated from the surface of the vacuum tank. This carbonaceous layer produced on the clean surface is called Adventitious Carbon (Barr and Seal 1995; Miller, Biesinger et al. 2002; Piao and McIntyre 2002; Mangolini, McClimon et al. 2014), which will be referred to as AC hereafter. A complete understanding of the source of this persistent carbonaceous layer is highly debatable and not well understood, though several mechanisms have been proposed (Barr and Seal 1995; Miller, Biesinger et al. 2002).

3.2 Samples

Background graphite samples were prepared from Rommenhöller CO_2 [AGA, presently Linde gases], which serves as our laboratory background material of infinite age. The activity of the Rommenhöller CO_2 is 0.15 ± 0.04 pMC. As the Rommenhöller CO_2 itself is an extremely old material, the activity level we determine is a combination of a possible residual activity of Rommenhöller CO_2, and contaminating modern carbon accumulated along the preparation of this CO_2 to a graphite target. Correspondingly, from long–term measurements, its spread shows the variability in that contamination.

Such background CO_2 samples (≈ 2 mg C) were "graphitized" in the routine way, that is reduced to elemental carbon in the presence of H_2 (≈ 2.5 × partial pressure of CO_2) and Fe (≈ 2.0-2.5 mg) at 600 °C (Aerts-Bijma, Meijer et al. 1997). For the extensive tests described here, these samples were subsequently stored under various CO_2-spiked laboratory air conditions, typically for more than a week, either in the form of powder (as produced) or pressed on aluminum AMS targets. For every test, a set of five samples was prepared for each storage condition within the test. Custom designed leak-tight containers were used to store the samples in

controlled conditions, i.e. in a specific gas mixture. Samples stored in dry Argon (4.6) served as a control storage condition. The control samples were placed in a dry Argon atmosphere as soon as they were prepared or pressed with the least possible exposure time to laboratory air. Initial storage experiments, performed previously (under less well-defined circumstances), indicated that samples stored in an atmosphere with water vapor were contaminated the most (even in a wet, initially pure Argon atmosphere, which however, may have gotten contaminated by outside air due to leakages in the polycarbonate desiccator used for storage back then). Hence for the storage tests, background samples were stored in humidified laboratory air spiked with CO_2 samples (1-5 %) with different radiocarbon activity. The activities of the CO_2 samples used to spike the laboratory air were 0.27, 50, 108, and 980 pMC. The 980 pMC CO_2 was prepared in-house for IntraCavity OptoGalvanic Spectroscopy (ICOGS) experiments and has been described elsewhere (Paul and Meijer 2015).

3.3 Results

As discussed in the previous sections, the graphite samples were stored under various CO_2-spiked laboratory air conditions to investigate their effect on the level of acquired contamination. Figure 3 shows the extent of contamination acquired by sets of five pressed aluminum targets stored in three different storage conditions. Five background graphite targets were pressed and were immediately stored in a dry argon atmosphere. These samples were designated as controls and are shown with open green circles in the top plots. The next set of five pressed background targets were stored in humidified laboratory air spiked with 5% CO_2 with activity 0.27 ± 0.02 pMC, shown with blue triangles in the middle plots. Additionally, a set of another five background targets were stored in humidified laboratory air spiked with 5% ^{14}C-enriched CO_2 (≈ 980 pMC), shown with red diamonds in the bottom plots. Figure 3 a) shows the counts recorded during the course of measurement for each storage condition and b) shows the corresponding frequency distribution of the counts. As mentioned earlier, the surface contamination is prominently visible during the initial parts of the measurement with relatively more counts in the first ≈

16 blocks, which subsequently decays to fewer counts representing the bulk background material. It is quite noticeable that the targets stored in an Argon atmosphere show a lower number of counts during the initial part of the measurement than those stored under the other two storage conditions. Targets stored in humidified laboratory air containing spiked CO_2, depleted in ^{14}C (resultant ^{14}C activity ≈ 1 pMC), still showed an overall increase in the number of counts. As described in Miller et al., (2002), deposition of a carbonaceous layer on a clean Fe surface happens very fast. Furthermore, the carbonaceous layer thickness tends to saturate within a few minutes of exposure and prolonged storage doesn't significantly alter the layer thickness nor the chemical composition. This implies that significant uptake of atmospheric CO_2 can already occur in the short time between the moment the samples were pressed and brought to the storage container. At the time these experiments were performed, we were unaware of the fact that the uptake process is so fast and thus requires as rapid as possible transport of the pressed material to the storage container. The five control targets were first pressed and immediately stored, but after that ten targets were pressed sequentially, after which five targets were stored in storage condition 2 and the other five were stored in storage condition 3. This longer exposure time to laboratory air would explain why the samples stored in the depleted CO_2 atmosphere still showed higher activity than the control ones. The targets stored in humidified laboratory air containing 5% enriched CO_2 (980 pMC) were contaminated the most. This case shows that the contaminating carbon percolates very deep into the sample bulk: the counts numbers do not get back to the background level, not even for the last block measurement. This possibly indicates that the carbonaceous layer formation was not complete during the exposure to laboratory air and sufficient number of sites were still available for the enriched CO_2 to interact with. One other feature observed in all storage experiments was that the number of blocks that would produce zero ^{14}C that would produce zero ^{14}C counts would always decrease upon storage, again indicating the presence of contaminants in the sample matrix. The frequency distribution of the counts shows this effect, which even happens under the control storage conditions (which corroborates the occurrence of adventitious carbon, probably from wall absorption).

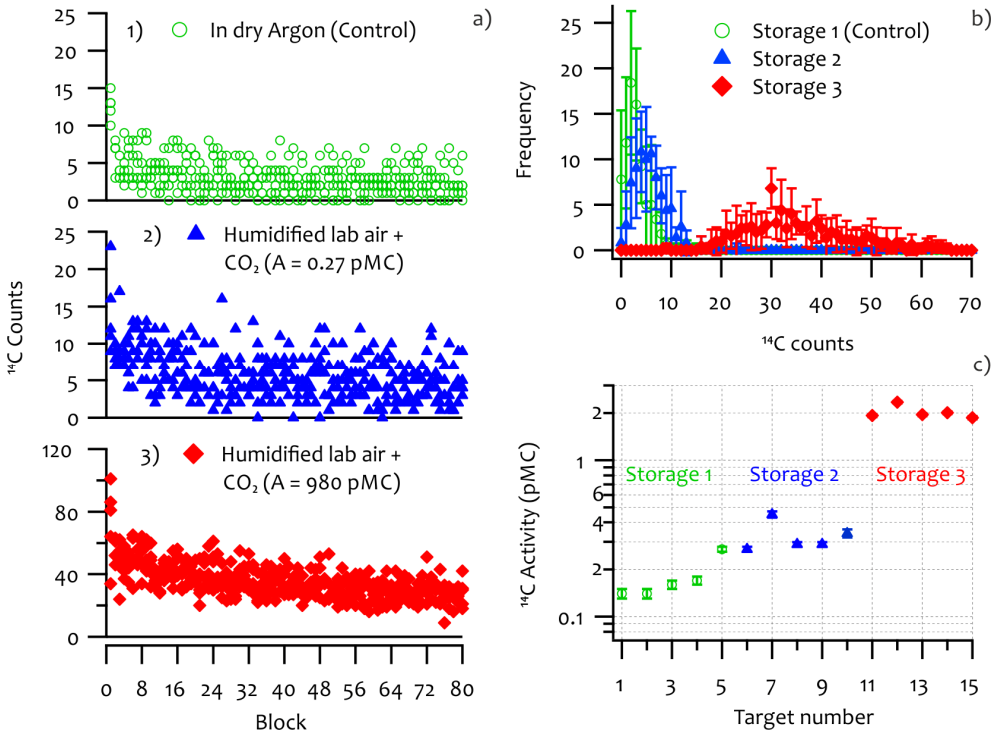

Figure 3: Storage test demonstrating the extent of acquired contamination in pressed targets on exposure to: Storage 1) Dry Argon, Storage 2) Humidified lab air + 5% CO_2 (0.27 ± 0.02 pMC) and Storage 3) Humidified lab air + 5% CO_2 (980 pMC). a) ^{14}C counts (raw data) detected during measurements of five pressed targets per storage condition. b) Average frequency distribution of the counts for five pressed targets per storage condition. c) Calculated ^{14}C activity (pMC) of the stored targets. For each storage condition, the results shown are the measurements of five samples that were pressed and stored for a period of 10 days before measurements were performed.

However, a large shift in the count distribution occurs as the extent of contamination increases. Remarkably though, a storage test performed earlier, with pressed graphite and graphite powder, with 5% CO_2 (760 pMC, and about threefold enriched in the abundances of the stable isotopes) in humidified lab air only showed a gain in contamination similar to the present ones stored in 5% CO_2 (0.27 pMC) in humidified lab air. The reason for this behavior is not understood; it was not investigated further since that storage test had not been performed as carefully as our new experiments, and there were even doubts at the time whether the spiked CO_2 was really enriched in ^{14}C. The newly prepared enriched CO_2 (980

pMC) showed enhanced acquired contamination in all the following storage tests, as expected. A summary of all the determined ^{14}C activities is shown in Figure 3c.

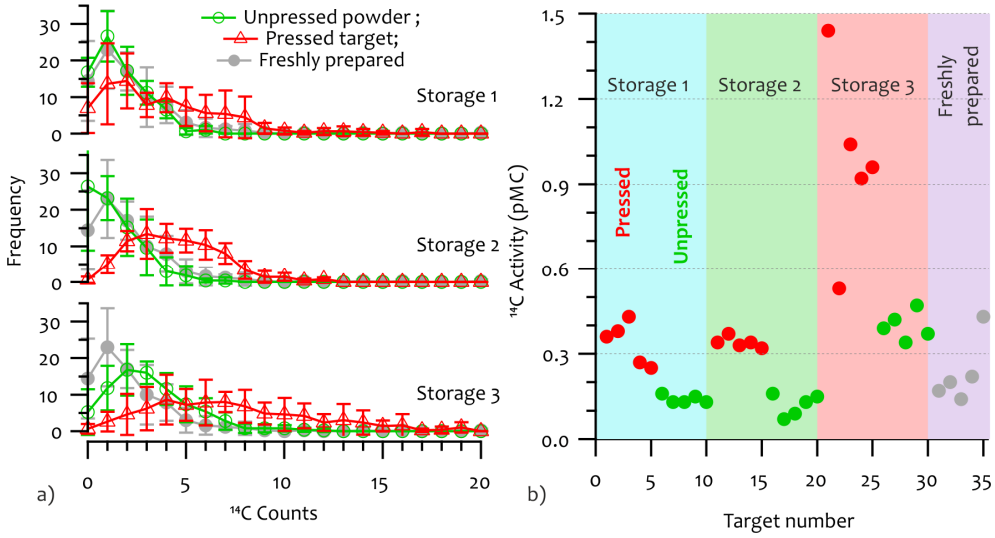

Figure 4: a) Frequency distribution of counts plot for storage tests with graphite in the form of powder (open circles) and pressed targets (open triangles) showing the difference in the level of acquired contamination: Storage 1) Humidified lab air + 1.5% CO_2 (A = 50 pMC), Storage 2) Humidified lab air + 1.5% CO_2 (A = 108 pMC) and Storage 3) Humidified lab air + 1.5% CO_2 (A = 980 pMC). The freshly prepared samples (gray circles) are plotted for comparison in each of the three graphs. b) Calculated ^{14}C activity (pMC) of the stored pressed targets (red), the stored graphite powder samples (green) and the freshly prepared targets (gray). For each storage condition, the results shown in a) are the averages for five pressed targets and five graphite powder samples, respectively, that were stored for a period of 10 days before measurements were performed.

Through these (and previous) storage tests it was also revealed, to our surprise, that the samples stored in the form of pressed graphite targets are more susceptible to contamination than the ones stored under the same conditions, but in the form of powder. As the effective exposed surface of graphite powder is much larger than that of the pressed targets, this is counter-intuitive. The effect is illustrated in Figure 4a, which shows the frequency distribution of counts of samples stored in three different storage conditions. Unpressed graphite powder (× 5 in each storage condition) and pressed targets (× 5 in each storage condition) were stored in humidified laboratory air spiked with ≈ 1.5 % CO_2 with an activity of

50, 108, and 980 pMC, respectively. The samples were stored in the test condition for a period of ten days. For comparison, the count distribution from a set of five freshly pressed targets is also shown (the same in all three graphs). These were transferred into the AMS sample chamber immediately after they were pressed, along with the other thirty targets from the test. In Figure 4a the stored unpressed samples are shown with open green circles, pressed targets are shown with open red triangles and freshly prepared targets with solid gray circles. The pressed targets in all storage conditions acquired contamination, the extent of which depended on the type of CO_2 the system was spiked with. Contamination was not visible on the graphite powder samples stored in the systems containing 50 pMC and 108 pMC CO_2, while the powder samples stored in the system containing 980 pMC CO_2 did show a shift in the count distribution, indicating a significant contamination take-up, but by far not as much as the pressed targets under that same storage condition. Shown in Figure 4b is the summary of all the ^{14}C activities determined for the 35 targets. ^{14}C activities corresponding to the pressed targets are shown with a red circle and the ones corresponding to the unpressed powder samples are shown with green circles. The freshly prepared samples are shown with gray circles.

3.4 Discussions

In the first phase of our storage tests we suspected the iron catalyst to be the mediator of the contamination on the samples. Since iron undergoes several different reactions during the production of graphite (Nemec, Wacker et al. 2010), it was our hypothesis that one of the reaction products, probably an oxide of Fe that survived during the graphitization reaction, exhibited very efficient carbon sequestration from atmospheric CO_2 on to the target surface. Thus, to remove any leftover iron oxides we hydrogenated the graphitization product (GP) at 600 °C and observed that it partially reacted, producing methane. We then graphitized a set of ten Rommenhöller CO_2 samples, and hydrogenated five of them in an attempt to passivate the samples. These samples were then pressed and left in open air for a week. We then measured these samples and found no improvement in the level of

acquired contamination. The results also showed that the reduction product, compared to the GP, was significantly depleted in ^{13}C ($\delta^{13}C$ from -2.2 ± 0.5‰ to -9.3 ± 0.7‰). We also tested the reactivity of high-purity, commercially available graphite (Alfa Aesar, 99.9995%) to hydrogenation reaction at 600 °C and found that the graphite failed to react.

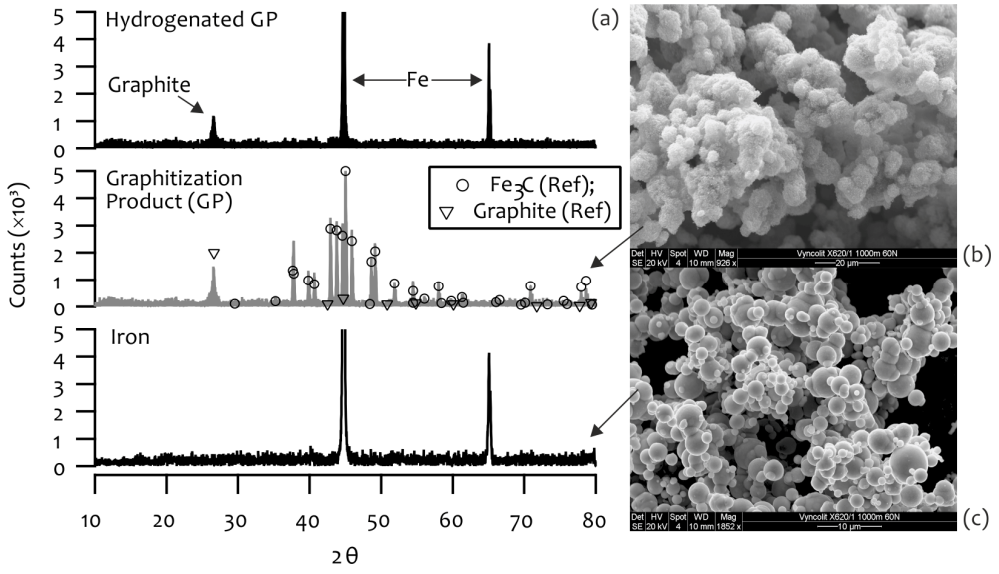

Figure 5: a) Powder X-Ray Diffraction pattern of Iron, Graphitization Product (GP) and GP after hydrogenation. GP primarily contains carbon in the form of Graphite and Iron Carbide (Fe_3C) as indicated by the PXRD pattern. Following hydrogenation at 600 °C, Fe_3C in GP is converted back to Fe releasing methane. SEM images of b) GP and c) Fe powder (Alfa Aesar, 325 mesh).

Thus, to understand the elemental composition of our GP, we then performed elemental analysis with Energy-Dispersive X-ray Spectroscopy (EDXS) to examine the presence of oxygen in the samples. The results showed no evidence of oxygen in the sample. Additionally, to understand the chemical composition of the GP, we also performed Powder X-Ray Diffraction (PXRD) measurements. Figure 5a shows the PXRD data of Fe (lowermost spectrum) and the graphitization product (GP, Fe + Carbon), (middle spectrum). The Scanning Electron Microscopic (SEM) images of the graphitization product and the iron power are shown in Figure 5b & c, respectively. These PXRD studies revealed that the carbon in our GP, commonly

referred to as graphite in the radiocarbon community, is predominantly a mixture of graphite and iron carbide (Fe_3C). The spectrum also reveals that no Fe is left in its original state. For identification of peaks, the standard reference spectra of Fe_3C and graphite are also shown, as circles and triangles, respectively, in the GP spectrum (Downs and Hall-Wallace 2003). Kim et al., 2010 measured the PXRD spectra of graphitization products with varying C/Fe mass ratio (1:1, 1:5, 1:10 and 1:15) at different temperatures (400, 500, 525 and 585 °C) (Kim, Kelly et al. 2010). Their PXRD spectrum of the graphitization product with 1:1 (C/Fe) mass ratio, prepared at 585 °C closely resembles that of the samples we prepare at 600 °C (≈ 1:1 C/Fe). It is evident from their measurements that the crystalline graphitic phase ($2\theta \approx 26.5°$) only appears, at detectable levels, at temperatures > 500 °C with 1:1 (C/Fe) mass ratio. Since Fe_3C reacts with H_2 at 600 °C producing methane (Kock, De Bokx et al. 1985), whereas the graphitic form of carbon remains intact, it is therefore possible to quantify the carbide phase by hydrogenation. Hence, we performed a hydrogenation reaction following the graphitization step. On completion of the graphitization reaction the reactor was evacuated and filled with ≈ 500 mbar of hydrogen and heated to 600 °C. The PXRD data of the hydrogenated product is also shown in Figure 5a (top spectrum). The result clearly shows that the iron carbide upon hydrogenation completely converts back to iron, leaving behind the unreacted graphitic carbon. The reaction product of hydrogenation, methane, was confirmed with a residual gas analyzer (Extorr XT100 RGA). Based on the amount of hydrogen consumed, it was calculated that ≈ 12% of the total carbon must have reacted to produce methane. Since it is evident from the PXRD data that the Fe present in GP is in the form of Fe_3C, we can calculate, based on the known amount of Fe added, that a maximum of ≈ 6 % of the C can be in the form of Fe_3C. This means that next to graphite and Fe_3C, yet another form of carbon must be present (amounting to ≈ 6 % of all C), which also reacts to produce methane during the hydrogenation reaction. The most likely candidate is filamentous carbon (Kock, De Bokx et al. 1985). Although interesting by itself, we did not investigate the exact structural form of carbon in the samples further, as it was deemed unnecessary for the proposed study.

As is seen in Figure 2, the first 8 blocks yield an excess of ≈ 25 counts above the mean accumulated counts from the rest of the measurement. We can thus calculate, based on the total "target surface to count detection" efficiency of our AMS instrument of ≈ 1%, that ≈ 0.04 µg modern carbon must have contaminated the surface in order to produce the additional counts. Similarly, observed from the other storage experiments shown in Figure 4, targets stored in storage condition-2 have ≈ 200 excess counts accumulated over the whole measurement when compared to the freshly prepared targets. This would correspond to ≈ 0.35 µg C accumulated during the storage period. This accumulated carbon is not necessarily present on the surface only, but, as is clearly demonstrated in Figure 3, carbon from storage condition-3 is capable of gradually percolating inside the sample matrix, leading to an overall increase in the observed counts.

During our extensive literature review, widely around this subject, we discovered recently that the presence of a thin layer of carbonaceous material leading to surface contamination is a phenomenon well known in the field of surface science, as Adventitious Carbon, since long. AC accumulation occurs on all air-exposed surfaces and is almost inevitable. In the fields of material science, this layer of unwanted contaminants, including AC, on a substrate surface is generally removed by sputter-etching with argon ions, by exposing the surface to photons from a xenon excimer lamp, or by the RCA cleaning procedure (developed by Werner Kern at the Radio Corporation of America), which is a multistep, wet cleaning procedure (Kern and Puotinen 1970). Unfortunately, none of these cleaning methods is practically suitable for decontaminating the target surface.

In addition to the experiments described here, we also performed several similar storage tests with commercially available high-purity graphite rods (Alfa Aesar, 99.9995% and Nilaco, 99.9995%; ^{14}C activity in both ≈ 0.2 pMC) and found no significant uptake of adventitious carbon on the graphite surface. As mentioned previously and shown in Figure 5a, we did not detect any residual Fe-oxides in the bulk GP (if any, their concentrations must thus be far below the detection limits). But, as shown by Miller et al., (2002), a clean iron surface produces, after exposure to CO_2, a thin oxide layer on iron along with a carbonaceous layer mainly in the

form of polymeric carbon. Also described in Miller et al., (2002) is an attempt to enrich the iron surface with ^{13}C by exposure to $^{13}CO_2$ (99% in ^{13}C). This attempt failed to show any enrichment in the ^{13}C content of the AC layer. The authors suggest that this might be caused by considerable dilution of their original pure ^{13}C labeled CO_2 by exchange with the much larger reservoir of unlabeled CO_2 adsorbed on the chamber. The results shown in this chapter make clear that ^{14}C labeled CO_2 can certainly contaminate a target surface, showing that CO_2 present around the target surface is definitely a source of AC and probably the most important one. Since we have not performed any storage tests with hydrocarbons (e.g. methane containing varying levels of ^{14}C), we cannot comment on the efficiency and the extent of contamination of those substances. As their concentrations are many orders of magnitudes smaller, it would be highly surprising if they would play a role at all. Likewise, the concentration of VOCs in a laboratory may be higher than in outside air due to the use of solvents etc., but it would still be far below the abundance of CO_2.

We also investigated the possible nature of the attachment of AC on the target surface. It is certainly possible that the initial extra counts observed during the measurements could arise from loosely adsorbed contaminants, which upon sputtering gradually escape and produce the additional counts. Thus to differentiate between loosely adsorbed contaminants and chemisorbed contaminants, we heated (80 ^oC) a set of five contaminated targets under vacuum for four hours. The samples were left in vacuum for approximately 12 hours, and then the container was filled with nitrogen at 1100 mbar. The container was opened just before the targets were placed inside the AMS sample chamber. The results showed no improvement in the level of acquired contamination when compared to a similar set of five untreated targets. These results reinforce the fact that the attachment of the carbonaceous layer on the target is through chemisorption and not just loosely adsorbed.

3.5 Conclusions

Through a series of experiments we learned that the level of acquired contamination is very much dependent on the type of environment the sample is in contact with. The level of contamination furthermore depends heavily on the form in which the samples are stored, i.e., the stored pressed targets are more vulnerable to contamination than the graphite powder. The contamination on stored graphite powder is barely visible when stored in an atmosphere spiked with contemporary CO_2 during an experimented period of ≈ 10 days, whereas the pressed targets are considerably contaminated. With enriched $^{14}CO_2$ spiked laboratory air, even powder graphite samples did show a noticeable contamination uptake, while the pressed targets were indeed contaminated to a very large extent. This also reinforces the fact that the contamination is indeed real and not just a detector artifact. Perhaps the most important finding was that a very similar phenomenon is known in the field of material science where they observe growth of a carbonaceous layer on all air exposed samples, an apparently unavoidable effect that is known as adventitious carbon. This phenomenon might very well explain our storage test results. The pressed targets, when exposed to air, acquire a thin layer of adventitious carbon on the surface, which is visible during the initial part of the measurement. As measurement progresses, the layer of adventitious carbon is removed by the sputtering process revealing the cleaner background material. Still, as indicated by the tests performed with enriched CO_2, the contamination of the pressed targets is not entirely limited to the surface but also affects the bulk, probably through diffusion. The stored graphite powder shows less acquired contamination, but it is very likely that also on the powder an adventitious carbon layer builds up. However, the sample is mixed well by stirring before pressing it, and this mixes the adventitious carbon layer into the sample matrix, thus diluting the effect. Still, long storage of graphite powder will contaminate the sample and lead to higher background values, even though this is hard to identify since the contamination is well-mixed throughout the sample. From the results presented in Miller et al., 2010, it is evident that the process of contamination leading to a buildup of a thin carbonaceous layer is always accompanied by an iron

oxide layer. Through our experiments, we also observe that in contrast to the graphitization product, a graphite rod alone fails to show a surface carbonaceous buildup, stored in similar conditions. It may be possible that this uptake of CO_2 leading to the production of the AC layer is occurring through electrochemical reduction of CO_2 in the presence of Fe and water vapor. We have also observed that, when a graphite rod (which normally is immune to contamination) is left in open air after it has been measured in the AMS, it shows a buildup of a carbonaceous layer, probably mediated through the deposited Cs on the surface.

This brings us to conclude that this process of surface contamination is, to a certain extent, inevitable. Although there are measures that can be taken to minimize the level of contamination, none will completely avoid it. Learning from the experience of the surface science community, the best recipe seems to be: store samples in the form of graphite powder, in a container filled with a dry and pure N_2 or Ar atmosphere, and if possible only for a limited period of time. Press the samples only when the instrument is ready for measurement. Once pressed, the samples must be transferred to the AMS sample chamber as soon as possible. As performed in most laboratories, the target surface should be sputtered clean before every measurement. This step of sputter-cleaning must be combined with the whole measurement procedure by adding some initial sputtering time (in our case a set of 8 or 16 blocks), the data of which must be excluded during the data analysis. In the light of the findings of this work, we will change our cleaning approach accordingly. Additional measures to avoid the adventitious carbon, such as pressing and transporting the samples in a CO_2-free, dry atmosphere, are very cumbersome, and will most likely not lead to the complete avoidance of the adventitious carbon (as this will even grow in the vacuum of the source chamber of the accelerator).

The implications of such surface contamination are of course not limited to background materials: all samples suffer from such a contamination, but it is mostly not noticeable. Still, sputtering a whole batch of samples, including backgrounds, unknowns and reference materials, is the best strategy. For very small samples the effects aggravate. Since the graphitization tube and the iron powder are generally

exposed to laboratory air before graphitization, they too carry an adventitious carbon layer, which could well become part of the Modern Carbon Contamination (MCC) (Santos, Southon et al. 2007; de Rooij, van der Plicht et al. 2010). It is therefore important to chemically remove this source of MCC for further reduction of the total accumulated contamination. The AC present on the reactor surface and on the iron powder may be removed by oxidation with O_2 followed by reduction with H_2 at 600 °C before starting the graphitization step, although the effectiveness is yet to be verified.

The AC contamination on samples can be avoided if the samples are introduced as CO_2 directly into the ionization chamber of the AMS. Indeed, experience with especially small samples shows lower levels of contamination when using such a gas source (Ruff, Szidat et al. 2010). Development of more efficient gas ion sources for AMS, among others, might thus improve the dynamic range of detection and make measurements of samples older than 50000 years possible. On the other hand, gas sources at the moment can only handle a limited amount of sample CO_2, and therefore counting statistics will be very limited for old samples. Now that we have unambiguously revealed one of the sources of contamination, the combination of careful sample and target handling (meaning basically fast throughput) and systematic sputtering of all targets might also lead to an effectively lower background, and thus to more reliable measurement of the oldest samples.

3.6 References

Aerts-Bijma AT, Meijer HAJ, van der Plicht J. 1997. AMS sample handling in Groningen. Nuclear Instruments & Methods in Physics Research Section B-Beam Interactions with Materials and Atoms 123(1-4):221-5.

Barr TL, Seal S. 1995. Nature of the use of adventitious carbon as a binding-energy standard. Journal of Vacuum Science & Technology a-Vacuum Surfaces and Films 13(3):1239-46.

Brown TA, Southon JR. 1997. Corrections for contamination background in AMS C-14 measurements. Nuclear Instruments & Methods in Physics Research Section B-Beam Interactions with Materials and Atoms 123(1-4):208-13.

de Rooij M, van der Plicht J, Meijer HAJ. 2010. Porous iron pellets for AMS ^{14}C analysis of small samples down to ultra-microscale size (10–25μgC). Nuclear Instruments & Methods in Physics Research Section B-Beam Interactions with Materials and Atoms 268(7-8):947-51.

Downs RT, Hall-Wallace M. 2003. The American Mineralogist Crystal Structure Database. American Mineralogist 88:247-50.

Kern W, Puotinen DA. 1970. Cleaning Solutions Based on Hydrogen Peroxide For Use in Silicon Semiconductor Technology. RCA Review 31(2):187-205.

Kim S-H, Kelly PB, Ortalan V, Browning ND, Clifford AJ. 2010. Quality of Graphite Target for Biological/Biomedical/Environmental Applications of ^{14}C-Accelerator Mass Spectrometry. Analytical Chemistry 82(6):2243-52.

Kirner DL, Taylor RE, Southon JR. 1995. Reduction in backgrounds of microsamples for AMS C-14 dating. Radiocarbon 37(2):697-704.

Kock A, De Bokx PK, Boellaard E, Klop W, Geus JW. 1985. The formation of filamentous carbon on iron and nickel catalysts: II. Mechanism. Journal of Catalysis 96(2):468-80.

Mangolini F, McClimon JB, Rose F, Carpick RW. 2014. Accounting for Nanometer-Thick Adventitious Carbon Contamination in X-ray Absorption Spectra of Carbon-Based Materials. Analytical Chemistry 86(24):12258-65.

Miller DJ, Biesinger MC, McIntyre NS. 2002. Interactions of CO_2 and CO at fractional atmosphere pressures with iron and iron oxide surfaces: one possible mechanism for surface contamination? Surface and Interface Analysis 33(4):299-305.

Nemec M, Wacker L, Gaggeler H. 2010. Optimization of the Graphitization Process at AGE-1. Radiocarbon 52(3):1380-93.

Paul D, Meijer HAJ. 2015. Intracavity OptoGalvanic Spectroscopy Not Suitable for Ambient Level Radiocarbon Detection. Analytical Chemistry 87(17):9025-32.

Piao H, McIntyre NS. 2002. Adventitious carbon growth on aluminium and gold-aluminium alloy surfaces. Surface and Interface Analysis 33(7):591-4.

Ruff M, Szidat S, Gaggeler HW, Suter M, Synal HA, Wacker L. 2010. Gaseous radiocarbon measurements of small samples. Nuclear Instruments & Methods in Physics Research Section B-Beam Interactions with Materials and Atoms 268(7-8):790-4.

Santos GM, Southon JR, Griffin S, Beaupre SR, Druffel ERM. 2007. Ultra small-mass AMS ^{14}C sample preparation and analyses at KCCAMS/UCI Facility. Nuclear Instruments and Methods in Physics Research Section B: Beam Interactions with Materials and Atoms 259(1):293-302.

Chapter 4:

Radiocarbon analysis of stratospheric CO_2 retrieved from AirCore sampling

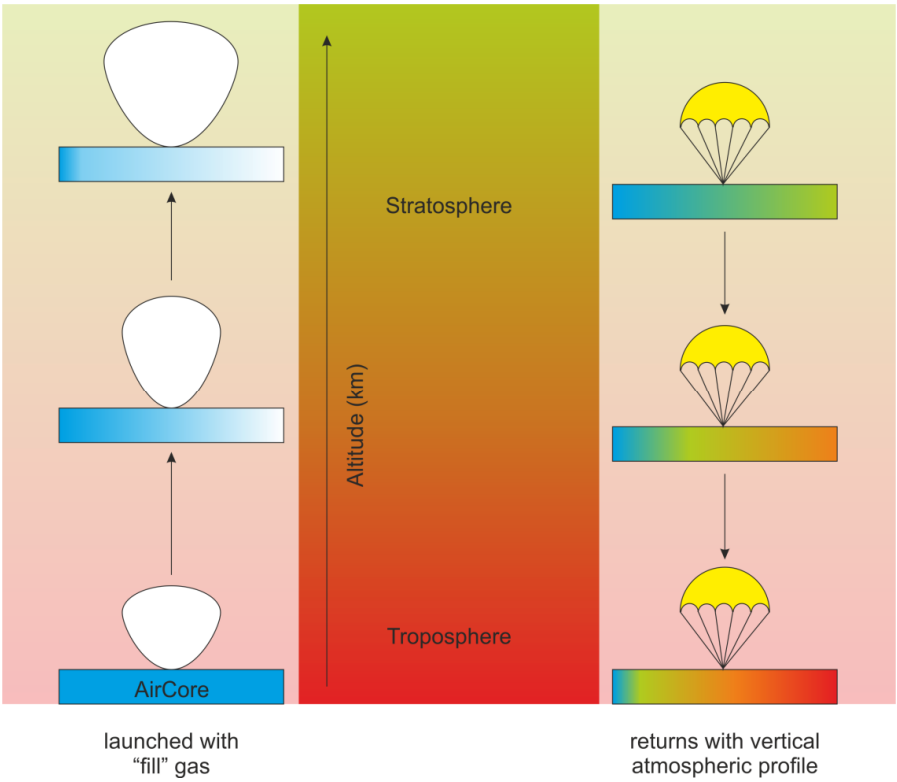

This chapter is under review in the journal Atmospheric Measurement Techniques Discussions

Paul, D., *Chen, H., Been, H. A., Kivi, R., and Meijer, H. A. J., Atmos. Meas. Tech. Discuss., DOI: 10.5194/amt-2015-377, 2016*

Cover image shows a pictorial summary of the AirCore sampling method.

Abstract

In this decade understanding the impact of human activities on climate has been one of the key issues of discussion globally. In that respect, the continuous rise of the concentration of greenhouse gases, e.g., CO_2, CH_4, etc. in the atmosphere, predominantly due to human activities requires continuous monitoring to understand the dynamics. Radiocarbon (^{14}C) is an important atmospheric tracer and one of the many used in the understanding of the global carbon budget, which includes the greenhouse gases CO_2 and CH_4. Measurement of radiocarbon in atmospheric CO_2 generally requires collection of large air samples (few liters) from which CO_2 is extracted and then the concentration of radiocarbon is determined using Accelerator Mass Spectrometry (AMS). However, the regular collection of air samples from the stratosphere, for example using aircraft and balloons, is prohibitively expensive.

Here we describe radiocarbon measurements in stratospheric CO_2 collected by the AirCore sampling method. AirCore is an innovative atmospheric sampling system, which comprises of a long tube descending from a high altitude with one end open and the other closed, and has been demonstrated to be a reliable, cost-effective sampling system for high-altitude profile (up to ≈ 30 km) measurements of CH_4 and CO_2. In Europe, AirCore measurements are being performed on a regular basis near Sodankylä (Northern Finland) since September 2013. Here we describe the analysis of samples from two such AirCore flights made there in July 2014, for determining the radiocarbon concentration in stratospheric CO_2. The two AirCore profiles were collected on consecutive days. The stratospheric part of the AirCore was divided into six sections, each containing ≈ 35 µg CO_2 (≈ 9.6 µgC). Each section was separately stored in a ¼ inch coiled stainless steel tubing (≈ 3 m) for radiocarbon measurements. A small-volume extraction system was constructed which enabled ≈ 100% CO_2 extraction from the stratospheric air samples. Also, a new small-volume high-efficiency graphitization system was constructed for graphitization of these extracted CO_2 samples, which were later measured at the Groningen AMS facility. Since the stratospheric samples were very similar in mass,

reference samples were also prepared in the same mass range to correct for contaminations. The results show that the $\Delta^{14}CO_2$ values for lower stratosphere up to about 18(± 1) km (first four samples from each profile) are very similar (10 ± 8‰) and represent the current tropospheric value. The next sample in each profile, corresponding to about 18(± 1)-22(± 2) km showed slight enrichment of 80 ± 20‰. The last section from one profile, corresponding to altitudes above 22(± 2), also showed enhanced $\Delta^{14}CO_2$ value of 79.1 ± 30‰. The last section from the other profile was spoiled during preparation.

4.1 Introduction

The concentration of Greenhouse Gases (GHG), with carbon dioxide as the most prominent example, has been and still is increasing, predominantly due to emissions from fossil fuel combustion. The consequences in terms of climate change are certainly detrimental (IPCC 2014a; IPCC 2014b) if the rapid increase in GHG concentrations is not regulated and properly accounted for. This brings in the necessity for better understanding and quantification of the sources, reservoirs, sinks and the transport mechanisms involved.

Carbon dioxide is a naturally occurring greenhouse gas produced mainly through respiration by aerobic organisms and decay of organic materials. It is also the product of combustion of any carbon-containing compound. Carbon in carbon dioxide exists in the form of three naturally occurring isotopes, i.e., ^{12}C, ^{13}C, and ^{14}C. Radiocarbon (^{14}C) is the only naturally occurring radioactive isotope of carbon ($t_{½}$ = 5730 ± 40 years), which is continuously produced through the reaction of thermalized neutrons from cosmic radiations with ^{14}N in the upper atmosphere (Lingenfelter 1963). The produced ^{14}C combines with oxygen to produce $^{14}CO_2$, which forms a trace component of atmospheric CO_2 (presently $^{14}CO_2/^{12}CO_2 \approx 1.2 \times 10^{-10}$%). $^{14}CO_2$ is an important atmospheric tracer, which helps in the understanding of the levels of anthropogenic emissions from fossil fuels. This is due to the fact that fossil fuel is virtually radiocarbon-free, which upon combustion produces CO_2, also radiocarbon-free. This CO_2 from fossil fuel dilutes the atmospheric $^{14}CO_2$ concentration upon release.

The concentration of CO_2 throughout the atmosphere is roughly well-mixed, with an observed annual rise in recent years of ≈ 2 ppm/year (Hartmann, Klein Tank et al. 2013). This rise in the concentration of CO_2 due to the burning of fossil fuels is at present the main cause for the decrease in the radiocarbon concentration in the atmospheric CO_2. Aircraft sampling of atmospheric CO_2 at various altitudes is regularly performed, which unfortunately only collects air samples up to upper troposphere/lower stratosphere (Brenninkmeijer, Lowe et al. 1995; Brenninkmeijer, Crutzen et al. 2007; Machida, Matsueda et al. 2008; Sweeney, Karion et al. 2015).

Although balloon based sampling has been demonstrated as a method for collecting stratospheric air for measurements of radiocarbon in stratospheric CO_2 (Hagemann, Gray et al. 1959; Ashenfelter, Gray et al. 1972; Nakamura, Nakazawa et al. 1992; Nakamura, Nakazawa et al. 1994), this method of sampling is extremely expensive and difficult to sustain for longer periods. Here we describe the use of the AirCore sampling method (Karion, Sweeney et al. 2010) as a viable tool for sampling stratospheric air for the measurements of radiocarbon in stratospheric CO_2. Although the sample sizes obtained through AirCore sampling are small (only ≈ 50 ml), they are just enough for performing quantitative radiocarbon measurements, with relatively good altitude resolution.

4.1.1 Sampling

Regular AirCore profiles of CO_2, CH_4, and CO have been made near Sodankylä (in Northern Finland, 67.4° N, 26.6° E) since September 2013 (Chen, Kivi et al. In preparation). We have collected the stratospheric part of the AirCore samples for several selected AirCore flights using a stratospheric air sampler (Mrozek, Veen et al. In preparation). Briefly, the AirCore that has been flown in Sodankylä comprises of a long coiled, thin-wall stainless steel tubing (≈ 100 m long, volume ≈ 1400 ml). The AirCore, before releasing with the help of a balloon, is first filled with a standard dry "fill-gas" with known CO_2, CH_4 and CO concentrations (CO_2 = 386.10 ± 0.09 ppm; CH_4 = 1880 ± 2 ppb; CO deliberately spiked to 7972 ± 5 ppb). The fill gas is a compressed air cylinder containing dry ambient air (sampled at Sodankylä, Finland) spiked with carbon monoxide. It should thus contain CO_2 with natural levels of radiocarbon. The accurate determination of the radiocarbon content in CO_2 of the fill gas was initially not deemed essential for this work, and has thus not been performed. The AirCore is then released with one end open to atmosphere. As the AirCore travels higher in the atmosphere, the fill-gas inside the AirCore is evacuated due to the drop in pressure. During its descent through the atmosphere, the evacuated AirCore equilibrates with the ambient pressure and thereby the tube gradually fills itself with atmospheric air. The open end of the AirCore is then closed automatically upon landing, preserving the collected air column until

analysis is performed, which is typically within a few hours after the AirCore has landed.

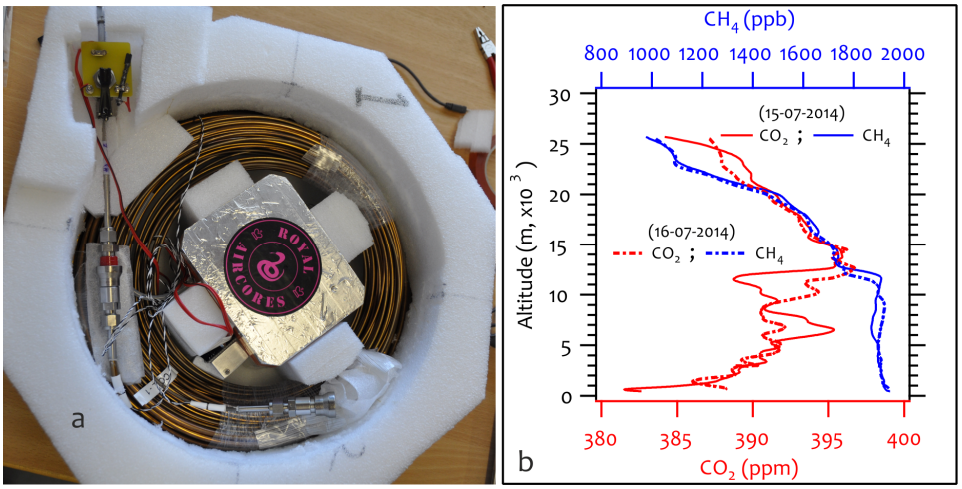

Figure 1: a) Picture of an AirCore, used during the sampling campaign at Sodankylä, constructed from a long thin walled stainless steel tubing (≈ 100 m long, wall thickness = 0.254 mm). b) Corrected vertical concentration profiles of CO_2 (red) and CH_4 (blue) retrieved through AirCore samplings performed on July 15, 2014 (solid line) and July 16, 2014 (dashed line) at Sodankylä. Mind the different scale span for CO_2 and CH_4.

For our goal, the AirCore, containing the vertical atmospheric profile, was connected to a Cavity Ring-Down Spectrometer (CRDS, Picarro Inc., CA model: G2401) for simultaneous measurements of the CO_2, CH_4 and CO concentrations. The sampling end of the AirCore was connected to a standard dry "push-gas" line, and the other end was connected to the CRDS analyzer. The sampled air column inside the AirCore was then "pushed" out with the push-gas, which is also the fill-gas, into the CRDS analyzer. The exhaust from the CRDS analyzer was connected to a Stratospheric Air Sampler (SAS) (Mrozek, Veen et al. In preparation). The SAS built at the University of Groningen, similar to the one described in Mrozek et al., comprises of a series of six connected stainless steel tubing (Swagelok, od = 6.35 mm, id = 4.57 mm, ≈ 50 ml), with each section measuring 3 m. The tubing sections were joined by three port two way valves (Swagelok SS-43GXS4), which allows uninterrupted transfer of the AirCore content into the SAS and subsequent isolation of each section for a desired analysis later. Each section in the SAS thus

represented an integrated sample from a determinable altitude range. Each section contained ≈ 50 ml stratospheric air (at STP), with ≈ 35 µg CO_2 (≈ 9.6 µgC). CO_2 samples from each section of the SAS were later extracted and processed for ^{14}C measurements at the Centre for Isotope Research, (CIO), Groningen, using Accelerator Mass Spectrometry (AMS). The AMS facility at CIO is a 2.3 MeV Tandetron built by High Voltage Engineering Europa (Gottdang, Mous et al. 1995).

Several AirCore profiles were collected at Sodankylä during a campaign in July 2014, out of which two stratospheric air profiles were preserved for radiocarbon measurements of stratospheric CO_2 described in this work. Figure 1a shows the picture of an AirCore that was used during the sampling campaign. Since the AirCore is initially filled with a fill-gas before release, there is a small fraction of the fill-gas still remaining in the AirCore, which is not evacuated completely. This leftover fraction of fill-gas contaminates the air from the highest sampled altitude. Fortunately, the impact on the samples from the highest altitude can be accurately corrected for when using fill gas with an enhanced CO of 7972 ± 5 ppb to label the mixing process (Chen, Kivi et al. In preparation). These corrected atmospheric profiles of CO_2 (red, solid and dashed lines) and CH_4 (blue, solid and dashed lines) from the two AirCore samplings are shown in Fig. 1b. The CO_2 profile is roughly well-mixed throughout the atmosphere, whereas the CH_4 concentration is rather constant in the troposphere and drops continuously with increasing altitude in the stratosphere, predominantly due to oxidation.

4.1.2 Extraction

Following the sample collection at Sodankylä, the SAS was brought back to Groningen for subsequent processing and measurement. CO_2 from the air samples in the SAS was extracted using an extraction system (total volume ≈ 20 ml) as shown in Fig. 2a. The detachable CO_2 trap, made from Pyrex, has two flow-through freezing tubes submerged in a liquid air bath (picture shown in Figure 3 of Appendix II). Each section of the SAS is individually connected to the extraction system. The extraction system is first evacuated for approximately an hour and then the air from the SAS is slowly expanded, during which the CO_2 trap is

submerged in liquid air. During this expansion of sample in the extraction system, a reference air (#1) is directed into the connected CRDS analyzer (Picarro G2301) through a 3-port 2-way valve. Once the pressure in the extraction system stabilized, the air from the extraction unit is directed into the CRDS analyzer to determine the CH_4 and the remaining CO_2 concentration in the extracted air. A flow rate of 3 sccm, using a mass flow controller (πMFC-LP P2A, MKS), was used for complete extraction of CO_2 and simultaneous determination of CH_4 in the CO_2-extracted-air. The extraction procedure was optimized by extractions performed with a reference-air (#2) filled "dummy" sampler (≈ 50 ml), similar to the SAS. The extraction efficiency was verified by comparison of the change in CO_2 signal with introduction of nitrogen (as zero-gas) and CO_2-extracted reference air into the CRDS analyzer from the dummy sampler. The process of optimization is shown in Fig. 2 b & c. Shown in Fig. 2b is a time series plot showing consecutive introduction of a zero gas (N_2, first two drops in the CO_2 and CH_4 signal; orange background) followed by CO_2 extracted reference air (#2, last two drops in the CO_2 signal; pink background). In between the consecutive measurements of N_2 (1 & 2) and CO_2 extracted reference air (3 & 4), reference air (#1) was measured and is shown with a cyan background. Figure 2c shows the superimposed CO_2 signals during introduction of the zero gas (N_2) and CO_2 extracted reference air (#2) from the dummy sampler into the CRDS analyzer. This method yielded an extraction efficiency of near 100%, which was also confirmed from the pressure of CO_2 in the CO_2 trap measured during the graphitization step discussed in the next section. Although the dummy loop was filled with N_2 and reference air (#2) with very similar pressure, the superimposed CO_2 signals, in Fig. 2c, show a small difference in the total running time of N_2 and CO_2 extracted reference air (#2). This is due to the fact that the reference air (#2) was cooled with liquid air during extraction, which led to a pressure drop, and thus a reduction of the total volume of air going through the CRDS analyzer before reaching the minimum differential pressure between the extraction system side and the CRDS analyzer side that the MFC could handle. As soon as the pressure in the extraction unit attained the minimum pressure (≈ 200 mbar), reference air (#1) was then directed into the CRDS analyzer and the extraction system was slowly evacuated while the CO_2 trap was still submerged in

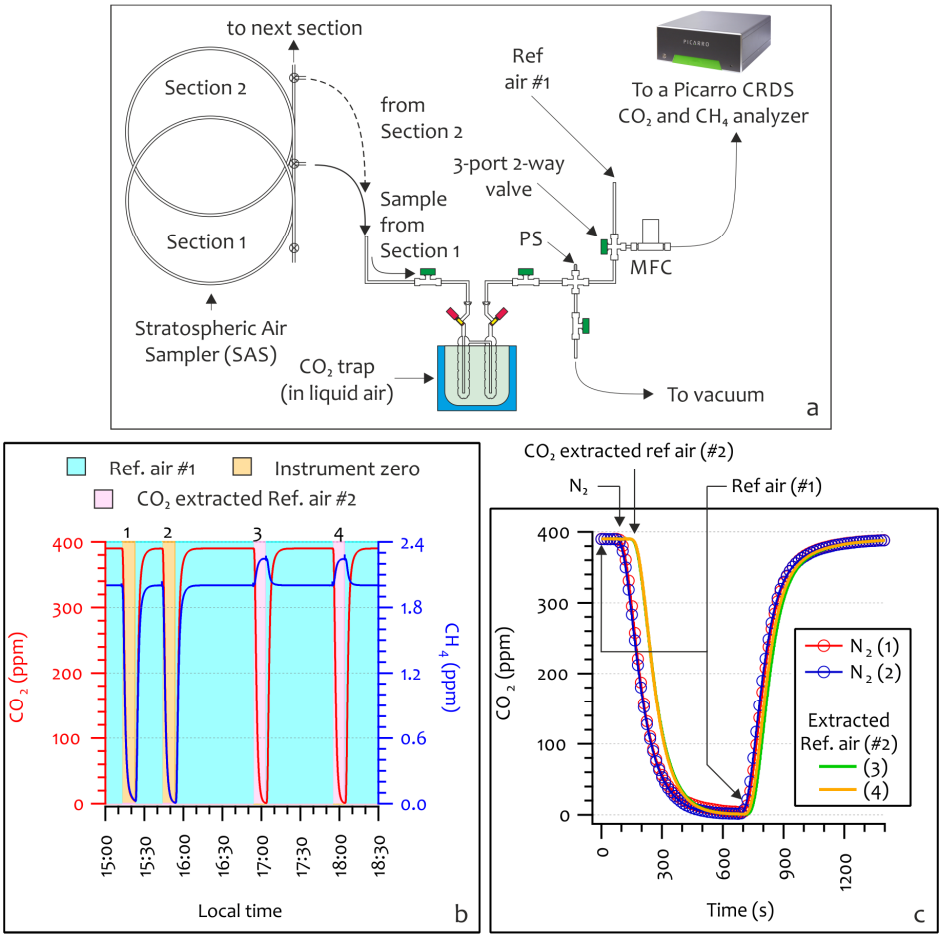

Figure 2: a) Schematic of the extraction system used for extraction of CO_2 from stratospheric air contained in the SAS. The CO_2 trap was submerged in a liquid air bath, which allowed quantitative freezing of CO_2 and avoided co-freezing of CH_4 and O_2. Using a CRDS analyzer (Picarro G2301), the concentration of CH_4 in the CO_2-extracted air was determined. The components indicated with abbreviations are as follows: MFC, mass flow controller; PS, pressure sensor. b) An example time-series showing a dummy sampler filled consecutively with N_2 (instrument zero, first two shown with an orange background) and reference air (#2, CO_2 extracted, last two shown with a pink background) to evaluate the extraction efficiency at a flow rate of 3 sccm. Reference air (#1) is directed through the Picarro analyzer when the extraction system is being made ready for the next extraction (shown with a cyan background). c) Superimposed CO_2 signal during the introduction of the zero gas (N_2) and the CO_2 extracted reference air (#2) showing a near 100% extraction efficiency.

the liquid air bath. Following the complete evacuation of air from the extraction unit, the CO_2 trap was disconnected and immediately taken for graphitization, described in the next section.

The use of liquid air, during the extraction of CO_2 from air, prevented the co-freezing of CH_4 (and of oxygen). A flow rate of 3 sccm (standard cubic centimeters per minute) ensured ≈ 100% removal of CO_2, while allowing simultaneous determination of the CH_4 concentration. The variability in the determination of methane in CO_2 extracted air was ≤ 5 ppb. The major source of variability in the determination of the CH_4 concentration is most likely the production of CH_4 from the metal-metal friction during the operation of the stainless steel valves, both in the sampler, the extraction system and the dummy sampler (Higaki, Oya et al. 2006). During the extraction of CO_2 from the SAS, dummy extractions were also performed with reference air (#2) and all extracted CO_2 samples were processed and measured by the AMS.

4.1.3 Graphitization

As the source of our present AMS facility is not yet capable of using gaseous CO_2, the CO_2 samples are reduced to elemental carbon, commonly referred to as graphite in the radiocarbon community. At the CIO, Groningen, the reduction of CO_2 (≈ 1-2 mg C – regular sample size) is carried out at 600 °C in the presence of H_2 (≈ 2.5 × partial pressure of CO_2) and Fe powder (Alfa Aesar, 325 mesh, 2 mg) (Aerts-Bijma, Meijer et al. 1997). A new graphitization system and procedure was devised later for the preparation of small samples (≈ 10-25 µgC) which featured the use of Fe in the form of a porous-pellet and not powder (de Rooij, van der Plicht et al. 2010). For graphitization of the CO_2 samples extracted from stratospheric air, described in this work, a modified and optimized preparation method of de Rooij et al., (2010) was used. A new low-volume graphitization reactor, shown in Figure 3 (also shown in Figure 4 of Appendix II), was designed in-house for the conversion of pure CO_2 into elemental carbon. The graphitization setup comprised of two sections, 1) the reactor region (marked in the blue box) and 2) the mass determination region (marked in the red box). The graphitization setup was

connected to a common vacuum line that also supported four other graphitization units. For evacuating the graphitization units, a turbo pumping station (Edwards, TS75W1001) was used.

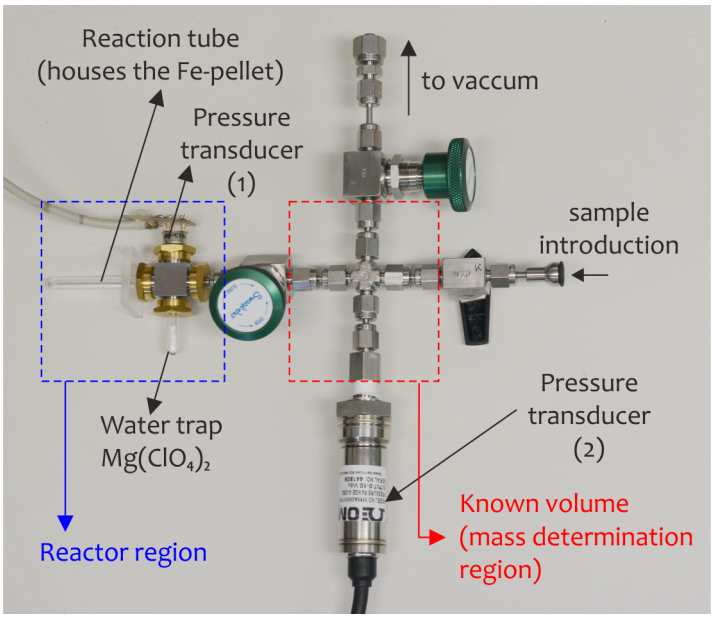

Figure 3: Newly designed reactor (≈ 1.5 ml, blue box) for preparation of ultra-small samples (3-50 µg C) for AMS measurements. Each section of the stratospheric air sampler contains ≈ 35 µg CO_2 sample that is reduced to graphite (≈ 9.6 µgC) on porous iron pellets at 500 °C in the presence of hydrogen (≈ 2.2 × partial pressure of CO_2). The mass determination section, comprising of a known volume, is used to determine the mass of the reference materials and the samples based on pressure measured at pressure transducer (#2). Pressure transducer (#1) is used to monitor the progress of the graphitization reaction.

The reactor region comprises of the reactor manifold, constructed from stainless steel, a reaction tube, a water trap tube and a pressure transducer. The reaction tube (OD = 6 mm, ID = 3 mm, length = 58 mm) and the water-trap tube (6 × 3 × 30 mm) connected on the manifold were constructed from fused silica. The total volume of the reactor thus achieved was ≈ 1.5 ml. Magnesium perchlorate was used to remove water produced during the reduction of CO_2 instead of Peltier-cooled water traps, that are in use for larger samples (Santos, Southon et al. 2007). We observed that the Peltier-cooled water traps retarded/prohibited the

reduction reaction for samples below 50 µg C. Although the reduction reaction is much more efficient and faster with the use of $Mg(ClO_4)_2$, care must be taken to avoid any $Mg(ClO_4)_2$ particle entering the heated section of the reactor tube, which mostly happened due to electrostatic repulsion produced through the operator. It seems likely that one of the thermal decomposition products of $Mg(ClO_4)_2$ (Devlin and Herley 1986) poisons the catalytic properties of Fe and thus significantly slows down or even prohibits the reduction reaction. $Mg(ClO_4)_2$ in the water trap was heated to 100 °C while evacuating the system, before the graphitization step, which released a significant amount of water, making the trap even more efficient during graphitization. Iron pellets (≈ 1.4 mg, 1.3 mm diameter, ≈ 0.4 mm thick) were prepared by pressing Fe powder (Alfa Aesar, 325 mesh) at 300 N (de Rooij, van der Plicht et al. 2010). The reactor temperature was set at 500 °C, and hydrogen equivalent to ≈ 2.2 times the CO_2 partial pressure (at STP) was used. Hydrogen is introduced into the reactor through the vacuum line, while the CO_2 in the reactor is frozen in the water trap with liquid N_2. While introducing hydrogen in the reactor, the valve connecting the common vacuum line and the pump is closed. The reaction temperature and hydrogen pressure were optimized for minimum CH_4 production, thereby minimizing the loss of sample during the graphitization process. To optimize the reaction condition, the production of CH_4 in the reactor was continuously monitored with a residual gas analyzer (Extorr, XT100) connected to the manifold through a 25 µm (id) GC capillary column. This manifold was identical to the one used for sample preparation, except for the additional port to connect the GC capillary column (not shown in Fig. 3). The reaction time for CO_2 samples < 50 µg C was typically less than 20 min with reaction efficiency better than 95 %. The reaction progress was determined by monitoring the change of pressure inside the reactor using a pressure transducer (#1) connected on the manifold.

The reactor region in the setup is connected to the mass determination region, which has a known volume. This known volume was used for determining the mass of the reference gases as well as of the stratosphere CO_2 samples. As contamination is a serious concern for radiocarbon measurements of ultra small

samples by AMS, it requires quantitative determination of the accumulated contaminants over the whole preparation process. Modern carbon contamination (MCC, containing contemporary levels of radiocarbon) and dead carbon contamination (DCC, originating from fossil materials with no radiocarbon) affect samples differently, depending on the age and mass of the sample (Brown and Southon 1997; Santos, Southon et al. 2007; de Rooij, van der Plicht et al. 2010). Very small samples such as those in the present work (≤ 10 µg C) are severely affected by both MCC and DCC. Hence, for such small samples determination of the accumulated contaminating carbon is essential. To determine the mass of accumulated contaminating carbon in a sample, reference materials (with masses similar to that of the sample) containing varying levels of radiocarbon are also prepared following identical preparation steps. The extent to which the reference materials deviate from the consensus value provides a direct measure of the accumulated contaminating carbon. With this information, correction of the radiocarbon values is possible (Brown and Southon 1997; Santos, Southon et al. 2007; de Rooij, van der Plicht et al. 2010). This correction to the reference samples is also applied to the stratospheric samples to remove the deviations arising from contamination, assuming that all samples accumulate similar contaminations following similar preparation steps. Hence an accurate determination of the sample mass is essential.

Following completion of the graphitization reaction, the graphitized iron pellets were pressed on AMS aluminum holders, so-called "targets". Since these pellets are too small and the amount of material is not enough to fill the hole of the targets, a clean unused iron pellet was first dropped into the target hole on top of which the graphitized pellet was placed. This procedure with two pellets allowed stable measurements, as the pressed target surface was much smoother this way (with only one pellet excessive fracturing of the pressed surface occurred, shown in Figure 5 of Appendix II). Each target is measured for forty minutes in the AMS and the data is analyzed offline.

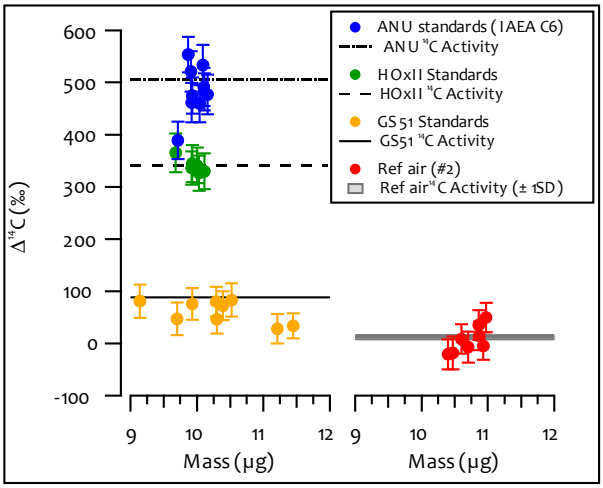

Figure 4: A summary of the derived ^{14}C activities (in $\Delta^{14}C$, ‰) of the reference materials and CO_2 extracted from reference air (#2) relative to HOxII. All the reference samples were prepared following identical preparation steps.

The concentration of CO_2 in stratospheric air, as observed in the two collected AirCore profiles (shown in Fig. 1), was between 387 and 397 ppm corresponding to 9.51-9.76 µg C in each section of the SAS. Since the mass of CO_2 from each section of the SAS was quite constant, reference samples and CO_2 samples from reference air (#2, from dummy loop) were prepared in the same mass range as the samples, a prerequisite for contamination correction. For correcting the ^{14}C in CO_2 measurements of the stratospheric air samples and CO_2 from reference air (#2), a set of three different reference materials was prepared with ^{14}C levels relevant for the present measurements. This set comprised of ANU Sucrose ($\Delta^{14}C$ = 506.1 ‰, IAEA C6), HOxII ($\Delta^{14}C$ = 340.6 ‰, SRM 4990C), GS51 ($\Delta^{14}C$ Activity = 88 ‰, local reference material prepared from cane sugar acquired in November 2002). Furthermore, a background material, Rommenhöller CO_2 (virtually free of ^{14}C) was also used. All the ^{14}C activities shown in this chapter are reported as $\Delta^{14}C$ (‰) (Mook and van der Plicht 1999), which indicates the enrichment/depletion in $^{14}C/C$ of CO_2 with respect to the preindustrial level of 0 ‰. Only HOxII measurements were used to correct all the other ^{14}C activities. The two other reference materials, IAEA C6 and GS51, were used to verify the effectiveness of the correction with a single reference standard, i.e. HOxII. Unlike the reference materials, which were

directly graphitized from CO_2, the CO_2 samples extracted from reference air (#2) were treated following identical preparation steps, as were the CO_2 samples from stratospheric air. Figure 4 shows a summary of all the corrected ^{14}C activities of the reference materials and CO_2 from reference air (#2) relative to HOxII standards.

4.2 Results

The two AirCore samples collected on July 15th and 16th, 2014 were used to determine the radiocarbon content in the two sets of stratospheric CO_2 samples. Stratospheric air samples from the two AirCore flights were transferred into the SAS for storage, after which the SAS were brought to Groningen for further analysis. CO_2 was extracted from the samples and graphitized, pressed and measured with the AMS. The air samples stored in the SAS represented an integrated sample corresponding to an altitude range, the extent of which depended on the ambient pressure at the altitude the sample was collected. The section of the AirCore profile that is transferred into the SAS can be determined based on the time it required for the sample to flow from the AirCore through the CRDS analyzer into the SAS. To verify the correctness of the altitude range derived from timing, CH_4 was used as a proxy for altitude. The decrease in the concentration of CH_4 in the stratosphere with increasing altitude is continuous and steep, making CH_4 a suitable proxy for the altitude check. In fact, CH_4 could even be used directly for altitude determination instead of the timing information. This was, however, less preferred due to the production of CH_4 from stainless steel surfaces as mentioned previously, which could corrupt the CH_4 signal in an unpredictable manner and to an unknown extent. Figure 5 (a) and (b) show the results of the altitude determination from the two stratospheric AirCore samples collected on July 15th and 16th, 2014. The blue circles show the AirCore CH_4 profile, the black solid line shows the corrected AirCore profile and the red solid line shows the predicted CH_4 concentration in each section of the SAS, based on the AirCore profile and the recorded sampling time and flow rate. Figure 5 (c) and (d) show the correlation between the CH_4 concentration as predicted based on

timing, shown in (a) and (b), against concentrations measured with the CRDS analyzer during extraction.

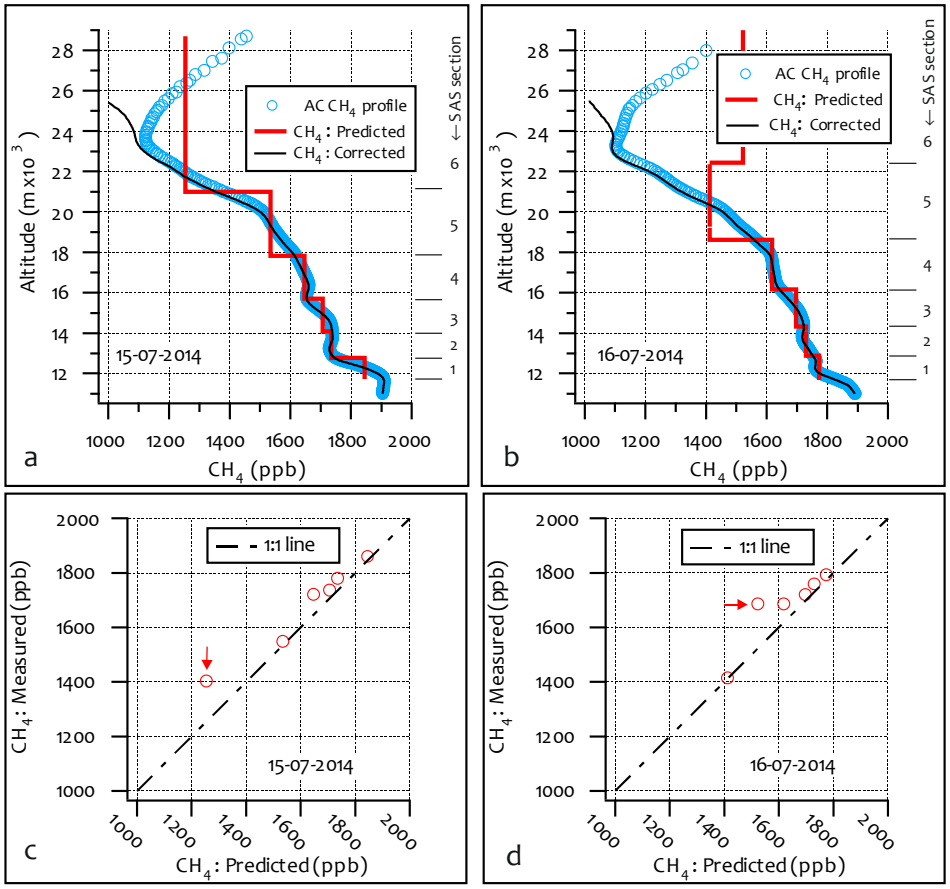

Figure 5. a) AirCore (AC) CH_4 profile (shown with blue open circles), the corrected AirCore profile (shown with a solid black line) and calculated CH_4 concentration for each section of the SAS for the samples collected on July 15, 2014. b) The same for the samples collected on July 16, 2014. c, d) Correlation between the calculated CH_4 concentration and the CH_4 concentration as measured by the CRDS analyzer while extracting the CO_2 from the samples. The measured CH_4 concentration values, for both profiles, are in good agreement with the calculated CH_4 concentrations for all samples except for the ones (indicated by arrows) corresponding to upper stratosphere, which are contaminated with leftover fill gas.

For most samples, the predicted CH_4 concentration was in good agreement with the concentration measured by the CRDS analyzer during extraction. The largest

deviation was observed for the sample representing the upper stratosphere (i.e.SAS section no. 6; marked with a red arrow in Fig. 5c & d) due to contaminations from leftover fill gas, which contains compressed dry ambient air (sampled at Sodankylä, Finland) spiked with carbon monoxide. This influence from the fill gas above 24 km causes the difference between the measured and the corrected vertical CH_4 profiles of the atmosphere shown in Fig. 5a & b. The AirCore profiles, shown in Fig. 5, were obtained as the air from the AirCore moved through the CRDS analyzer into the sampler. During this transfer, behind the analyzer there is a small additional mixing of samples through diffusion which is not captured in the presented AirCore profile data. While diffusion in principle has slightly affected all the samples, the ones near the upper stratosphere are affected the most due to the large difference in the CH_4 concentration of the sample and the fill gas. This contamination of upper stratospheric air (SAS section no. 6) with the leftover fill gas in the AirCore, due to diffusion, is predominantly the cause of the large observed deviation.

As timing is our primary parameter for altitude calculation, reliable knowledge of the timing during the filling of the SAS is crucial, i.e., the time when the valves at both ends of the SAS were closed during the filling process. "Timing" also includes here the accurate knowledge of the flow rate at which the sample from the AirCore is transferred to the SAS. A timing problem was observed in the dataset shown in Fig. 5b, which could have been caused by any of the previously mentioned reasons. By introducing a "best fit" timing offset of -33 sec, we moved the whole predicted profile slightly upwards, and then the resultant predicted altitude range showed a good agreement with the measured concentrations, as seen in Fig. 5d. Control of the SAS filling process should, however, be improved, a topic for future research.

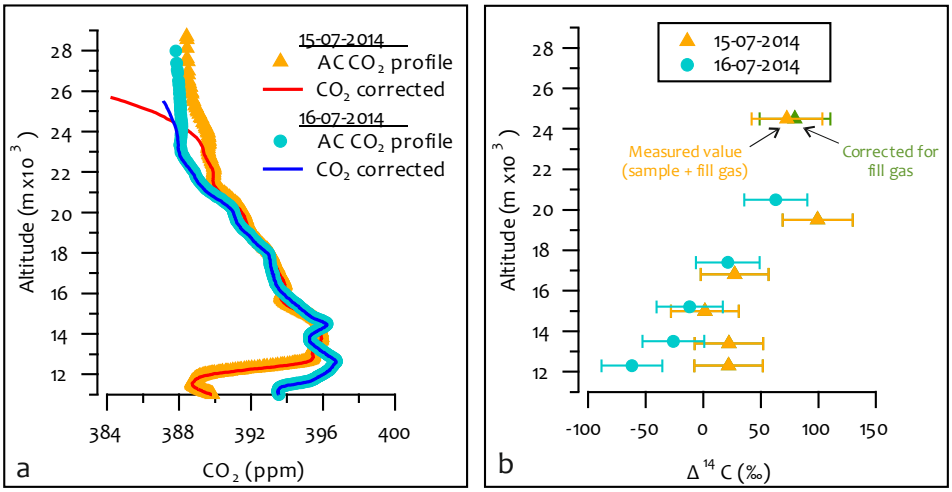

Figure 6. a) AirCore (AC) CO_2 profiles (orange triangles for July 15, 2014 and cyan circles for July 16, 2014) and their corresponding corrected AirCore CO_2 profiles (red line for July 15, 2014 and blue line for July 16, 2014). b) The $\Delta^{14}C$ values (‰, orange triangles representing samples from July 15, 2014 and cyan circles representing samples from July 16, 2014) in each section of the SAS. The $\Delta^{14}C$ value (green triangle) shown next to the sample from upper stratosphere sampled on July 15, 2014, is corrected for the fill gas contamination. The last CO_2 sample extracted from the AirCore sampled on July 16, 2014 was lost. The uncertainties in the $\Delta^{14}C$ values correspond to measurement uncertainties arising from limited counting statistics.

Fig. 6a shows the CO_2 concentrations retrieved from the two AirCore samples described in this chapter (orange triangles for July 15, 2014 and cyan circles for July 16, 2014) and the respective corrected AirCore profile (red line for July 15, 2014 and blue line for July 16, 2014). Figure 6b shows the measured radiocarbon concentration in the extracted CO_2 samples, with orange triangles representing samples from July 15, 2014 and cyan circles representing samples from July 16, 2014. The present $\Delta^{14}C$ value for tropospheric CO_2 is ≈ 20‰ (Hua, Barbetti et al. 2013; Levin, Kromer et al. 2013; Graven 2015). The uncertainties in the $\Delta^{14}C$ values, shown in Fig. 6b, are about ±30‰, entirely caused by counting statistics. The sample from the upper stratosphere of the AirCore sampled on July 16th (sample 6) was lost during the graphitization process due to a leak in the reactor. As the production of ^{14}C from the reaction of ^{14}N with cosmogenic neutron is maximum in the stratosphere, CO_2 in the stratosphere is enriched in ^{14}C relative to

the tropospheric CO_2. The transport of this enriched stratospheric CO_2 into the troposphere (stratosphere-to-troposphere transport, STT) increases the $\Delta^{14}C$ value of the troposphere whereas the transport of tropospheric CO_2 into the lower stratosphere (troposphere-to-stratosphere transport, TST) dilutes the $\Delta^{14}C$ value of the stratosphere. This mixing in the two layers of atmosphere, very distinct in their chemical composition, through STT and TST is known as stratospheric-tropospheric exchange (STE). Caused by the nuclear bomb tests conducted during 1950's and early 1960's, the atmospheric $\Delta^{14}C$ was enriched due to anthropogenic production of ^{14}C, famously known as the bomb spike. As most of the ^{14}C was produced in the stratosphere, the stratosphere-troposphere gradient was very large in those days (Ashenfelter, Gray et al. 1972; Nakamura, Nakazawa et al. 1992; Nakamura, Nakazawa et al. 1994). Following the Nuclear Test Ban Treaty signed in October 1963, the stratosphere-troposphere gradient gradually returned towards pre-bomb conditions, and the tropospheric $\Delta^{14}C$ has continuously dropped to a present value of ≈ 20‰. (Nakamura, Nakazawa et al. 1992; Nakamura, Nakazawa et al. 1994; Zahn, Neubert et al. 1999; Hesshaimer and Levin 2000).

As mentioned in the previous section, during the extraction and graphitization of the stratospheric samples, CO_2 from reference air (#2) was also extracted, graphitized and measured. AMS measurements of the 8 CO_2 samples extracted from reference air (#2, ≈ 10 µgC each), after contamination corrections yielded a mean $\Delta^{14}C$ value of 7 ± 9‰ that is in close agreement with the directly measured value of a 2 mgC sample extracted from reference air (#2) that yielded a $\Delta^{14}C$ value of 12 ± 4‰. This gives confidence in the applied contamination corrections.

The two CO_2 profiles shown in Fig. 6a are very similar, with slight differences near the tropopause (11-12 km, ≈ 4 ppm). The $\Delta^{14}C$ values in Fig. 6b corresponding to the lower stratosphere, sections 2, 3 and 4 of the SAS, also show very similar values for the two profiles (mean of these two times 3 values is 8 ± 8 ‰) that closely represents the current troposphere. The $\Delta^{14}C$ values corresponding to SAS section 5, in both profiles, shows some enrichment in $^{14}CO_2$ due to constant production of radiocarbon in the stratosphere. In Fig. 6b, the $\Delta^{14}C$ value drops for the last sample (collected on July 15, 2014), which confirms the contamination of

stratospheric CO_2 (enriched in ^{14}C) with the CO_2 from fill-gas (natural levels of ^{14}C, although the exact $\Delta^{14}C$ value is not known), as mentioned previously. The extent of contamination in the last sample from the fill gas was determined from the CO profile, since the concentration of CO in the stratosphere is low and fairly constant (≈ 15 ppb) whereas the concentration of CO in the fill gas is high and known (7972 ppb). This lead to a small correction (from 72.6 ‰ to 79.1 ± 30 ‰), shown with a green triangle, for contamination with ≈ 11% fill gas for which we assumed a $\Delta^{14}C$ value of 20 ‰. The three $\Delta^{14}C$ values observed for the lower altitude samples for the July 16, 2014 profile (Fig. 5b), especially the sample close to the troposphere-stratosphere boundary (11-13 km) have ^{14}C values that are, in part significantly, lower than present day tropospheric air. The occurrence of a polluted air mass causing this can be ruled out due to the absence of a simultaneous rise of CO at such altitudes. The most probable explanation is thus contamination somewhere in the SAS sampling or extraction process.

The results for these very first data sets are, due to various uncertainties (in timing and other issues such as possible sample contamination) not accurate enough to deduce any transport processes in the atmosphere; rather are these results a proof-of-principle showing that the AirCore sampling for radiocarbon determination in stratospheric air is feasible. As the sampling method is relatively cheap, regular sample collections are affordable, leading to better understanding of the ^{14}C budget and STE transport mechanisms involved.

4.3 Conclusions

The results presented in this chapter show that AirCore sampling is, in principle, a viable sampling method for the purpose of radiocarbon measurements in stratospheric CO_2. In this proof-of-principle experiment we achieved a measurement uncertainty of ≈ ± 30 ‰, mostly limited by the AMS counting statistics. The $^{14}CO_2$ content in the stratosphere (up to ≈ 18 ± 1 km) seems very well-mixed with $\Delta^{14}C$ values being ≈ 10 ± 8 ‰, very close to the present-day troposphere. Samples from higher than 18 km, are likely to be slightly enriched in $^{14}CO_2$ (≈ 80 ± 20 ‰), as expected in this production region of ^{14}C.

Since the sampling technique is relatively cheap, it is feasible to couple an AirCore "SAS" sampling program to a regular AirCore launch program, such as the one that is regularly being carried out at Sodankylä, Finland throughout the year. The stratospheric samples required for radiocarbon measurements could always be taken from any AirCore sampling and need not have to be dedicated campaigns with special protocols as long as the sample size obtained is adequate for AMS measurements. As indicated by the results in Fig. 5, one of the major challenges we faced in this work is the altitude determination for each section of the SAS. In that respect, it would help if we can avoid the contamination of the CH_4 signal due to the production of CH_4 from stainless steel valves and connectors. Replacing every stainless steel valve with valves made from polymeric material might be unfeasible, but some sections can certainly be modified in the future versions. For example, currently the extraction system is completely constructed from stainless steel components, which in future can be completely replaced with glass components. This would partially reduce the extent of contamination of stratospheric air with CH_4 produced because of metal-metal friction. The other important source of uncertainty in the projection of altitude is the accurate knowledge of the timing, based on which the altitude is calculated. Future experiments would require careful laboratory bookkeeping for more accurate altitude determination. Through these experiments we also learned that the samples that were collected at the top of profiles are contaminated with the fill gas, thus collecting an air column from a slightly lower altitude range would introduce less contamination. The $\Delta^{14}C$ values for the contaminated samples (last sections of SAS) can also be corrected if the extent of contamination is well defined, which would require a careful characterization of the sample transfer process, from the AirCore to the SAS, or accurate measurements of CO_2 and CH_4 concentrations for these same air samples. Thus it is certainly critical to treat the stratospheric samples very carefully, and rigorous testing of the sampling process is needed to rule out leakages, potential contaminations arising from memory effects of the sampler wall and the extent of sample profile integrity as the sample from the AirCore moved into the SAS through the CRDS analyzer. Additionally, the graphitization process also requires careful monitoring since incomplete reduction

would result in a lower sample mass than expected in addition to isotopic fractionation, and thus a less accurate contamination correction based on reference materials (that are then relatively larger in mass). Thus it is important to have very consistent reaction efficiencies. It is also important that the mass of the reference material, used for correction, closely matches that of the samples.

Difficulties with altitude determination and possibilities of various contamination sources notwithstanding, we successfully demonstrated a new way of stratospheric ^{14}C sampling, for which we have successfully dealt with small (≈ 10 µg C) samples. This is thanks to our small and efficient extraction system with near 100% extraction efficiency. With the installation of the newly designed small volume graphitization reactor, we also achieved reaction efficiencies better than 95 % for samples as small as ≈10 µg C. The ^{14}C ion counts can be increased further with the use of smaller Fe pellets (< 1 mg) due to the increase in the number density of the carbon atoms in the sputtered volume of the AMS target. This would improve the counting statistics and thus the AMS measurement uncertainties. Alternatively, the use of a state-of-the-art AMS facility with a gas ionization source (Ruff, Wacker et al. 2007; Ruff, Szidat et al. 2010) would lead to less contamination (thanks to the avoidance of the graphitization step) and a higher number of accumulated counts (thanks to the higher efficiency) and thus a higher precision even with such small samples. Renewal of the current AMS system in Groningen is foreseen in the near future.

4.4 References

Aerts-Bijma AT, Meijer HAJ, van der Plicht J. 1997. AMS sample handling in Groningen. Nuclear Instruments & Methods in Physics Research Section B-Beam Interactions with Materials and Atoms 123(1-4):221-5.

Ashenfelter TE, Gray J, Sowl RE, Svendsen M, Telegadas K. 1972. A Lightweight Molecular Sieve Sampler for Measuring Stratospheric Carbon-14. Journal of Geophysical Research 77(3):412-9.

Brenninkmeijer CAM, Lowe DC, Manning MR, Sparks RJ, vanVelthoven PFJ. 1995. The ^{13}C, ^{14}C and ^{18}O isotopic composition of CO, CH_4, and CO_2 in the higher southern latitudes lower stratosphere. Journal of Geophysical Research-Atmospheres 100(D12):26163-72.

Brenninkmeijer CAM, Crutzen P, Boumard F, Dauer T, Dix B, Ebinghaus R, Filippi D, Fischer H, Franke H, Frieβ U, Heintzenberg J, Helleis F, Hermann M, Kock HH, Koeppel C, Lelieveld J, Leuenberger M, Martinsson BG, Miemczyk S, Moret HP, Nguyen HN, Nyfeler P, Oram D, O'Sullivan D, Penkett S, Platt U, Pupek M, Ramonet M, Randa B, Reichelt M, Rhee TS, Rohwer J, Rosenfeld K, Scharffe D, Schlager H, Schumann U, Slemr F, Sprung D, Stock P, Thaler R, Valentino F, van Velthoven P, Waibel A, Wandel A, Waschitschek K, Wiedensohler A, Xueref-Remy I, Zahn A, Zech U, Ziereis H. 2007. Civil Aircraft for the regular investigation of the atmosphere based on an instrumented container: The new CARIBIC system. Atmospheric Chemistry and Physics 7(18):4953-76.

Brown TA, Southon JR. 1997. Corrections for contamination background in AMS C-14 measurements. Nuclear Instruments & Methods in Physics Research Section B-Beam Interactions with Materials and Atoms 123(1-4):208-13.

Chen H, Kivi R, Heikkinen P, Kers B, de Vreis M, Hatakka J, Laurila T, Sweeney C, Tans P. In preparation. High-latitude balloon observations of CO_2/CH_4/CO using AirCore: evaluation of Sodankylä TCCON retrievals.

de Rooij M, van der Plicht J, Meijer HAJ. 2010. Porous iron pellets for AMS ^{14}C analysis of small samples down to ultra-microscale size (10–25μgC). Nuclear Instruments & Methods in Physics Research Section B-Beam Interactions with Materials and Atoms 268(7-8):947-51.

Devlin DJ, Herley PJ. 1986. Thermal decomposition and dehydration of magnesium perchlorate hexahydrate. Thermochimica Acta 104:159-78.

Gottdang A, Mous DW, van der Plicht J. 1995. The HVEE C-14 system at Groningen. Radiocarbon 37(2):649-56.

Graven HD. 2015. Impact of fossil fuel emissions on atmospheric radiocarbon and various applications of radiocarbon over this century. Proceedings of the National Academy of Sciences of the United States of America 112(31):9542-5.

Hagemann F, Gray J, Machta L, Turkevich A. 1959. Stratospheric Carbon-14, Carbon dioxide, and Tritium. Science 130(3375):542-52.

Hartmann DL, Klein Tank AMG, Rusticucci M, Alexander LV, Brönnimann S, Charabi Y, Dentener FJ, Dlugokencky EJ, Easterling DR, Kaplan A, Soden BJ, Thorne PW, Wild M, Zhai PM. 2013. Observations: Atmosphere and Surface. In: Stocker TF, Qin D, Plattner G-K, Tignor M, Allen SK, Boschung J, Nauels A, Xia Y, Bex V, Midgley PM, editors. Climate Change 2013: The Physical Science Basis. Contribution of Working Group I to the Fifth Assessment Report of the Intergovernmental Panel on Climate Change. Cambridge, United Kingdom and New York, NY, USA: Cambridge University Press. p 159–254.

Hesshaimer V, Levin I. 2000. Revision of the stratospheric bomb $^{14}CO_2$ inventory. Journal of Geophysical Research-Atmospheres 105(D9):11641-58.

Higaki S, Oya Y, Makide Y. 2006. Emission of Methane from Stainless Steel Surface Investigated by Using Tritium as a Radioactive Tracer. Chemistry Letters 35(3):292-3.

Hua Q, Barbetti M, Rakowski AZ. 2013. Atmospheric Radiocarbon for the Period 1950–2010. Radiocarbon 55(4):2059-72.

IPCC. 2014a. Climate Change 2014: Impacts, Adaptation, and Vulnerability. Part A: Global and Sectoral Aspects. Contribution of Working Group II to the Fifth Assessment Report of the Intergovernmental Panel on Climate Change [Field, C.B., V.R. Barros, D.J. Dokken, K.J. Mach, M.D. Mastrandrea, T.E. Bilir, M. Chatterjee, K.L. Ebi, Y.O. Estrada, R.C. Genova, B. Girma, E.S. Kissel, A.N. Levy, S. MacCracken, P.R. Mastrandrea, and L.L. White (eds.)]. Cambridge, United Kingdom and New York, NY, USA: Cambridge University Press. 1132 p.

IPCC. 2014b. Climate Change 2014: Impacts, Adaptation, and Vulnerability. Part B: Regional Aspects. Contribution of Working Group II to the Fifth Assessment Report of the Intergovernmental Panel on Climate Change [Barros, V.R., C.B. Field, D.J. Dokken, M.D. Mastrandrea, K.J. Mach, T.E. Bilir, M. Chatterjee, K.L. Ebi, Y.O. Estrada, R.C. Genova, B. Girma, E.S. Kissel, A.N. Levy, S. MacCracken, P.R. Mastrandrea, and L.L. White (eds.)]. Cambridge, United Kingdom and New York, NY, USA: Cambridge University Press. 688 p.

Karion A, Sweeney C, Tans P, Newberger T. 2010. AirCore: An Innovative Atmospheric Sampling System. Journal of Atmospheric and Oceanic Technology 27(11):1839-53.

Levin I, Kromer B, Hammer S. 2013. Atmospheric $\Delta^{14}CO_2$ trend in Western European background air from 2000 to 2012. Tellus Series B-Chemical and Physical Meteorology 65.

Lingenfelter RE. 1963. Production of Carbon 14 by Cosmic-Ray Neutrons. Reviews of Geophysics 1(1):35-55.

Machida T, Matsueda H, Sawa Y, Nakagawa Y, Hirotani K, Kondo N, Goto K, Nakazawa T, Ishikawa K, Ogawa T. 2008. Worldwide Measurements of Atmospheric CO_2 and Other Trace Gas Species Using Commercial Airlines. Journal of Atmospheric and Oceanic Technology 25(10):1744-54.

Mook WG, van der Plicht J. 1999. Reporting ^{14}C activities and concentrations. Radiocarbon 41(3):227-39.

Mrozek DJ, Veen Cvd, Hofmann M, Chen H, Kivi R, Röckmann T. In preparation. CF-IRMS method for analysis of $\Delta^{17}O$ in stratospheric CO_2 from small air samples collected with an AirCore.

Nakamura T, Nakazawa T, Nakai N, Kitagawa H, Honda H, Itoh T, Machida T, Matsumoto E. 1992. Measurement of ^{14}C Concentrations of Stratospheric CO_2 by Accelerator Mass Spectrometry. Radiocarbon 34(3):745-52.

Nakamura T, Nakazawa T, Honda H. 1994. Seasonal variations in ^{14}C concentrations of stratospheric CO_2 measured with accelerator mass spectrometry. Nuclear Instruments and Methods in Physics Research Section B: Beam Interactions with Materials and Atoms 92(1-4):413-6.

Ruff M, Wacker L, Gaeggeler HW, Suter M, Synal HA, Szidat S. 2007. A gas ion source for radiocarbon measurements at 200 kV. Radiocarbon 49(2):307-14.

Ruff M, Szidat S, Gaggeler HW, Suter M, Synal HA, Wacker L. 2010. Gaseous radiocarbon measurements of small samples. Nuclear Instruments & Methods in Physics Research Section B-Beam Interactions with Materials and Atoms 268(7-8):790-4.

Santos GM, Southon JR, Druffel-Rodriguez KC, Griffin S, Mazon M. 2007a. Magnesium perchlorate as an alternative water trap in AMS graphite sample preparation; a report on sample preparation at KCCAMS at the University of California, Irvine. Radiocarbon 46(1):165-73.

Santos GM, Southon JR, Griffin S, Beaupre SR, Druffel ERM. 2007b. Ultra small-mass AMS ^{14}C sample preparation and analyses at KCCAMS/UCI Facility. Nuclear Instruments and Methods in Physics Research Section B: Beam Interactions with Materials and Atoms 259(1):293-302.

Sweeney C, Karion A, Wolter S, Newberger T, Guenther D, Higgs JA, Andrews AE, Lang PM, Neff D, Dlugokencky E, Miller JB, Montzka SA, Miller BR, Masarie KA, Biraud SC, Novelli PC, Crotwell M, Crotwell AM, Thoning K, Tans PP. 2015. Seasonal climatology of CO_2 across North America from aircraft measurements in the NOAA/ESRL Global Greenhouse Gas Reference Network. Journal of Geophysical Research: Atmospheres 120(10):5155-90.

Zahn A, Neubert R, Maiss M, Platt U. 1999. Fate of long-lived trace species near the Northern Hemispheric tropopause: Carbon dioxide, methane, ozone, and sulfur hexafluoride. Journal of Geophysical Research-Atmospheres 104(D11):13923-42.

Chapter 5:

Conclusion and outlook

In this thesis, various aspects of radiocarbon have been described, starting with detection, to contamination and finally to an application. Although the research described here is broadly diverse, radiocarbon is what links them all. Chapter 1 provides a general introduction. Chapter 2 describes the evaluation of IntraCavity OptoGalvanic Spectroscopy as a possible method to detect radiocarbon at natural levels and below. Chapter 3 describes the investigation of radiocarbon contamination from contemporary sources on background AMS samples. Chapter 4 describes the determination of radiocarbon concentration by AMS in stratospheric CO_2 samples collected using the AirCore sampling method. In the following paragraphs, description of each chapter with their conclusions and possible future implications and developments are described.

In **Chapter 2**, we report our investigation of the possibility of using IntraCavity OptoGalvanic Spectroscopy (ICOGS) as a tool to detect radiocarbon (^{14}C) in CO_2 and found that the method did not work. Since the results published by the Murnick group at Rutgers showed the method to be effective for natural ^{14}C concentrations, and we intended to use ICOGS for dating and atmospheric monitoring applications, initially we tested the sensitivity of ICOGS with CO_2 containing near contemporary ($^{14}C/^{12}C$ = 108.8 pMC) and background ($^{14}C/^{12}C$ < 0.1 pMC) levels of radiocarbon. We could not unambiguously differentiate these two CO_2 samples, with radiocarbon concentration 3 orders-of-magnitude apart. Many attempts were made to reproduce the Murnick group results, by adjusting parameters such as the cell pressure, flow rate, laser modulation frequency, laser wavelength, etc. The repeated failures in this concentration regime led us to investigate the concentration range much higher than contemporary in an attempt to track down the limit of detection our instrument could deliver. Thus we prepared a set of nine local reference CO_2 samples containing elevated levels of radiocarbon ($^{14}CO_2/^{12}CO_2 \approx 10^{-11}$ to 10^{-3}). To our surprise and disappointment, we did not detect any significant change in the optogalvanic signal as a function of changing radiocarbon concentration, not even at such high ^{14}C concentrations. Optogalvanic spectroscopy has previously been demonstrated as a viable tool to detect $^{13}CO_2$ in CO_2 and was also commercialized, known as Laser Assisted Ratio Analyzer

(LARA). Owing to the measurement precision of LARA (≈ 1‰ in $\delta^{13}C$), it was possible to use LARA for analysis of CO_2 in breath samples. But, with ICOGS, through our extensive tests we can now conclude that it is not a suitable analytical technique for detection of radiocarbon for most application purposes. It may only be useful, if the ^{14}C concentration in the samples are excessively high (probably $^{14}CO_2/^{12}CO_2$ > 0.1 %), which however can easier be done alternatively using a scintillation counter. Since the Groningen ICOGS setup is very similar to the setup at Rutgers, and from the experiments we performed at Rutgers in the initial phase of this thesis research period, we are confident that the results published in the journal Analytical Chemistry (2008) are erroneous and the conclusion that the method can detect radiocarbon with limit of detection similar to AMS is wrong.

Thus AMS still seems to be the “best” radiocarbon detection method, with a wide detection dynamic range and with the capability to handle small samples and samples even in the form of pure CO_2. Other methods, based on cavity ring-down spectroscopy has been successfully used for the detection of radiocarbon, but the detection limits achieved thus far are suitable for pharmaceutical applications and not yet promising for atmospheric and dating applications.

The $^{14}CO_2$ laser in the present ICOGS setup is unique as it can emit a large number of $^{14}CO_2$ specific lines. This laser could possibly be used for cavity ring-down spectroscopy of $^{14}CO_2$. Of course the greatest challenge lies in the availability of highly reflective mirrors used for the construction of a high-finesse cavity and a suitable detector at wavelengths around 11-12 µm. In developing such an instrument, the availability of the nine enriched CO_2 samples in-house, prepared during the ICOGS research, would be extremely useful during the optimization and the calibration process. Acquiring such radioactive materials from the only, foreign vendor has required cumbersome paperwork, complicated transport management and a long lead time. Such time and effort would be saved for a follow-up project.

In **Chapter 3**, we describe a study to understand the source of modern carbon contamination (containing contemporary levels of radiocarbon) on background AMS "graphite" samples (highly depleted levels of radiocarbon). It has been known

for long, that upon prolonged exposure to air, AMS samples become contaminated with carbon from the surroundings. Although this contamination from modern carbon happens on all samples, the effects are pronounced in the case of very old samples (≥ 35000 years) and smaller samples (< 200 µg C). During an AMS measurement, a sample is measured eighty times at ten different spots (eight times per spot), with each measurement lasting 30 sec. Such a 30 sec measurement is called a *block*. It is observed that during AMS measurements of background samples, the initial block measurements always yield higher ^{14}C counts than the later ones. The extent of these initial higher counts (during the first ≈ 16 blocks) of course depends on the time duration the sample was exposed to air. This indicates that the surface of the sample is relatively enriched in contrast to the inner bulk which is exposed while sputtering. In this chapter we investigate atmospheric carbon dioxide as a possible source of this contaminating modern carbon. Since carbon dioxide is by far the largest modern carbon containing fraction in the atmosphere, it being the culprit is plausible. Hence we performed a series of storage tests to investigate this phenomenon. Samples were stored in CO_2-spiked (1-5 %; with varying ^{14}C concentration), humidified air to aggravate the contamination process. We found that the pressed targets were more prone to contamination than the unpressed graphite samples. When stored under enriched (980 pMC) CO_2-spiked humidified air, the unpressed graphite samples also showed contamination uptake, although the extent of the contamination is not as severe as in the case of pressed targets in the same condition. We also learned that the contaminating carbon is not loosely bound to the surface and inside the pores and crevices. It seems likely that the contaminant is chemisorbed on the target surface and also penetrates into the sample matrix, although to a lesser extent. We also observed that a pure graphite rod (Alfa Aesar, 99.9995% metal basis) does not show any contaminant uptake when exposed to laboratory air for prolonged periods, contrary to pressed targets. Surprisingly, once the graphite rod has been measured, and is then exposed to laboratory air, it shows a buildup of modern carbon on the surface, similar to the pressed targets. This indicates that the uptake of carbon on the graphite surface must be mediated through an electrochemical reduction process that involves the metals, Fe in the case of the

normal samples (Fe is the catalyst for the production of graphite, and thus amply present in the target) and Cs in the case of a previously exposed graphite rod (Cs is the sputtering material in the source). During this study we also learned that a similar phenomenon is long known in the field of material science, where they observe deposition of carbonaceous material on any clean surface upon exposure to air. This carbonaceous layer is known as Adventitious Carbon. It has been seen that the formation of this carbonaceous layer happens very fast (within few minutes of exposure) and that the layer thickness and the chemical composition does not change significantly after prolonged exposures. The exact mechanism of the formation of adventitious carbon layer is not well understood, but possible explanations to our observations may already be available in the literature.

In this chapter, we have unambiguously shown CO_2 to be a prominent source of modern carbon contamination on AMS targets, if not the only one. Through these results we conclude that it may not be possible to completely get rid of adventitious carbon and one may only take measures to minimize it. Since every sample, after being pressed on the targets, is exposed to laboratory air for some time after preparation and during transfer, contamination is practically unavoidable. The best strategies we learned from this study are: 1) Before the graphitization step, the reactor and the Fe powder must be cleaned to remove any carbonaceous contaminant already present on the surface of the reactor and the iron powder; 2) Samples must be transferred to the AMS sample chamber as soon as they are pressed; 3) If storage is unavoidable due to technical faults or unavailable slots, it is best to store the samples in the form of unpressed powder preferably in an dry Argon or Nitrogen atmosphere; 4) Each sample should be sputter-cleaned before the actual measurement is performed and in fact these two steps must be combined (e.g., 96 block measurement instead of 80 blocks, the first 16 cleaning blocks are thus disregarded during analysis); 5) The use of efficient gas ion sources, that are continuously being improved, tremendously reduces the extent of contamination incurred by samples. Gas sources are explicitly used for small samples, for which avoiding contamination is even more beneficial. Some of the

above mentioned improvements have been partially implemented at the Groningen AMS facility with the others foreseen in near future.

In **Chapter 4**, determination of radiocarbon concentration in stratospheric CO_2, retrieved from an AirCore, is described. The AirCore sampling method, invented at NOAA, is a very innovative sampling technique used for atmospheric vertical profiling of various greenhouse gases e.g. CO_2 and CH_4. AirCore sampling in Europe has regularly been performed at Sodankylä, Northern Finland since September 2013. The stratospheric parts of two such AirCore samples, collected in July 2014 at Sodankylä, were used in this study to determine the radiocarbon concentration in stratospheric CO_2. The stratospheric parts of the AirCore samples were divided into six sections on-site and stored in stratospheric air samplers (SAS), which were brought to Groningen for further analysis. Each section of the SAS contained ≈ 35 µg CO_2 that would produce ≈ 9.6 µg carbon (µgC). We developed a small-volume extraction system (20 ml) that allowed quantitative extraction of CO_2 (≈ 100%) from the stratospheric air samples. To perform AMS measurements in our facility, CO_2 samples have to be converted to graphite. Since these samples were very small, it was not possible to use the regular reactors used for graphitization in our lab. Hence we also designed a new high-efficiency, small-volume graphitization system (efficiency > 95%, volume ≈ 1.5 ml) for the reduction of CO_2 to graphite. Following the graphitization step, the samples were measured using an AMS. Since the reported AMS measurements are always normalized to reference materials, we prepared reference materials in the very similar mass range as the samples themselves. Oxalic Acid II (HOxII, 134.06 pMC) measurements were used to correct all the other ^{14}C activities. The other reference materials, i.e., IAEA C6 (150.61 pMC) and GS51 (108.8 pMC) were used to verify the effectiveness of the implemented correction.

During this proof-of-principle experiment, we successfully developed and demonstrated a small-volume quantitative extraction system, an efficient and optimized graphitization system and graphitization procedure, and data normalization protocol. One of the biggest challenges we faced during this work was the determination of the corresponding altitude for each section of the SAS.

The altitudes were determined based on the time the sample required to travel from the AirCore into the SAS through the cavity ring-down spectrometer. The determined altitudes were verified using the CH_4 concentration in each section as a proxy. Although the CH_4 measurements were to some extent compromised by the CH_4 produced from the stainless steel valves, it was still a reasonably good altitude indicator due to the large differences in the CH_4 concentration in stratosphere with increasing altitude. The predicted first five (≈ 12-22 km) CH_4 concentrations are in good agreement with the measured values. The last section in both AirCore profiles, corresponding to upper stratosphere (≈ 22 km and above) was contaminated with the fill gas. The radiocarbon measurements of the stratospheric CO_2 samples show that the radiocarbon concentrations up to about 18 km (first four samples from each profile) are very similar (10 ± 8‰) and represent the current tropospheric value. The next sample in each profile, corresponding to about 18-22 km showed slight enrichment of 80 ± 20‰. The last section from one profile, corresponding to altitudes above 22, also showed an enhanced $\Delta^{14}CO_2$ value of 80 ± 30‰. The last section from the other profile was spoiled during preparation.

Through this study, we successfully demonstrated that the AirCore sampling method is indeed a viable sampling technique to collect air samples from stratosphere for the determination of radiocarbon in CO_2. There are several improvements possible that can definitely improve the quality of future radiocarbon measurements in stratospheric CO_2. As discussed in the Chapter 4 and mentioned here, production of CH_4 from the valves was a major source of contamination that corrupted the CH_4 signal in an unpredictable manner. The extraction system can be completely constructed from glass, which would partly reduce the production of the “extra” CH_4. Since CH_4 is produced through the friction on stainless steel valves and the quick-connect connectors, some of the stainless steel valves can be replaced with valves constructed from other materials such as brass. This would reduce the CH_4 contamination further and would thus improve the altitude prediction. A better bookkeeping and careful documentation of the sample transfer process and timing, i.e., when the sample is transferred from the AirCore into the SAS, is essential. During the graphitization reaction, carbon was deposited on

small porous iron pellets that weighed ≈ 1.4-1.5 mg. Reducing the size of the iron pellet further, e.g. ≈ 1 mg, would increase the number density of the carbon atoms on the sputtered surface and would increase the ion counts and thus the measurement precision. Again, use of a gas ion source would allow direct measurements with pure CO_2 instead of the traditional graphite sputtering method, and this would produce contamination-free high precision measurements (the latter through acquiring more counts). At CIO, a new accelerator facility including such a gas source is foreseen in the near future. Further, to make use of the radiocarbon measurements in models, more and more accurate measurements are required. Regular measurements would also allow monitoring the seasonal variations in the stratospheric radiocarbon concentrations caused by the stratosphere troposphere exchange.

Summary

The research described in this thesis is broadly divided into three different research projects linked together by their common factor: radiocarbon. Radiocarbon (^{14}C, $t_{½}$ = 5730 ± 40 years) is the only naturally occurring radioactive isotope of carbon, with very low abundance (natural concentration of $^{14}CO_2/^{12}CO_2 \approx 1.2 \times 10^{-12}$). ^{14}C is produced in the upper atmosphere through the reactions of ^{14}N with thermalized neutrons originating from cosmic radiation. The produced ^{14}C is oxidized to $^{14}CO_2$ and thus forms a trace component of CO_2. Radiocarbon in the form of $^{14}CO_2$ is then taken up by plants through photosynthesis, which is then transferred to animals that feed on plants and so on. Thus radiocarbon is taken up by all living organisms. When an organism dies, the uptake of radiocarbon stops and the leftover radiocarbon slowly decays to ^{14}N. This process forms the very basis of radiocarbon dating. In addition to dating organisms, ^{14}C is also used to determine the age of groundwater reservoirs and oceanic water masses (in which "age" is to be understood as the time passed since the last contact and thus CO_2 exchange with the atmosphere).

^{14}C is present in the atmosphere predominantly in the form of CO_2 and CO_2 is by far the largest carbon containing fraction of the atmosphere. CO_2 is a naturally occurring greenhouse gas produced mainly through respiration by aerobic organisms, decay of organic materials and volcanic activities. It is also produced anthropogenically through the combustion of fossil fuels and biomass burning. $^{14}CO_2$ is an important atmospheric tracer, which helps in the understanding and quantification of the levels of anthropogenic emissions from fossil fuels. This is due to the fact that fossil fuel is virtually radiocarbon-free, which upon combustion produces radiocarbon-free CO_2 which dilutes the atmospheric $^{14}CO_2$ concentration upon release. As the concentration of CO_2 in our atmosphere is rising rapidly, monitoring of these greenhouse gases and understanding of their sources, sinks and transport mechanisms become extremely important. Thus radiocarbon is used as an important tracer to better understand the global carbon cycle. Apart from

dating and atmospheric applications, radiocarbon is also used in various forensic and pharmaceutical applications.

Since the natural concentration of ^{14}C in CO_2 is ≈ 1 ppt, detection of such low concentrations requires specialized equipment. To date, Accelerator Mass Spectrometry is the best available method for the detection of ^{14}C with extremely high precision and a very wide dynamic range. For AMS measurements, samples are first combusted to CO_2 and this CO_2 is then reduced to graphite in the presence of Fe and H_2. The graphite is then pressed on aluminium targets (cathodes), and is then measured in the AMS. To avoid interferences from the highly abundant isobar ^{14}N, graphite targets are sputtered with Cs ions to produce $^{14}C^-$. The $^{14}C^-$ is then accelerated and with the help of a stripper gas, e.g., Ar converted to $^{14}C^{3+}$, which is detected with a gas ionization detector. The charge state of the produced carbon cation is dependent on the applied acceleration voltage and is thus different for different instrument types. Simultaneous measurement of $^{12}C^{3+}$ and $^{13}C^{3+}$ is also performed to determine the isotopic ratio. Before the successful demonstration of AMS, proportional gas counting was used for the detection of radiocarbon, which was also accurate, but had a very low measurement throughput and required very large samples. Alternative methods based on cavity ring-down spectroscopy have recently been demonstrated for radiocarbon detection, with detection limits suitable for pharmaceutical (labeled) applications, but not (yet) for atmospheric studies and dating.

As mentioned before, the research described in this thesis consists of three different research projects. In **Chapter 2**, evaluation of IntraCavity OptoGalvanic Spectroscopy (ICOGS) as a possible radiocarbon detection technique is described. ICOGS was first described by the Murnick group at Rutgers University, USA in 2008 as a radiocarbon detection method with sensitivity comparable to that of an AMS. Motivated by their results, four other research groups around the world started the development of ICOGS for their respective applications. At Groningen, the ICOGS project was started in close collaboration with the Murnick group at Rutgers. The construction of the ICOGS setup at Groningen was completed in mid 2012, prior to which the author had spent 11 months at Rutgers learning the

technical know-how of the instrument. Since the ICOGS system was intended for radiocarbon dating and atmospheric monitoring applications, initial tests were performed with CO_2 containing contemporary levels of radiocarbon (modern) and CO_2 containing depleted levels of radiocarbon (dead). Several experiments were performed to unambiguously differentiate these samples, separated by 3 orders of magnitude in radiocarbon concentration. Measurements were performed by adjusting several parameters which included the cell pressure, flow rate, laser modulation frequency and the laser wavelength. These experiments were performed in a continuous flow mode. None of the experiments performed at Groningen, with these two samples, provided any evidence of an unambiguous radiocarbon signal. Thus it was very clear that the limit of detection possible with the ICOGS instrument at Groningen was higher than the investigated concentration range. To determine the achievable limit of detection, we decided to explore a concentration regime much higher than contemporary. Thus, a series of nine local reference CO_2 samples were prepared in-house, with ^{14}C concentration 10 to 1 billion times the contemporary concentration, to explore the capabilities of ICOGS. Due to limited sample size and strict regulations concerning the release of radioactive substances, the following experiments with CO_2 enriched in ^{14}C were performed in batch mode. No significant optogalvanic signal was observed, not even with the highly enriched CO_2 samples, although one set of experiments performed showed a significant rise in the optogalvanic signal at 10^{-4} to 10^{-3} $^{14}CO_2/^{12}CO_2$ levels. Nevertheless, through the experiments described in Chapter 2, it was shown that ICOGS is not a viable analytical technique for radiocarbon detection. The high detection limits achievable with the ICOGS setup at Groningen makes it impracticable for any possible radiocarbon application. Thus the development project of ICOGS at Groningen has been terminated.

In **Chapter 3**, research with storage experiments, to understand the process of contamination of background AMS samples with modern carbon, is described. Reducing the levels of contamination is of course a serious challenge faced during any high-sensitivity measurement and the same holds true for detection of radiocarbon by AMS. The problem is even more challenging when the sample is

old (> 35000 years). This is due to the exponential relation between the radiocarbon content of a sample and its age. When samples containing contemporary levels of radiocarbon are contaminated with dead carbon, their radiocarbon content are merely slightly diluted, making them to appear only slightly older. When, however, an old sample is contaminated with modern carbon, the amount of radiocarbon is significantly increased, making them to appear much younger. In practice, the contamination of graphite samples is of course a combination by both dead and modern carbon. The effect of this contamination is visible over a very small age-range only when the sample is near contemporary. On the other hand, the effect of contamination on background samples is visible over a much wider range of age. In addition to background samples, smaller samples (1-200 µgC) are also affected heavily by contamination during the preparation steps, as the influence of a fixed amount of contamination increases with decreasing sample size.

In this chapter, a post-preparation contamination phenomenon is described. This phenomenon has been known for some time and was studied at the CIO, Groningen for the past few years. As mentioned earlier, for performing AMS measurements, the samples are combusted to CO_2 which is subsequently reduced to graphite. This graphite is finally pressed on aluminium targets which are used for the measurements. Measurements are performed at 8 different spots on the target and each spot is measured 10 times, producing eighty measurements in total. Each measurement on a spot is performed for 30 sec, which is referred to as a block. Thus the total measurement time for each target is 40 min. It is observed that, when a pressed background sample is left in open air for a day or so, the initial blocks (≈ 16) produce a higher number of counts than the later ones, indicating an enriched surface in contrast to the bulk. It was also observed that the pressed samples showed a much higher level of acquired contamination than the graphite powder exposed to similar conditions. Thus, to identify the source of this modern carbon contamination that the samples acquired after preparation, several storage tests were performed. During these tests, samples are stored in humidified air spiked with CO_2 containing various levels of radiocarbon. Since CO_2 is the by

far the largest modern carbon containing fraction in air, it certainly is plausible to assume it being the culprit. Hence storage tests were performed with air spiked with CO_2. From these storage tests, it was again confirmed that the pressed targets were more prone to contamination. It was also revealed that the graphite powder, when stored in humidified air spiked with enriched CO_2 (980 pMC), also acquired contamination but to a lesser extent. It was initially presumed that a reaction product, probably an oxide of Fe that survived the graphitization reaction was responsible for the carbon uptake from air. PXRD and EDXS measurements, however, revealed no evidence of leftover oxides, and provided a clear picture of the composition of the graphitization product. The graphitization product comprises of a combination of graphitic carbon, filamentous carbon and iron carbide (Fe_3C). Although it was unambiguously shown that CO_2 is one of the sources of modern carbon contamination if not the only one, it was still not clear what the underlying mechanism was. It was then discovered that a similar phenomenon is already known in the field of material science. It has been known for long that any clean surface when exposed to air gets contamination with a carbonaceous layer known as Adventitious Carbon. Although the source and mechanism of adventitious carbon formation is not very well understood, the documented literature provides possible explanations through analogous results as we have observed. We learned that this process leading to the formation of the adventitious carbon layer is extremely fast and happens within the first few minutes of exposure to air. The carbonaceous layer on Fe surfaces is also accompanied by an iron oxide (FeO) layer. Through experiments performed in our lab, we also learned that the contaminating carbon is not loosely attached on the target surface, but that the attachment is possibly thorough chemisorption. It is also seen that a pure graphite rod (commercially available) does not show a buildup of an adventitious carbon layer when left exposed in open air for prolonged periods. Surprising enough, when the same graphite rod is exposed to air for a day or so after it has been measured, it shows buildup of contaminating carbon similar to the pressed targets. This indicates that the process of buildup of this carbonaceous layer on targets is possibly mediated through the metals, Fe in the case of normal samples (Fe is the catalyst for the production of graphite, and thus amply present in the target) and Cs

in the case of a previously exposed graphite rod (Cs is the sputtering material in the source). From the extensive tests described in this chapter, we finally concluded that this process of contamination is simply unavoidable. Measures can be taken to minimize it but possibly none to completely evade it. From the understandings gained during this work, several recommendations have been proposed in chapter 5 that would lead to minimum sample contamination and thus smaller uncertainties in the measurements.

In **Chapter 4**, determination of radiocarbon in stratospheric CO_2 samples collected with the AirCore sampling method is described. The AirCore sampling method is a very innovative sampling method, first developed at NOAA. The AirCore sampling method is used to determine atmospheric vertical profiles of greenhouse gases such as CO_2 and CH_4. These measured profiles are further used in the validation of satellite measurements. The AirCore comprises of a very long (≈ 100 m), thin walled (≈ 0.254 mm) stainless steel tubing. The AirCore is first filled with a fill gas, with known CO_2, CH_4 and CO concentration. The AirCore is then released with the help of a weather balloon, with one end open and the other closed. As the AirCore travels higher in altitude, due to the decreasing pressure, the fill gas is evacuated from the AirCore. Once the balloon has ruptured in the stratosphere, the AirCore falls back, and during this descent the AirCore equilibrates with the ambient pressure and thereby gradually fills itself with air. The open end of the AirCore is automatically closed upon arrival. Within a few hours of the AirCore recovery, the profile is measured for CO_2, CH_4 and CO concentrations using a cavity ring-down spectrometer. In Europe, AirCore measurements are regularly being performed at Sodankylä, Northern Finland. Two such AirCore samples collected at Sodankylä were used for this study. The stratospheric part of the AirCore was transferred into a stratospheric air sampler (SAS) and was divided into six sections. Each section of the SAS contained ≈ 50 ml stratospheric air with ≈ 35 µg CO_2 (≈ 9.6 µg C). For such small air samples, a small-volume extraction system (≈ 20 ml) was developed, which enabled ≈ 100% CO_2 extraction efficiency while allowing simultaneous measurements of CH_4 in the air after CO_2 extraction. The extraction procedure was optimized using a dummy extraction loop, similar to SAS, filled with

reference air. The extracted CO_2 was then graphitized in a newly designed, small-volume reactor (≈ 1.5 ml) with reaction efficiencies > 95%. In this version of the reactor, $Mg(ClO_4)_2$ was used to remove the water produced in the graphitization reaction. The reaction time was typically around 20 minutes for samples < 30 µgC. Following the conversion of CO_2 to graphite, the samples were pressed and measured with the AMS. As described in the previous section, smaller samples are extremely vulnerable to contamination; thus to correct for such contaminations, reference samples were also prepared in the very similar mass range as were the samples. Since the reported radiocarbon activities are normalized to reference materials, HOxII (134.06 pMC) was used for normalization. Other reference samples were used to verify the correctness of the applied normalization. The radiocarbon measurements of the stratospheric CO_2 samples show that the radiocarbon concentrations up to about 18 km (first four samples from each profile) are very similar (10 ± 8‰) and represent the current tropospheric value. The next sample in each profile, corresponding to about 18-22 km showed slight enrichment of 80 ± 20‰. The last section from one profile, corresponding to altitudes above 22, also showed an enhanced $\Delta^{14}CO_2$ value of 80 ± 30‰. The last section from the other profile was lost during preparation. Through the results presented in this chapter, it was demonstrated that the AirCore sampling method is indeed a viable and a valuable sample collecting method that would make regular measurements of radiocarbon in stratospheric CO_2 possible. Several technical improvements, enlisted in chapter 5, would make high-precision measurements (better than what was achieved in this proof-of-principal work) in future possible.

Samenvatting

Het in dit proefschrift beschreven onderzoek is verdeeld in drie zeer verschillende projecten die met elkaar verbonden zijn door hun gemeenschappelijke factor: ^{14}C, ook wel "radiokoolstof" genoemd. ^{14}C (halveringstijd $t_{½}$ = 5730 ± 40 jaar) is de enige van nature voorkomende radioactieve isotoop van koolstof, met een zeer lage concentratie (de natuurlijke concentratieverhouding van $^{14}CO_2$ / $^{12}CO_2 \approx 1{,}2 \times 10^{-12}$). ^{14}C wordt aangemaakt in de hogere atmosfeer, door de reacties van ^{14}N met thermische neutronen afkomstig van kosmische straling. De geproduceerde ^{14}C wordt geoxideerd tot $^{14}CO_2$ en wordt daarmee een bestanddeel van het natuurlijke CO_2. ^{14}C in de vorm van $^{14}CO_2$ wordt vervolgens opgenomen door planten via fotosynthese, en belandt zo ook in dieren die zich voeden met planten, enzovoort. Op die manier wordt ^{14}C opgenomen door alle levende organismen. Zodra een organisme sterft stopt de opname van ^{14}C; het in het organisme aanwezige ^{14}C vervalt langzaam tot ^{14}N. Dit proces vormt de basis van koolstofdatering. Behalve voor het dateren van organismen wordt ^{14}C gebruikt om bijvoorbeeld de leeftijd van grondwaterreservoirs en oceaanwater te bepalen (waarbij "leeftijd" moet worden begrepen als de tijd verstreken sinds het laatste contact en dus CO_2-uitwisseling met de atmosfeer).

^{14}C is dus in de vorm van CO_2 aanwezig in de atmosfeer en CO_2 is verreweg de grootste koolstofhoudende fractie van de atmosfeer. CO_2 is een natuurlijk voorkomend broeikasgas dat voornamelijk wordt geproduceerd door middel van respiratie door aerobe organismen, afbraak van organische materialen en door vulkanische activiteit. Ook wordt het door de menselijk handelen geproduceerd, namelijk door de verbranding van fossiele brandstoffen en door verbranding van biomassa. $^{14}CO_2$ is een belangrijke atmosferische tracer, die helpt bij het begrijpen en kwantificeren van de antropogene CO_2-emissies door het verbranden van fossiele brandstoffen. Dit komt door het feit dat de fossiele brandstoffen nagenoeg geen ^{14}C bevatten, zodat bij verbranding ^{14}C-vrij CO_2 ontstaat dat de atmosferische $^{14}CO_2$ concentratie verdunt. Aangezien de CO_2-concentratie in onze atmosfeer

snel stijgt, is het monitoren van dit broeikasgas, en het begrijpen van bronnen, putten en transportmechanismen ervan belangrijk. Op die manier is ^{14}C in gebruik als een belangrijke tracer om beter inzicht in de wereldwijde koolstofcyclus te krijgen. Behalve ouderdomsdatering en atmosferische toepassingen wordt ^{14}C ook in diverse forensische en farmaceutische toepassingen gebruikt.

De natuurlijke concentratie van ^{14}C in CO_2 is slechts ongeveer 1 ppt, en detectie van zulke lage concentraties vereist gespecialiseerde apparatuur. Op dit moment is massaspectrometrie m.b.v. een deeltjesversneller (Accelerator Mass Spectrometry, AMS) de beste methode die beschikbaar is voor de detectie van ^{14}C, gekenmerkt door zeer hoge nauwkeurigheid en een breed dynamisch bereik. Voor AMS-metingen worden monsters eerst verbrand tot CO_2 en dit CO_2 wordt vervolgens gereduceerd tot grafiet bij aanwezigheid van Fe en H_2. Het grafiet wordt vervolgens in aluminium houders ("targets" of ook "kathoden") geperst en wordt dan gemeten in de AMS. Om storingen door de zeer overvloedig aanwezige isobaar ^{14}N te voorkomen, worden de grafiet targets beschoten met Cs-ionen zodat negatieve $^{14}C^-$ -ionen worden geproduceerd (^{14}N vormt geen negatieve ionen). Dit $^{14}C^-$ wordt vervolgens versneld en dan door botsingen met een strippergas, bijvoorbeeld Ar, omgezet tot $^{14}C^{3+}$-ionen, welke worden gedetecteerd met een gasionisatie-detector. De ladingstoestand van het geproduceerde koolstof-kation is afhankelijk van de toegepaste versnellingsspanning en derhalve verschillend voor verschillende AMS-installaties. De ionen van de stabiele koolstofisotopen $^{12}C^{3+}$ en $^{13}C^{3+}$ worden gelijktijdig ook gemeten, om de isotoopverhoudingen te bepalen.

Voordat AMS succesvol werd ingevoerd, waren voor de detectie van ^{14}C proportionele gastelbuizen in gebruik. Dit was ook een nauwkeurige meetmethode, maar de metingen duurden lang en vereisten veel monstermateriaal. Alternatieve methoden, gebaseerd op Cavity Ring-Down Spectroscopie (CRDS) zijn recentelijk gedemonstreerd voor het meten van ^{14}C, echter met detectiegrenzen die het geschikt maken voor farmaceutische toepassingen (met ^{14}C-labelling), maar (nog) niet voor atmosferische studies en datering.

Het in dit proefschrift beschreven onderzoek bestaat, zoals boven vermeld, uit drie verschillende onderzoeksprojecten. In hoofdstuk 2 is de evaluatie van IntraCavity Opto-Galvanische Spectroscopie (ICOGS) als een nieuwe mogelijke detectietechniek voor ^{14}C-datering beschreven. ICOGS werd voor het eerst beschreven door de groep van Murnick aan de Rutgers Universiteit, (Newark, New Jersey, VS) in 2008, als een ^{14}C detectiemethode met een gevoeligheid vergelijkbaar met die van AMS. Gemotiveerd door hun resultaten zijn vier andere onderzoeksgroepen over de hele wereld begonnen met de ontwikkeling van ICOGS voor hun diverse toepassingen. In Groningen werd een ICOGS project gestart in nauwe samenwerking met de Murnick groep. De bouw van de ICOGS setup in Groningen werd medio 2012 voltooid. Daaraan voorafgaand had de auteur 11 maanden in de groep van Murnick gewerkt en daar de technische know-how van het instrument verworven. Aangezien in Groningen het ICOGS systeem bestemd zou worden voor datering en atmosferische monitoring, werden de eerste tests uitgevoerd met CO_2 met een hedendaags ("modern") ^{14}C niveau en met CO_2 dat vrijwel geen ^{14}C bevatte ("dood"). Een groot aantal experimenten werd uitgevoerd waarin gepoogd werd deze monsters, die zo'n drie ordes van grootte verschillen in hun ^{14}C-concentratie, ondubbelzinnig te onderscheiden. Metingen werden uitgevoerd in een scala van omstandigheden, waarbij parameters zoals celdruk, gasflow, de modulatiefrequentie en golflengte van de laser werden gevarieerd. Deze experimenten werden uitgevoerd bij een continue stroom van monstergas door de meetcellen ("continuous flow mode"). Geen van deze Groningse experimenten met deze twee monsters gaf ook maar enig bewijs van een eenduidig ^{14}C-signaal. Dit maakte heel duidelijk dat de ^{14}C-detectielimiet met het ICOGS instrument in Groningen hoger lag dan het onderzochte concentratiegebied. Om de detectielimiet te kunnen bepalen hebben we besloten om te gaan werken met veel hogere ^{14}C-concentraties. Daartoe is door ons een reeks van negen CO_2-monsters bereid, met ^{14}C-concentraties van 10 tot 1 miljard keer de hedendaagse concentratie. Gezien de beperkte hoeveelheid bereid monstergas en de strikte voorschriften met betrekking tot het vrijkomen van radioactieve stoffen moesten experimenten met deze ^{14}C-verrijkte CO_2-monsters uitgevoerd worden met een vaste portie gas in de cellen ("batch mode"). Zelfs met

de meest verrijkte CO_2-monsters werd geen significant opto-galvanisch signaal waargenomen, alleen één reeks experimenten vertoonde een significante stijging van het optogalvanisch signaal tussen de twee meest ^{14}C-verrijkte monsters (die met $^{14}CO_2$ / $^{12}CO_2$ verhoudingen van 10^{-4} en 10^{-3}). Het is al met al door de in hoofdstuk 2 beschreven experimenten duidelijk aangetoond dat ICOGS geen levensvatbare analysetechniek voor ^{14}C is. Vanwege de hoge detectielimieten die de ICOGS setup in Groningen laat zien is ICOGS onbruikbaar. Daarom is het ICOGS-project in Groningen stopgezet.

In hoofdstuk 3 wordt onderzoek naar het proces van verontreiniging van achtergrond ("dode") AMS-monsters met moderne koolstof beschreven. Het zo laag mogelijk houden van verontreinigingsniveaus is uiteraard een serieuze uitdaging bij iedere meting met hoge gevoeligheid, en zo geldt dit ook voor ^{14}C-metingen met AMS. Het probleem is nog navranter wanneer het monster oud is (> 35.000 jaar). Dit komt door de exponentiële relatie tussen de radioactieve inhoud van een monster en de leeftijd. Wanneer monsters met modern ^{14}C-niveau worden verontreinigd met dode koolstof wordt hun ^{14}C-niveau slechts licht verdund, waardoor ze slechts in geringe mate ouder lijken. Wanneer echter een oud monster verontreinigd wordt met moderne koolstof wordt de hoeveelheid ^{14}C aanzienlijk verhoogd, waardoor ze significant jonger schijnen. In de praktijk is de verontreiniging van grafietmonsters natuurlijk een combinatie van zowel dood als modern koolstof. Op een modern of vrijwel modern monster heeft deze verontreiniging alleen een merkbare invloed in een zeer kleine ouderdomsinterval. Het effect van verontreiniging op oude (achtergrond-) monsters is echter merkbaar over een grote range van ouderdom. Behalve zulke zeer oude monsters worden ook kleinere monsters (1-200 µgC) sterk beïnvloed door verontreiniging tijdens de voorbereidende stappen, omdat de invloed van een vaste hoeveelheid verontreiniging toeneemt bij afnemende monstergrootte.

In dit hoofdstuk 3 wordt een verontreinigingsfenomeen beschreven dat inwerkt op reeds tot grafiet geprepareerde monsters. Dit fenomeen is al enige tijd bekend en er is de afgelopen jaren bij het CIO ook al aan gewerkt. Zoals eerder vermeld worden voor het uitvoeren van AMS-metingen de monsters verbrand tot CO_2, dat

vervolgens wordt gereduceerd tot grafiet. Het grafiet wordt dan in aluminium targets geperst die voor de meting worden gebruikt. De metingen worden uitgevoerd op 8 verschillende plekken op het grafietoppervlak en elke plek wordt 10 keer gemeten, in het totaal dus 80 metingen. Elke individuele meting op één plek duurt 30 seconden, aangeduid als een "blok". De totale meettijd voor een monster is dus 40 minuten. Wanneer een geperst achtergrondmonster in de open lucht wordt gelaten, voor een dag of zo, blijkt dat de eerste blokken (≈ 16) een hoger ^{14}C-signaal (een groter aantal "counts") leveren dan de latere. Dit wijst op een verrijking aan het oppervlak t.o.v. het totale monster. De geperste monsters vertoonden ook een veel hogere verontreiniging dan grafietpoeder blootgesteld aan soortgelijke omstandigheden. Om de bron van deze verontreiniging met moderne koolstof die de monsters oplopen na preparatie op te sporen zijn diverse opslagtests uitgevoerd. Bij deze tests werden monsters bewaard in bevochtigde lucht, verrijkt met CO_2 met verschillende ^{14}C-niveaus. Aangezien CO_2 veruit de grootste moderne-koolstof-fractie in lucht is, ligt het voor de hand CO_2 van het veroorzaken van de verontreiniging te verdenken. Daarom zijn de opslagtests uitgevoerd in lucht met extra toegevoegd CO_2. Door deze opslagtests werd opnieuw bevestigd dat de in een target geperste monsters gevoeliger zijn voor verontreiniging dan het nog niet geperste grafietpeoder. Grafietpoeder bleek weliswaar ook verontreinigd te worden als het wordt bewaard in bevochtigde lucht met toegevoegde, in ^{14}C verrijkte CO_2 (980 pMC), maar in veel mindere mate. Aanvankelijk werd verondersteld dat een reactieproduct, waarschijnlijk een oxide van Fe dat de grafitisatie had overleefd, verantwoordelijk was voor opname van koolstof uit de lucht. PXRD en EDXS metingen leverden echter geen bewijs voor overgebleven oxiden, maar gaven wel een duidelijk beeld van de samenstelling van het grafitisatieproduct. Het grafitisatieproduct bestaat uit een combinatie van grafiet-koolstof, koolstof in de vorm van filamenten, en ijzercarbide (Fe_3C). Hoewel ondubbelzinnig werd aangetoond dat CO_2 één van de bronnen van verontreiniging met modern koolstof is (zo niet de enige), was het nog steeds niet duidelijk wat het onderliggende mechanisme was. Verder zoekend werd ontdekt dat een soortgelijk verschijnsel binnen het vakgebied van materiaalkunde al lang bekend is: ieder schoon oppervlak wordt bij blootstelling aan lucht verontreinigd met een

koolstofhoudende laag, die "Adventitious Carbon" ("onvoorziene koolstof") wordt genoemd. Hoewel de bron en het mechanisme van de vorming van onvoorziene koolstof niet goed worden begrepen biedt de materiaalkunde-literatuur mogelijke verklaringen aan de hand van resultaten analoog aan wat wij hebben gezien. Het proces dat leidt tot de vorming van de laag onvoorziene koolstof blijkt extreem snel te zijn: het gebeurt in de eerste paar minuten na blootstelling aan lucht.

De koolstof-laag op Fe oppervlakten is vergezeld van een ijzeroxide (FeO) laag. Door experimenten in ons laboratorium hebben we vastgesteld dat de verontreinigende koolstof niet losjes geadsorbeerd zit op het monsteroppervlak, maar sterk gebonden is door chemisorptie. Een staaf puur grafiet (een commercieel product) die voor een langere periode in de open lucht wordt bewaard laat geen opbouw van een onvoorziene koolstoflaag zien. Wanneer dezelfde grafietstaaf echter na het meten in de AMS een dag of wat blootgesteld wordt aan de lucht ontstaat er wèl een laag verontreinigende koolstof, net als bij de geperste monsters. Dit geeft aan dat de opbouw van deze koolstofhoudende laag waarschijnlijk wordt gemedieerd door de aanwezigheid van metalen, Fe bij normale monsters (Fe is de katalysator voor de productie van grafiet en daarmee ruimschoots aanwezig in het geperste monster) en Cs bij een eerder gemeten grafietstaaf (Cs is het sputtermateriaal in de bron van de AMS).

De uitgebreide tests die in hoofdstuk 3 worden beschreven hebben ons uiteindelijk tot de conclusie gebracht dat dit verontreinigingsproces helaas onvermijdelijk is. Maatregelen kunnen worden genomen om het te minimaliseren, maar niet om het volledig te vermijden. De inzichten opgedaan tijdens dit werk hebben geleid tot een aantal aanbevelingen die we doen in hoofdstuk 5, waarmee de verontreiniging van monsters kan worden geminimaliseerd en dus de meetnauwkeurigheid wordt verhoogd.

Hoofdstuk 4 is de beschrijving van ^{14}C-metingen aan stratosferische CO_2-monsters die verzameld zijn met de AirCore bemonsteringsmethode. AirCore is een zeer innovatieve bemonsteringsmethode, die ontwikkeld is bij NOAA (Earth System Research Laboratory, Boulder, CO, VS). De AirCore bemonsteringsmethode wordt

gebruikt om atmosferische verticale concentratieprofielen van broeikasgassen zoals CO_2 en CH_4 te bepalen. Deze gemeten profielen worden o.a. gebruikt in de validatie van satellietmetingen. De AirCore bestaat uit een zeer lange (≈ 100 m), dunwandige (≈ 0,254 mm) RVS buis. De AirCore wordt aanvankelijk gevuld met een vulgas, met bekende CO_2, CH_4 en CO-concentraties. Dan wordt de AirCore, met één uiteinde open en het andere gesloten, opgelaten met een weerballon. Tijdens het stijgen van de AirCore stroomt als gevolg van de afnemende druk het vulgas geleidelijk uit de AirCore weg. Nadat de ballon in de stratosfeer is gescheurd valt de AirCore terug, en tijdens deze afdaling blijft de AirCore in evenwicht met de omgevingsdruk en daardoor vult hij zich geleidelijk met lucht. Het open einde van de AirCore wordt automatisch gesloten bij aankomst op de grond. Binnen enkele uren na het terugvinden van de AirCore worden de CO_2-, CH_4- en CO-profielen gemeten met behulp van een "Cavity Ring-Down" spectrometer.

In Europa worden AirCore metingen regelmatig uitgevoerd in Sodankylä, Noord-Finland. Twee van zulke AirCore-monsters die verzameld zijn op Sodankylä werden gebruikt in deze studie. Het stratosferische deel van de AirCore-inhoud werd daartoe overgebracht in een stratosferischelucht-sampler (SAS), die is verdeeld in zes secties. Elke sectie van de SAS bevatte ≈ 50 ml stratosferische lucht met ≈ 35 µg CO_2 (≈ 9,6 µg C). Voor deze kleine luchtmonsters is een speciaal klein-volume extractiesysteem (≈ 20 ml) ontwikkeld, waarmee ≈ 100% CO_2 extractie-efficiëntie kon worden bereikt, terwijl bovendien in de lucht na de CO_2-extractie gelijktijdig metingen van de CH_4-concentratie konden worden verricht. De extractie-procedure is geoptimaliseerd met behulp van een dummy extractieloop, vergelijkbaar met de SAS, gevuld met referentielucht. De geëxtraheerde CO_2 werd vervolgens gegrafitiseerd in een eveneens nieuw ontworpen, klein-volume reactor (≈ 1,5 ml) met een grafietopbrengst van > 95%. In de reactor is magnesiumperchloraat ($Mg(ClO_4)_2$) in gebruik om het water af te vangen dat in de grafitisatiereactie wordt gevormd. De reactietijd is rond de 20 minuten voor monsters <30 ug C. Na de omzetting van CO_2 in grafiet werden de monsters geperst en gemeten met de AMS. Zoals beschreven in de vorige paragraaf zijn kleine monsters zeer gevoelig voor verontreiniging; om te corrigeren voor deze

verontreinigingen werden ook referentiemonsters gemaakt in hetzelfde massabereik als de monsters. Als referentiemateriaal, nodig voor de normalisatie van de ^{14}C-activiteiten is HOxII (134,06 pMC) gebruikt. Er zijn ook andere referentiemonsters gebruikt om de juistheid van de toegepaste normalisatie te controleren.

De ^{14}C-metingen van de stratosferische CO_2-monsters laten zien dat de ^{14}C-concentraties tot ongeveer 18 km hoogte (dat zijn de eerste vier monsters van elk profiel) constant zijn (10 ± 8 ‰) en overeen komen met de actuele waarde in de troposfeer. Het volgende monster in beide profielen, afkomstig van ongeveer het 18-22 km hoogteinterval, vertoonde een geringe verrijking van 80 ± 20 ‰. Het hoogste deel van het ene profiel, afkomstig van hoogtes boven 22 km, toonde ook een verhoogde $\Delta^{14}CO_2$ waarde van 80 ± 30 ‰. Het hoogste deel van het andere profiel ging verloren tijdens de preparatie.

De resultaten in dit hoofdstuk laten zien dat de AirCore bemonsteringsmethode inderdaad een levensvatbare en waardevolle methode is, die regelmatige metingen van ^{14}C van stratosferisch CO_2 mogelijk kan maken. Diverse technische verbeteringen, toegelicht in hoofdstuk 5, zullen nauwkeurige metingen (nauwkeuriger dan in het huidige "proof-of-principle" werk is getoond) in de toekomst mogelijk maken.

(vertaling H.A.J. Meijer)

Appendix I

Recently, the Murnick group from Rutgers University have submitted comments on our paper "Intracavity OptoGalvanic Spectroscopy is not suitable for ambient level radiocarbon detection", which is Chapter 2 of this thesis, to the journal Analytical Chemistry. Through these comments, Murnick and coauthors state that our experiments were not correctly performed and that the conclusions we derived were incorrect. We certainly do not agree with the comments submitted by Murnick and coauthors and have submitted our response to the comments. The comments and reply are currently under review. In the following section the comments and our response to them (as submitted to Analytical Chemistry) are shown.

Comments on "Intracavity OptoGalvanic Spectroscopy is not suitable for ambient level radiocarbon detection" by Daniel Murnick, Junming Liu and Mark DeGuzman.

In a recent paper in Analytical Chemistry, Paul and Meijer[1] reported a series of survey experiments with a new intracavity optogalvanic system. Data obtained were heuristically reduced in an attempt to calibrate the system for radiocarbon analysis. In our opinion, the title of the paper does not describe the work reported and the conclusions reached are not supported by the data presented. No theoretical explanations are given for the manner in which their system was designed nor for the method by which their data were analyzed. In this comment, some of the major inconsistencies in their work are pointed out and it is shown that with a more careful analysis of their data their conclusions can be refuted.

In 2008 a new intracavity laser spectroscopy, given the acronym ICOGS, was introduced[2]. Though the basic physics of the technique was described at that time, the experiments reported were complex and required a thorough understanding of gas laser and glow discharge physics to properly carry out. Due to gaps in a full theoretical understanding it was noted then that many variables had to be carefully controlled both with respect to the laser and the sample discharge cell in order to

obtain consistent results. In particular, it was pointed out that measurements using an external reference discharge cell were crucial for control and stabilization of laser and system variables. Typically, if one is to claim that a particular experiment is incorrect, it is necessary to provide either a valid theoretical basis for that claim and/or to demonstrate unequivocally that the reported results could not be reproduced under identical conditions. Paul and Meijer do neither.

Their work begins by stating that a new two internal cell laser system is to be used, eliminating the crucial external reference cell, containing highly enriched radiocarbon, which had been used in the original ICOGS system. It then makes the logically inconsistent assumption that an internal reference with natural abundance radiocarbon is equivalent to an enriched external cell. In order to determine the effect of the internal cell, it must first be compared with an external cell including benchmark tests such as stability and Allan variance measurements. This was not done. Further, as previous studies[2,3] and the authors own work show the total ICOGS radiocarbon signal with natural abundance radiocarbon present has a high background component such that the analysis technique they describe is non-quantitative and can only be used to test stability. Further, the so-called reference cell signal cannot be used to lock the laser to the center of the $^{14}CO_2$ resonance; but rather to near the peak of the laser gain profile. In the set of experiments with enriched $^{14}CO_2$ reported by Paul and Meijer the sample itself is used as its own reference. No control or benchmark experiments are presented to validate their system or analysis.

Difficulties are apparent in the first set of experiments presented in Figure 2 of Paul and Meijer. The time variation in the transversely irradiated $^{12}CO_2$ ratios as well as the ICOGS $^{14}CO_2$ ratios indicates possible problems with their experimental system. These ratios should be constant and should exhibit a linear Allan variance. Possible experimental variables influencing their measurements but not carefully controlled by the authors are temperature, pressure and gas flow rate drifts. Most importantly, without a well-understood external reference cell the $^{14}CO_2$ laser wavelength was unstabilized. The figure clearly shows inconsistent results. Depending on chopping rate, pressure, temperature and exact laser power and

lock point used the expected separation in the case studied can be small but should be constant. The ^{14}C concentration depends on the $^{12}CO_2$ ratio and requires a rigorous de-convolution algorithm. In the absence of a well-characterized and stable reference cell, all dependent variables must be constant to quantitatively compare samples with the configuration used. The data displayed simply indicates that that was not the case for the experiments described.

The independent batch mode experiments using enriched $^{14}CO_2$ described in the Paul and Meijer work are interesting, but have little relationship to the title or conclusions of their paper. Again, there is no reference cell used and, significantly, there is no $^{12}CO_2$ monitoring shown. As the experiments are done in batch mode there must be time dependent dissociation present that does not come to equilibrium for possibly many hours. This would have been obvious with $^{12}CO_2$ monitoring. Nevertheless, with a more careful analysis of their data some valid conclusions might have been drawn.

The graphs and corresponding raw data shown in Figure 1, were kindly sent to us in mid 2014 by one of the authors, Dipayan Paul, and are similar to Figure 3 of Paul and Meijer. There is a significant pressure change observed over the course of the measurements that is less obvious in Figure 3 of Paul and Meijer due to a scale change. No pressure dependent studies were carried out in their work but the sensitivity to pressure is documented in their references 7 and 10. Their laser is stabilized on the peak of the ICOGS signal which is not necessarily the peak of the $^{14}CO_2$ resonance-obviously not for the P(20) line where, as the authors note, it is due to a very close accidental coincidence in $^{12}CO_2$. The laser-off feed through signal, given as 0.4mV, should have been subtracted as a vector from the total signal for proper analysis. The total background also consists of ionization from high lying states and off resonant enhancement of other absorbing transitions. For 100% CO_2 the ionization level background along with the non-resonant CO_2 far wing background can be found from the signal vector for dead CO_2. Then, by subtracting that vector, the remaining $^{14}CO_2$ vector, amplitude and phase, can be determined. We have attempted to do that with the data set supplied by Mr. Paul in 2014 sharing the results shown in Figure 2 with the authors at that time.

Figure 2a shows the $^{14}CO_2$ amplitudes and Figure 2b the corresponding phases of the resultant vector at the chopping frequency when all calculable backgrounds are subtracted. Note that contrary to the conclusions of Paul and Meijer there is a clear and consistent separation in amplitude from dead (taken as zero ^{14}C amplitude and plotted at a ^{14}C ratio of 10^{-15}) to modern and beyond for all wavelengths studied. The points at 10^{-9} concentration, in the data set provided, are above the trend lines-possibly due to variations in discharge system parameters for what we were told was the first measurement in the series. The phases for all but the P(20) line are the same for all concentrations, as expected, except for the highest concentration where some of the ICOGS theory[4] assumptions may need modification. The P(20) phase variation is likely due to the large effect of the nearby $^{12}CO_2$ background resonance and the fact that the laser stabilization is not at the proper wavelength.

It would be interesting to carry out similar vector decompositions for the data summarized in Figure 5 of Paul and Meijer. It should be noted that the statistical uncertainties for the data of Figure 1, and of Figure 3 of Paul and Meijer are significantly smaller than what is shown in Figure 5 of their work. Paul and Meijer state that is because they have averaged three independent measurements and show the standard deviation about the mean. The fact that independent measurements vary significantly from run to run confirms to us that the lack of a reference cell and corresponding control of crucial experimental variables by Paul and Meijer is the true cause for their variability. As the uncontrolled variables mainly effect the background, and the heuristic analysis method used by Paul and Meijer ignores background contributions, the variability in the numbers they quote for power normalized total signal are not surprising.

In summary we would conclude that Paul and Meijer's work, though confusing, has made a contribution to ICOGS science for analysis of radiocarbon. Their hypothesis that an internal reference cell with contemporary levels of $^{14}CO_2$ can be substituted for an external reference cell with enriched radiocarbon is unproven. Contrary to the conclusions in Paul and Meijer, their survey measurements with enriched $^{14}CO_2$ without an external reference cell or proper stabilization of their $^{14}CO_2$ laser still shows clear validity for the ICOGS technique reported in reference

1 when analyzed carefully. Their work may lead to advancing the development of intracavity optogalvanic instrumentation for radiocarbon detection.

Figures from the comments submitted by Murnick and coauthors:

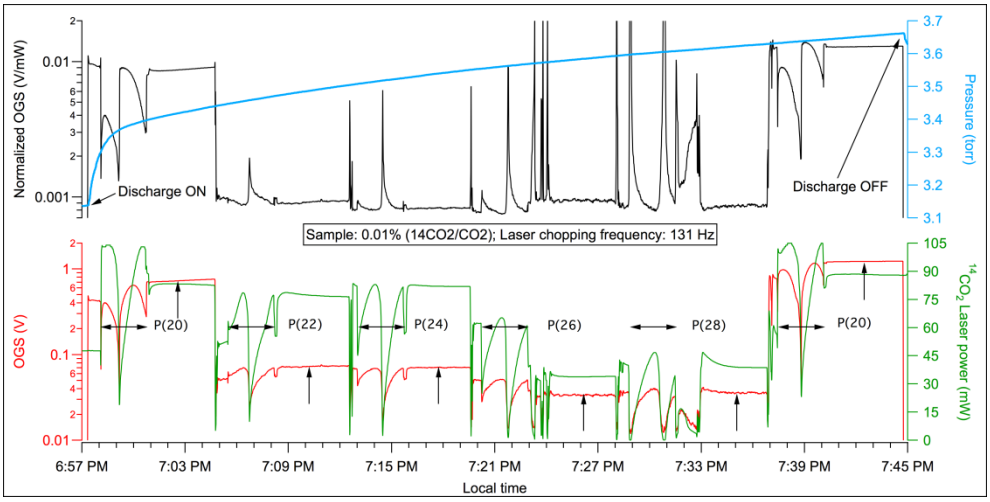

Figure 1: Data obtained with the system of Paul and Meijer similar to that of Figure 3 of reference 1 and analyzed, in 2014, as described in the text.

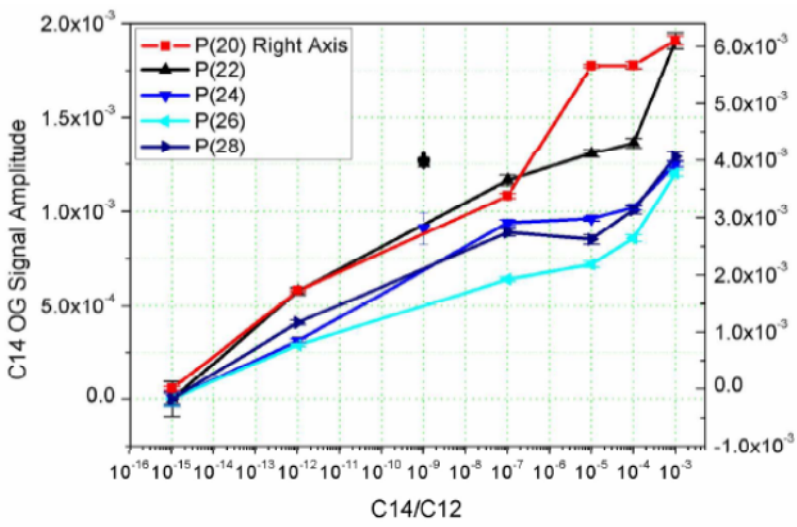

Figure 2 (a)) Amplitude of 14CO2 contribution to the total ICOGS signal at the fundamental chopping frequency as determined by proper background subtraction from the data of Figure 1.
279x182mm (150 x 150 DPI)

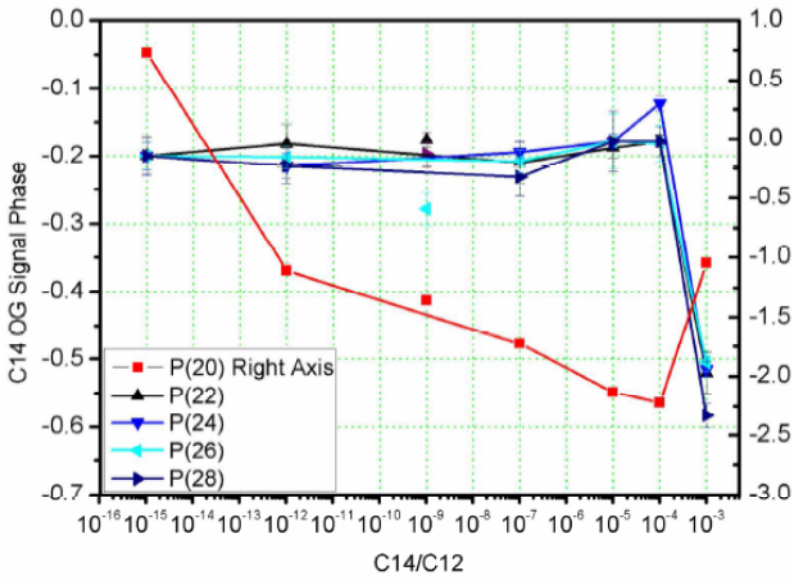

Figure 2 (b) Corresponding phase of the 14CO2 contribution. In both cases, the scale for the P(20) line is on the right.
279x203mm (150 x 150 DPI)

Figure 2: (a) Amplitude of $^{14}CO_2$ contribution to the total ICOGS signal at the fundamental chopping frequency as determined by proper background subtraction from the data of Figure 1. (b) Corresponding phase of the $^{14}CO_2$ contribution. In both cases, the scale for the P(20) line is on the right.

References from the comments submitted by Murnick and coauthors:

[1] Dipayan Paul, and Harro A.J, *Anal. Chem.*, **2015**, *87* (17), pp 9025–9032

[2] Murnick DE, Dogru O, Ilkmen E.. *Anal. Chem*. **2008,** 80(13):4820-4.

[3] Persson A, Eilers G, Ryderfors L, Mukhtar E, Possnert Gr, Salehpour M*, Analy. Chem* **2013,** 85(14):6790-8

[4] H. J. Kimble, *IEEE J. Quantum Electron*. **1980**, QE-16 (4), 455-461

Response to comments submitted by Daniel Murnick et al. on our paper "Intracavity OptoGalvanic Spectroscopy is not suitable for ambient level radiocarbon detection" by Dipayan Paul and Harro A. J. Meijer

It is highly disappointing to see that Dr. Daniel Murnick and co-authors still claim that ICOGS is a viable analytical technique for radiocarbon detection and that they use our data without our prior consent to support their theory, which we do not agree with. Since 2010, groups from three universities (University of Groningen (Paul and Meijer 2015), Uppsala University (Eilers et al. 2013; Persson et al. 2013; Persson and Salehpour 2015), and Columbia University (Carson et al. 2016)) participated in a consortium with the Murnick Group, following the 2008 Analytical Chemistry paper (Murnick et al. 2008) (will be referred to as Mu2008 as used in our manuscript), to develop and apply ICOGS for various applications. As stated in our paper (Paul and Meijer 2015), we have spent a considerable amount of time (Dipayan Paul ~11 months and Harro Meijer ~3 months) in the Murnick Group during the first year of our involvement with ICOGS. During our stay at Rutgers, we participated in the day-to-day experiments performed in the Murnick group to understand the technical details required for the construction of our own system. Even after severe reproducibility problems we faced at Rutgers, we still decided to investigate the possibilities with ICOGS back at Groningen. Following this, we constructed the ICOGS setup at the University of Groningen in close collaboration with the Murnick group, and this was completed in mid-2012. Since then we have performed experiments at length to detect radiocarbon unambiguously, but we have not succeeded. This process was described in our paper (Paul and Meijer 2015).

Thus far, none of the groups participating in the ICOGS consortium (including the Murnick lab itself) could reproduce the results published by Murnick et al. (2008 (Murnick et al. 2008), 2010 (Murnick et al. 2010)). From our own experience, the set-ups in Murnick's lab have systematically been unable to actually determine the ^{14}C content of unknown gases. During our stay at the lab in 2011, our home lab in Groningen provided a series of ten ^{14}C-calibrated CO_2 gases, ranging from "dead" to ≈150% modern. In spite of a great deal of effort, no reproducible results could be

obtained, neither in the way exactly reproducing the 2008 paper, nor in any other way (shown in figures below).

To our information, that situation is still the case: the Murnick lab can simply not produce any measurement result on a CO_2 with a ^{14}C concentration unknown to them. This is clearly evident from the number of publications (only one) the Murnick group has delivered since the 2008 publication: since they just could not reproduce their own work, the 2010 paper simply reused the data from the Mu2008.

About a year ago, after we received the "calibration plot" shown in Murnick's comments (Figures 2a & b), we again sent the raw results of our measurements on two samples with ^{14}C concentrations unknown to them, with the question to determine their ^{14}C content, but the answer has been silence. We never understood the physical basis of the so-called "vector model" proposed by Murnick (July 2012), nor were we convinced by this method of analysis, which as mentioned only worked with samples known on forehand and was never reproducible. Soon after sending us the analysis results (shown in Figures 2a & b of Murnick et al.'s comments), one of the coauthors (Mr. Junming Liu) also expressed his disagreements and questioned the validity of Murnicks vector model through personal communication (available on request). Mr Junming Liu's coauthorship in the comments submitted by Dr. Murnick is quite puzzling to us, given his contrasting opinion in the past.

Because of our experience at Rutgers, we decided to adapt the set-up in Groningen, as was described in our paper: more careful gas handling, and as the most crucial improvement: the simultaneous measurement of reference and sample under identical circumstances. The criticism about not being able to stabilize on a ^{14}C transitions is wrong for two reasons: first, the laser itself is lasing on a $^{14}CO_2$ medium, and thus coupled to the proper transitions. In our experiments, we deliberately scan the laser frequency around the heart of these lines. Second, if one needs an external cell, filled with CO_2 of which 5-10% is $^{14}CO_2$, to observe a proper signal, and one allegedly cannot stabilize the laser on the intracavity

reference cell, this already shows that there is no consistent $^{14}CO_2$ signal to be observed at natural abundances (of 10^{-12}!).

Murnick et al. still talk about their set-up as if there is signal present, even at natural abundances, and that we have supposedly not done a proper job, by not investigating Allan variances, not properly subtracted backgrounds, not done a phase-dependent signal analysis, and whatnot. Bottom line is, however, that there IS no signal at all! If a system would be sensitive enough to produce a sizeable signal at ^{14}C concentrations around (and as is even claimed, below) 10^{-12}, then even a "sloppy" experiment at 10^{-5} – 10^{-3} $^{14}C/^{12}C$ concentration would show a tremendously high and robust signal. As we have shown, there is none, and we performed all but a sloppy experiment. As explained in the paper, due to radioactivity safety requirements, we were not able to perform continuous flow-dual cell experiments with these radioactive CO_2's, but we nevertheless did a careful job in single cell "batch mode". Perhaps, with considerable extra effort, as we write in the paper, we would find signal at the high end of concentrations that we use but that is where the story ends.

If, for some mysterious reason, the signal of the system would have a logarithmic response, such that at 10^{-5}-10^{-3} abundances the signal would be only incrementally higher than at 10^{-12}, this would immediate lead to the conclusion that the system would be unsuited for ^{14}C measurements (and certainly for dating): how would one then expect to observe the difference between two more closely lying concentrations?

Indeed Murnick et al. reacted on raw data sent by us in the past by sending us the present Figure 2 of their comment. Already at that time we had to conclude that this is based on no more than wishful thinking: the exact treatment of these data is tuned towards the desired outcome. Especially the indicated errors are absolutely unrealistically low. What we see in their Figure 2 is a linear amplitude signal ranging from 0 to about 1.5 x 10^{-3} (thus hardly exceeding the noise level) over a ^{14}C concentration range of 11-12 orders of magnitude! Figures like our figure 3, or the figure 1 that Murnick et al. reproduce, but especially our figure 2 show

significant day-to-day (and even sample-to-sample) variability which is larger than the whole range of the calibration curve of Murnick et al.'s Figure 2. The 10^{-9} point is symptomatic for that. Next day, the shape of the curves would look entirely different again. That is why we produce in our figure 5 an honest average of three attempts, such that the variability of the system is visible. Data treatment like suggested by Murnick et al. does not improve that situation at all. Of course, one could argue that there is a slightly negative trend in the curves of figure 5a, but given the enormous range of ^{14}C concentration and the size of the error bars, taking such a trend line seriously is, again, wishful thinking. For all but the "contaminated" P(20) line (which we disregard based on its severe overlap with a normal $^{12}CO_2$ line), such a "trend" is entirely based on the slightly higher signal for "dead" CO_2 alone, and we describe in detail in the paper why even this is not significant. Figure 5b serves to demonstrate the large sample-to-sample fluctuations that occur.

Murnick et al. have to face the disappointing truth: ICOGS does not deliver ^{14}C signals, neither from natural abundance CO_2 nor from considerably enriched. We, too, would have loved to have shown ^{14}C measurements delivered by ICOGS (not in the least because the work formed the heart of the PhD thesis work of D. Paul), but scientific integrity has required from us that we published the paper with the outspoken title.

Below, we add some detailed responses to the comments submitted by Murnick et al. (cited in italics)

"In a recent paper in Analytical Chemistry … their conclusions can be refuted." (first paragraph)

Our paper does not attempt to show a calibration of the system at all. The sole goal of the paper is to determine a $^{14}CO_2$ concentration range, where a "clear and unbiased" optogalvanic signal (OGS) is observed based on the measurement and analysis procedure described in the 2008 Analytical Chemistry paper (Mu2008) and the thesis work of Dr. Erhan Ilkmen (former PhD student from the Murnick

group). As reported, we did not succeed, and neither did the other groups who were trying this.

If the analysis is “so” complex, and monitoring parameters is “so” necessary, then it is practically impossible that the results published in Mu2008 are trustworthy (many parameters were not monitored back then, their signal could have just been an artifact and not signal at all).

“In 2008 a new … identical conditions. Paul and Meijer do neither.” (second paragraph)

Here Murnick and coauthors start with a statement that suggests that ICOGS works and the only requirement is careful monitoring of parameters and that would result in “consistent results”. This certainly was not the case back in 2011, one such example among many others is shown in the figures below. This is one of the examples of measurements performed during our stay. In the experiments shown here (performed at Rutgers during 2011), we participated equally both in performing the measurements and analysis thereafter. Several different data analysis strategies have been used by the Rutgers group so far to detect the radiocarbon concentrations in a given sample. One such method used extensively during 2011 is shown below. Measurements of CO_2 samples were performed by injecting CO_2 (with known radiocarbon content, ranging from "dead" to ≈ 50 times modern) in a steady flow of N_2 (buffer gas, examples shown in Figure 1). A slope corresponding to each injection was determined from the C14 Ratio vs. C12 Ratio plots which was used as a measure of the radiocarbon content in the CO_2 sample, and thus in the calibration plots (Figure 2).

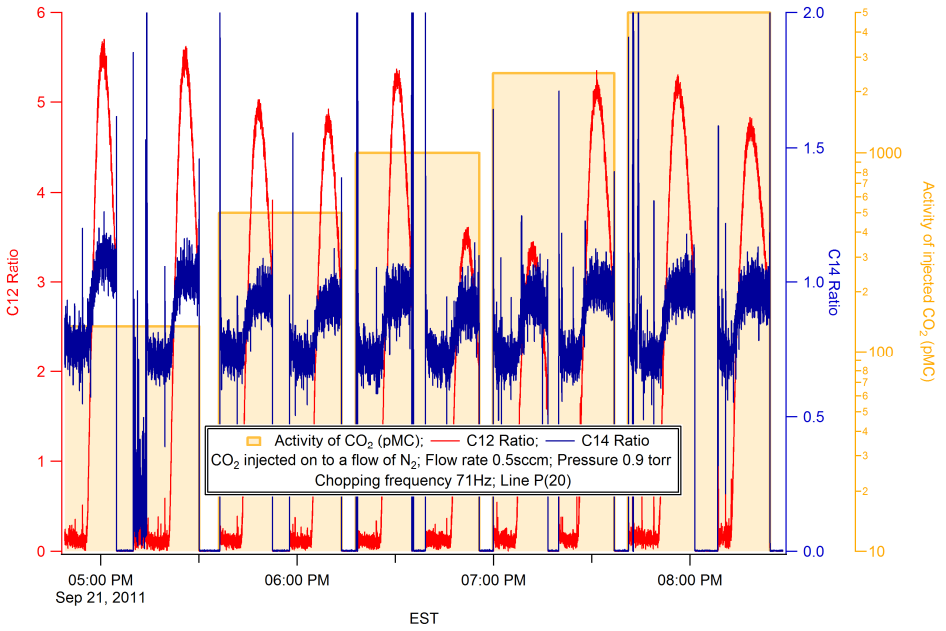

Figure 1: CO_2 samples with varying ^{14}C activity injected on to a flow of nitrogen.

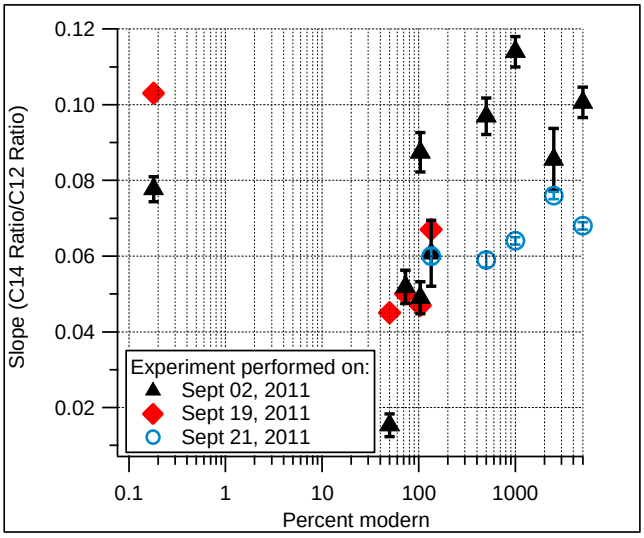

Figure 2: Summary of all measurements performed on Sept 02, 2011 (Figure 1); Sept 19, 2011 and Sept 21, 2011 (not shown), showing the large variability between measurements and lack of reproducibility. Mind the logarithmic x-axis.

"Their work begins by … validate their system or analysis." (third paragraph)

Since the optogalvanic signal in an external (enriched) reference cell scales with the laser power, except for the P(20) laser transition at 11.7677 µm, we really don't see the point why an external reference cell is critical. Murnick et al. say that the use of an external reference cell is critical without supporting this with any data. This point has never been emphasized in any of the earlier publications (Murnick et al. 2008; Murnick et al. 2010) from the group and in contrast, successful use of an external reference cell containing natural levels of radiocarbon has also been described (Ilkmen 2009) (page 35, paragraph 2 of the PhD thesis of Dr. Erhan Ilkmen). Moreover, the Murnick group has never shown that the signal observed with the external reference cell is produced solely from $^{14}CO_2$ molecules and that the signal actually scales with the $^{14}CO_2$ concentration (containing varying levels of radiocarbon). In fact, their external reference cell is not well characterized and most importantly, is in a very different pressure regime than the samples themselves. The reference cells are typically filled at pressures of around 5 torr (not consistent all the time) and have to be stabilized with a discharge glowing for weeks before they become any usable, meaning that the pressure would be much higher than when filled. Also, these reference cells are filled with different (inconsistent) levels of $^{14}CO_2$ in CO_2 or N_2 every time they are filled. And no "benchmark experiments" were presented nor performed for the data shown in the Mu2008 paper and in the thesis work of Dr. Erhan Ilkmen, which forms the very basis of Mu2008.

Here at Groningen, we have performed Allan Variance analysis, mostly to characterize the noise in the system and also to determine the optimal integration time. But presenting these analyses only makes sense when there is already an unambiguous signal present. And there is none.

"Difficulties are apparent in the … for the experiments described." (fourth paragraph)

This criticism is not true; all parameters were controlled and monitored. This includes temperature (in the room, near the internal cells and the chiller

temperature: for cooling the laser), pressure (in both cells), flow (in both cells) and the $^{14}CO_2$ laser power (emitted).

"The independent batch mode experiments …conclusions might have been drawn." (fifth paragraph)

For the reference cell argument, see above. The batch mode experiments were performed to determine a $^{14}CO_2$ concentration where a clear and distinct optogalvanic signal was observed. This method of analysis we used was widely used by the Murnick group before the proposed "vector-model" (in fact also for their Mu2008 paper). The use of a reference cell would remove the fluctuations caused by the laser (which was very stable during our measurements anyway, as seen from the power) and the ^{12}C normalization removes the fluctuations in the discharge (which also was quite stable). Since all the experiments were performed in similar fashion, they are comparable. And had there been a clear and large signal, it would have certainly been visible here.

Murnick et al. state that the laser-discharge equilibration takes "many hours", thereby criticizing our batch mode experiments. However, in the experiments previously performed in the Murnick group (in batch mode), the discharge was allowed to stabilize for a minute or so before measurements were performed (Ilkmen 2009) (Figure 4.8 and 4.9 on page 56, description on page 57 of the PhD thesis of Dr. Erhan Ilkmen). So, if few hours of stabilization are required, are the calibration curves by the group credible at all?

"The graphs and corresponding … at the proper wavelength." (sixth and seventh paragraphs)

Murnick and coworkers turned our data from chaotic, random behavior (figure 3a, our data analysis) which we believe to be realistic, into an almost straight line (their figure 2a, reproduced here figure 3b). How they perform this process in a reliable and credible way (that is without working towards a desired result) remains a mystery to us. Anyway, if such a complicated analysis procedure is required to

extract the radiocarbon signal, how was it even possible to see a radiocarbon signal with the data published in Mu2008?

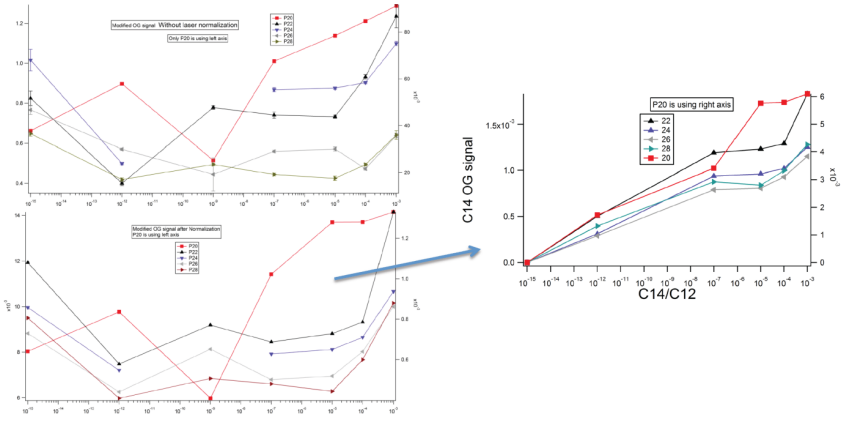

Figure 3: a) (left) data from one of our experiments, showing no relation between the ICOGS signal and the ^{14}C concentration of the sample. b) (right) the "calibration curve" deduced by Murnick et al. from the exact same data.

"It would be interesting to … normalized total signal are not surprising." (eighth paragraph)

The large standard deviation observed in Figure 5 of our paper is indeed due to large variations in the optogalvanic signal and is also observed with the Rutgers ICOGS setup. It is not because of a lack of reference cell, but because of the intrinsic variability in the RF discharge process. We disagree that performing vector decompositions would be interesting; we simply do not believe this method to be any good, because there simply is no ^{14}C signal! If Murnick et al. still claim that their new method of analysis is how it should be, then it must be independently verifiable with unknowns and not just with known samples. And it would also imply that their original Mu2008 measurements were incorrect, as they did not use this method back then.

"In summary we would conclude that … instrumentation for radiocarbon detection." (last paragraph)

Obviously, we totally disagree with this final paragraph based on all arguments in this reply, as well as in our paper. ICOGS is not feasible for ^{14}C detection, and if Murnick et al firmly believe it does, they have to produce good quality results for the ^{14}C level of several CO_2 gases unknown to them. So far, they have not done that, and it is our firm conviction they never will.

References:

Carson CG, Stute M, Ji Y, Polle R, Reboul A, Lackner KS. 2016. Invalidation of the intra-cavity opto-galvanic method for radiocarbon detection. Radiocarbon DOI: 10.1017/RDC.2016.5, 2016.

Eilers G, Persson A, Gustavsson C, Ryderfors L, Mukhtar E, Possnert G, Salehpour M. 2013. The Radiocarbon Intracavity Optogalvanic Spectroscopy Setup at Uppsala. Radiocarbon 55(3–4):237-50.

Ilkmen E. 2009. Intracavity Optogalvanic Spectroscopy for Radiocarbon Analysis with Attomole Sensitivity [Doctoral Thesis]. Newark: Rutgers, The State University of New Jersey.

Murnick D, Dogru O, Ilkmen E. 2010. C-14 analysis via intracavity optogalvanic spectroscopy. Nuclear Instruments & Methods in Physics Research Section B-Beam Interactions with Materials and Atoms 268(7-8):708-11.

Murnick DE, Dogru O, Ilkmen E. 2008. Intracavity optogalvanic spectroscopy. An analytical technique for C-14 analysis with subattomole sensitivity. Analytical Chemistry 80(13):4820-4.

Paul D, Meijer HAJ. 2015. Intracavity OptoGalvanic Spectroscopy Not Suitable for Ambient Level Radiocarbon Detection. Analytical Chemistry 87(17):9025-32.

Persson A, Eilers G, Ryderfors L, Mukhtar E, Possnert G, Salehpour M. 2013. Evaluation of Intracavity Optogalvanic Spectroscopy for Radiocarbon Measurements. Analytical Chemistry 85(14):6790-8.

Persson A, Salehpour M. 2015. Intracavity optogalvanic spectroscopy: Is there any evidence of a radiocarbon signal? Nuclear Instruments and Methods in Physics Research Section B: Beam Interactions with Materials and Atoms 361: 8-12.

Appendix II

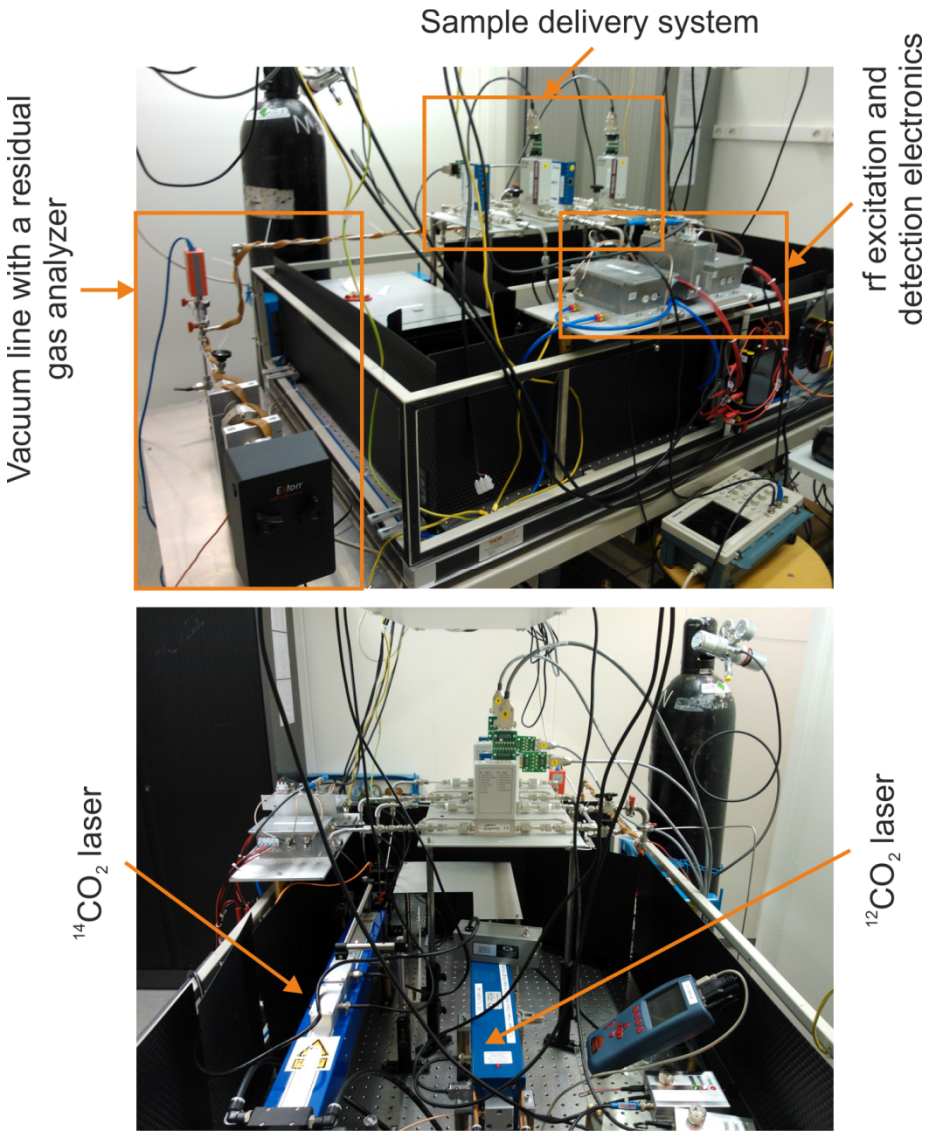

Figure 1: The IntraCavity OptoGalvanic Spectroscopy setup at CIO, Groningen (from Chapter 2).

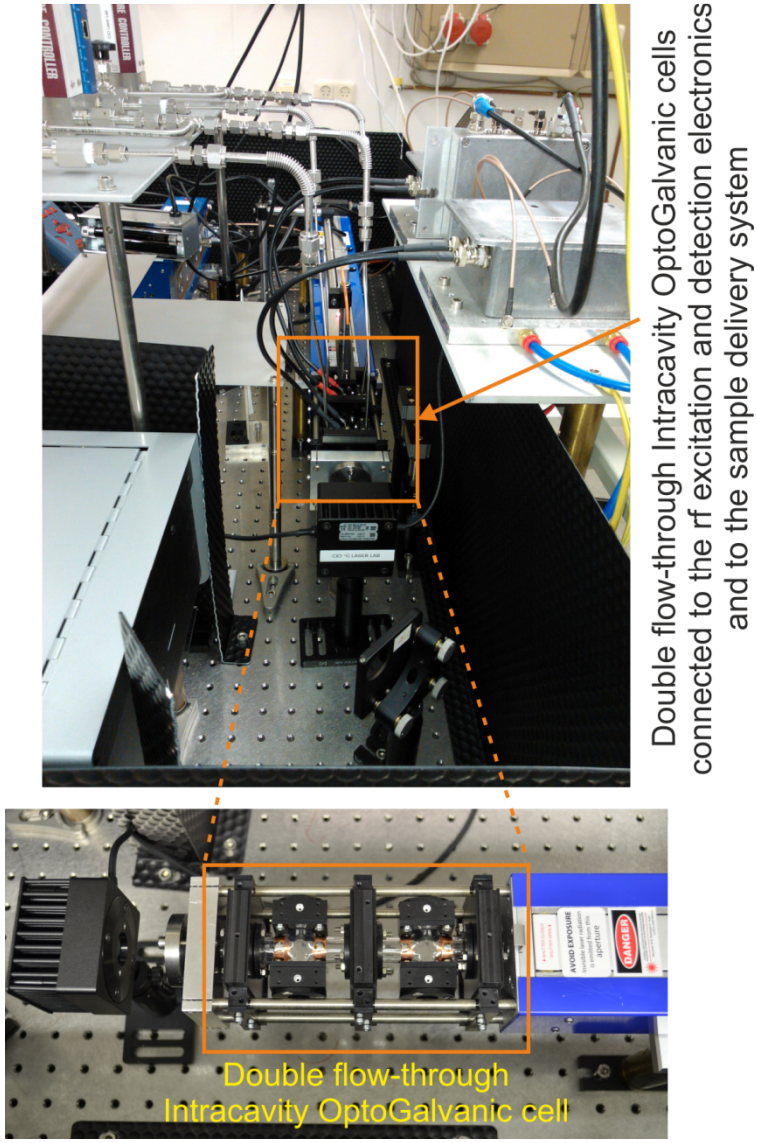

Figure 2: The IntraCavity OptoGalvanic Spectroscopy setup at CIO, Groningen (from Chapter 2).

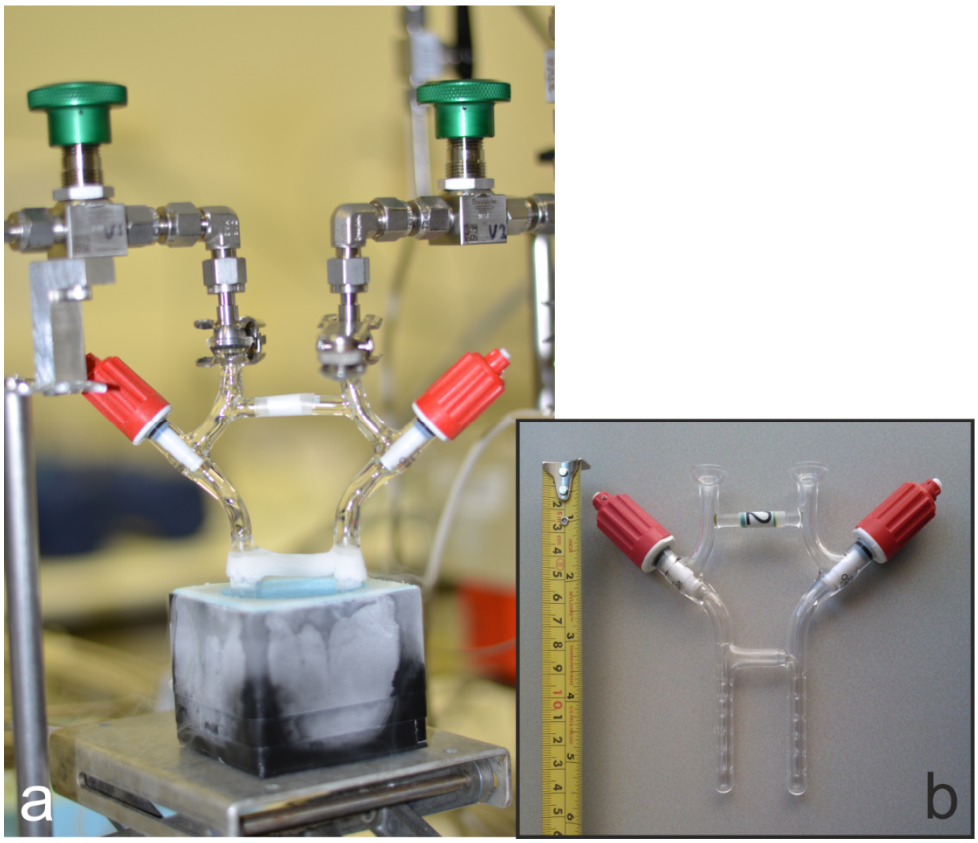

Figure 3: a) The detachable flow-through freezing tube submerged in liquid air during an extraction (described in Chapter 4). b) The detachable flow-through freezing tube.

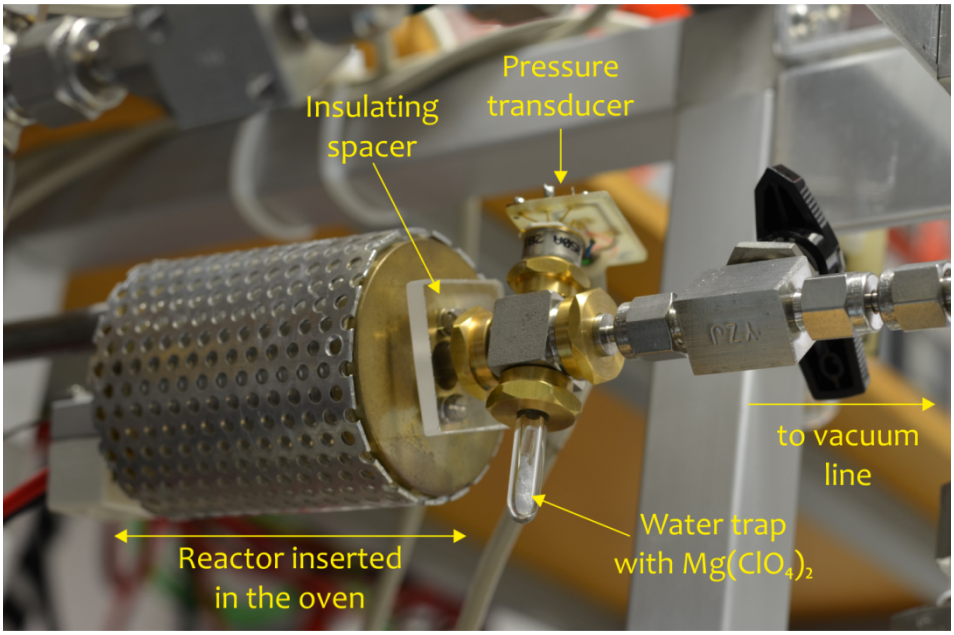

Figure 4: Setup of the graphitization system used for the graphitization of stratospheric CO_2, described in Chapter 4.

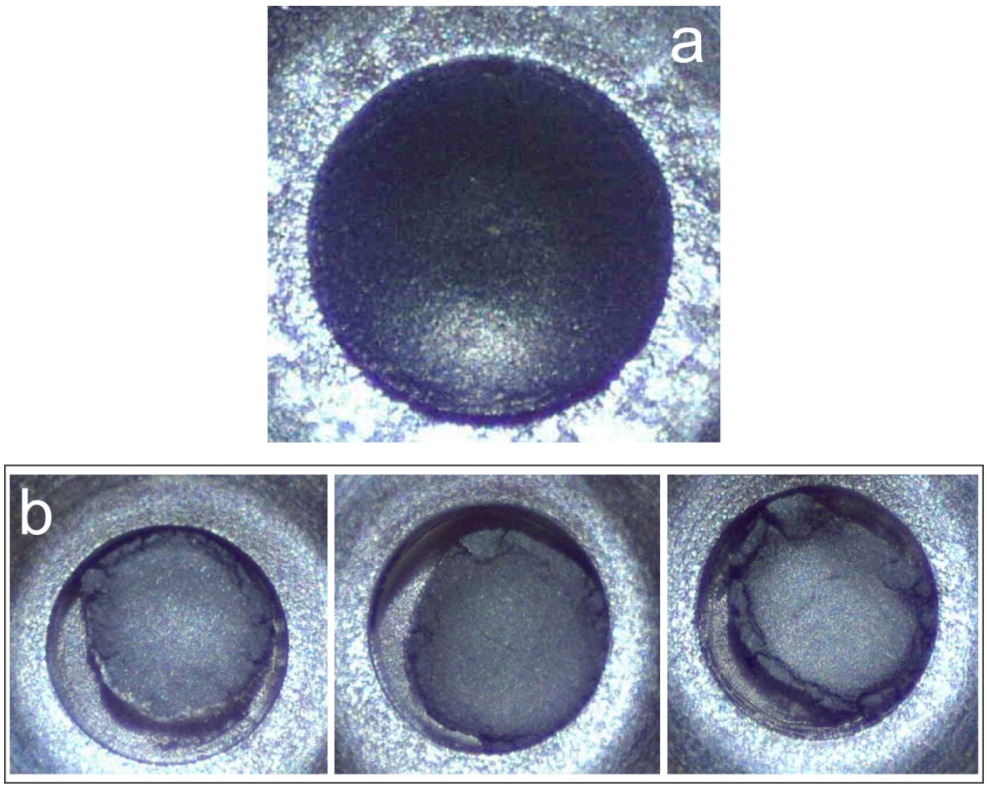

Figure 5: a) Close-up of a regular AMS target with pressed graphite (graphite + iron powder ~ 4-4.5 mg), b) Close-up of a small sample AMS target with pressed graphite (graphite + iron powder < 1.5 mg) without a blank iron filling pellet underneath as described in Chapter 4.

Acknowledgments

I guess everyone doing a “PhD” has a very similar overall story to tell about this epic journey. But nevertheless, the experience gained during these eventful years is pretty unique and definitely leaves behind wonderful memories to be cherished later. During this journey, I worked and made friends with many individuals who in some way or the other influenced this delightful ride for which I am ever grateful.

The first chapter started at Rutgers University, Newark. I would like to thank Prof. Daniel Murnick and his group for the welcoming and a very cooperative research environment. Thank you Dr. Murnick for your encouragements, the extensive research discussions and for involving me in all the discussions with the pharmaceutical partners, which was certainly beneficial! I am thankful to Erhan Ilkmen, Mark DeGuzman, Cantwell Carson, Andrew Reynolds, Michael Gray, Michael Bellanich, Bill Thomas, Johnny Gonzalez and Tulu Bacha for the wonderful time we spent at Rutgers (from research – interesting lunch discussions – “optics” golf sessions – Hamburgao & Red Robbins… and the list is endless). Mark, I really appreciate your prompt efforts with the multiple laser gas fills that we had to do. I also thank Yong Zhang and Michael Adams at the Access Laser Company for the innumerous discussions, tips on laser alignments and the support. Outside lab, Shajesh, you were a great company and support, thanks! And of course, thank you Mrs. Wheeler for your kind support with all the administrative issues! I wish the ICOGS project had been a success, we could have continued this collaboration much longer.

Following Rutgers, the next chapter begun at Groningen. In terms of the work culture, Netherlands was completely a different experience. Although this was first introduced (briefly) to me by my supervisor, Prof. Harro Meijer, while on a three-month sabbatical at Rutgers, I got the real picture upon arrival. Harro, I would like to thank you for being a wonderful mentor. I’ve enjoyed every moment of my stay at CIO, all because of the enthusiastic coworkers around and your constant

encouragements. The ICOGS work was quite frustrating and demotivating at times, but your support and trust helped a lot. Although it was always a bit difficult to keep up with your pace, in terms of futuristic thinking, your quick calculations, and of course for your superfast corrections/comments on the manuscripts and the chapters, it was a great training. I always received very constructive and helpful feedbacks from you, whenever required, and almost-always without a prior appointment!

Next, I would like to thank the three pillars (Henk Jansen, Henk Been and Bert Kers) that enthusiastically and reliably supported my research work at CIO. Thanks a lot for the unconditional helps and suggestions. I have learned a lot from you all, and I can definitely say that you have significantly enriched (not radioactively!) my knowledge with your wisdom!

Anita: thank you for your help with planning the sample preparations and the discussions/suggestions on sample contamination and sample preparation. It was indeed a great pleasure working with you. Dicky, Trea, Fsaha and Margot: Thanks a lot for the innumerous samples you prepared during the past years. I cannot thank you enough for your help and patience. It is unfortunate and sad that Trea is not longer with us but I'll certainly cherish her support and the first sample preparation training with her at CIO. Fsaha: I would especially thank you for patiently preparing the iron pellets. Sanne: thank you for preparing the CO_2 reference standards and for the innumerous discussions. Janette: thanks a lot for explaining me and sharing your experiences with the CO_2 extraction system.

Hans (van der Plicht): thanks a lot for helping me with many of the AMS related questions I had and for sharing various interesting facts, experiences on radiocarbon related research. Huilin: thanks a lot for your suggestions and insightful discussions during the radiocarbon in stratospheric CO_2 study. Wouter: thanks a lot for giving me the opportunity to work on the dryer development project while I was finishing up my thesis write-up.

Mark and Marcel: thanks a lot for eagerly helping me with all the electronics issues and for your useful suggestions. Hans (Roeloffzen): thanks a lot for your computer related helps. Patricia: thanks a lot for your help with all the administrative issues.

Apart from research, time spent with the lunch group was fun and relaxing. Thanks a lot to Steven, Charlotte, Linda, Truls, Bert (Scheeren), Katrin, Uli, Wei, Ivar, Panteha, Alex, Herman, Navin and Huilin.

I would like to thank all members of CIO for making my stay so pleasant.

I would also like to thank all the members of the reading committee, Prof. J. van der Plicht, Prof. E. Kerstel and Prof. W. Peters for your approval.

Since the research described in this thesis required several custom-built parts, it would have had been difficult without the skillful support from the Machine shop: Bert, Harry, André, Koos, Rieks, Henk, Udo, Dave, Willem, Ricardo, Hielke, Jannes, Frits, and Rick; the Glass shop: Maarten, Harold and Wouter; and the Electronic shop: Hans and Wigger. Jan-dirk van Hoogen and Klaas Veldman: thank you very much for your help with the arrangements required for shipping and receiving the $^{14}CO_2$ laser. Erik J. Bunskoeke: thank you for making the necessary arrangements required for acquiring the $^{14}CO_2$ sample and for providing me with a lab space to prepare the diluted $^{14}CO_2$ samples. Jacob Baas: thank you for helping me with the PXRD measurements.

Outside work, life wouldn't have had been fun without my friends from India. Soumya, Sandeep, Sujatadi, and Ayan: thanks a lot for all the wonderful times we spent and the elaborate dinners we had. Neha and Pavan: thank you for the great weekends we had together with good food and lovely music. Pranav, Vaishali and Nobina: thank you guys for all the fun-filled weekends with delicious food and nice movies (mostly horror!) and of course badminton. Tara and Divya: thank you for the nice time we spent together and for all the restaurant explorations. Asishda and Reema boudi: thank you for the good time, good food and interesting discussions. Saurabh, Raj bhai: thanks for the nice and fun-filled times. Tamalikadi: thanks a lot

for the nice time, delicious food and your suggestions. You all have been my family far from home.

I would also like to thank all the friends I met through the Groningen Indian Students Association (GISA), especially, Suresh, Vineet, Milon, Tushar, Rama, Pallavi, Varsha, Ekta, Sumit, Arijit, Kumar, Soma and many others for all the wonderful events. I also thank all my house mates (current and previous), especially Ram, Gaurav, Nilesh, Sarrvesh, Agnes, Martin and Daniel for the nice time.

I would like to extend my sincere gratitude to the electricity company RWE/Essent for generously funding my PhD research project for which I am extremely grateful.

At last but not the least, I would like to thank my family for the constant support and love. Baba and Mam: thanks for being strong during the tough times we had been through. It was what kept me going. Swati: I certainly cannot imagine my life being complete without you. Thanks a lot for your patience, encouragement, support and love.

Curriculum vitae

September 2015 – Present: Temporary researcher at the Center for Isotope Research, University of Groningen, the Netherlands.

December 2010 – April 2016: Ph.D. research under the supervision of Prof. Dr. Harro A. J. Meijer at the Center for Isotope Research, University of Groningen, the Netherlands.

January 2008 – June 2010: M.Sc. under the supervision of Dr. Hans D. Osthoff at the Department of Chemistry, University of Calgary, Canada.

June 2006 – December 2007: Research Associate at the Analytical R&D facility of Dr. Reddy's Laboratory, Hyderabad, India.

2004 – 2006: M.Sc. in Analytical Chemistry from the University of Pune, Pune, India.

2001 – 2004: B.Sc. in Chemistry from S. P. College, Pune, India.

List of Publications

1) **Paul, D.**, and Meijer, H. A. J.: Intracavity OptoGalvanic Spectroscopy Not Suitable for Ambient Level Radiocarbon Detection, *Analytical Chemistry*, **87**, 9025-9032, 10.1021/acs.analchem.5b02226, 2015.

2) **Paul, D.**, Been, H. A., Aerts-Bijma, A. T., and Meijer, H. A. J.: Contamination on AMS sample targets by modern carbon is inevitable, *Radiocarbon, 2016,* DOI: 10.1017/RDC.2016.9.

3) **Paul, D.,** Chen, H., Been, H. A., Kivi, R., and Meijer, H. A. J.: Radiocarbon analysis of stratospheric CO_2 retrieved from AirCore sampling, *Atmospheric Measurement Techniques Discussions,* DOI: 10.5194/amt-2015-377, 2016.

From previous work:

4) **Paul, D.**, Furgeson, A., and Osthoff, H. D.: Measurements of total peroxy and alkyl nitrate abundances in laboratory-generated gas samples by thermal dissociation cavity ring-down spectroscopy, *Review of Scientific Instruments*, **80**, 114101, http://dx.doi.org/10.1063/1.3258204, 2009.

5) **Paul, D.**, and Osthoff, H. D.: Absolute Measurements of Total Peroxy Nitrate Mixing Ratios by Thermal Dissociation Blue Diode Laser Cavity Ring-Down Spectroscopy, *Analytical Chemistry*, **82**, 6695-6703, 10.1021/ac101441z, 2010.

6) Furgeson, A., Mielke, L. H., **Paul, D.**, and Osthoff, H. D.: A photochemical source of peroxypropionic and peroxyisobutanoic nitric anhydride, *Atmospheric Environment*, **45**, 5025-5032, 10.1016/j.atmosenv.2011.03.072, 2011.